Electronic Supplementary Information for

Synthesis and catalytic performance of ruthenium complexes ligated with rigid *o*-(diphenylphosphino)aniline for chemoselective hydrogenation of dimethyl oxalate

Xiaolong Fang, Chunyan Zhang, Jin Chen, Hongping Zhu*, and Youzhu Yuan*

State Key Laboratory of Physical Chemistry of Solid Surfaces, National Engineering Laboratory for Green Chemical Productions of Alcohols–Ethers–Esters, iChEM, College of Chemistry and Chemical Engineering, Xiamen University, Xiamen, 361005, China

Content:

S1. General Methods

The manipulations were performed under a dry Ar or N_2 atmosphere by using Schlenk line and glovebox techniques. Organic solvents, such as toluene, *n*-hexane, tetrahydrofuran, and diethyl ether, were dried by refluxing with sodium/potassium benzophenone under N_2 prior to use. The esters used for the catalytic test were distilled before use. ^{1}H (500 MHz), ^{13}C{^{1}H} (125 MHz), and ^{31}P{^{1}H} (202 MHz) NMR spectra were recorded using a Bruker Avance II 500 MHz spectrometer. Infrared spectra were obtained using a Nicolet FT-IR 330 spectrometer. Elemental analysis was performed using a Thermo Quest Italia SPA EA 1110 instrument. Commercial reagents were purchased from Aldrich, J&K, or Alfa-Aesar Chemical Co. and used as received. The compounds *o*-$Ph_2PC_6H_4NH_2$,[1] *o*-$Ph_2PC_6H_4NMe_2$,[2] $(PPh_3)_3RuCl_2$,[3] $(PPh_3)_3RuHCl$,[4] $(PPh_3)_3RuHCl(CO)$,[5] $(Ph_2P(CH_2)_2NH_2)_2RuCl_2$,[6] $(Ph_2P(CH_2)_3NH_2)_2RuCl_2$,[7] $(o\text{-}Ph_2PC_6H_4CH_2NH_2)_2RuCl_2$,[8] and $(PPh_3)(o\text{-}PPh_2C_6H_4NMe_2)RuCl_2$ (**8**)[9] were prepared according to the literature procedure.

Hydrogenation was performed in a 100 mL Parr stainless steel autoclave with a Teflon lining. Ru complex, THF solvent, ester substrate, and/or NaOMe, and *p*-xylene (50 μL) as an internal standard were charged into the lining in a glovebox. The autoclave was sealed and retrieved. Afterwards, the autoclave was purged through three successive cycles of pressurization/venting with H_2 (10 bar) by maintaining at ca. 5 °C in an ice-water bath. The autoclave was pressurized with H_2 (50 bar), closed, and placed in a temperature-controlled heating mantle. After the reaction was completed, the autoclave was quickly cooled to ca. 5 °C and vented. The solution was analyzed using GC (FULI company, 9790II) equipped with a KB-Wax column (60 m × 0.32 mm × 0.33 μm) after purification by going through a short, silica-filled column.

S2. Synthesis of Ruthenium(II) Complexes

[(PPh_3)(*o*-$Ph_2PC_6H_4NH_2$)$RuCl_2$]$_2$ (1) A mixture of $(PPh_3)_3RuCl_2$ (0.48 g, 0.5 mmol) and *o*-$Ph_2PC_6H_4NH_2$ (0.14 g, 0.5 mmol) in toluene (40 mL) was stirred and allowed to heat to 100 °C. After 12 h, the reaction mixture was cooled to room temperature; a large amount of orange solid of **1** was precipitated, collected, and washed with *n*-hexane (2 mL). Yield: 0.31 g for **1**·toluene, 87%. The solution NMR (^{1}H, ^{13}C{^{1}H}, and ^{31}P{^{1}H}) analysis showed two sets of the data, suggesting a partial dissociation into a monomeric (PPh_3)(*o*-$Ph_2PC_6H_4NH_2$)$RuCl_2$ (**1a**).[10] This suggestion is confirmed by low-temperature ^{31}P{^{1}H} NMR studies (see Fig. S8, *vide infra*). A clear assignment of the resonances for the phenyl ring protons and carbons of these two species is not possible. ^{1}H NMR (500 MHz, $CDCl_3$, 298 k, ppm): δ = 3.28 (d, $^2J_{HH}$ = 15.0 Hz, 2 H, NH_2, for **1**), 3.45 (d, $^2J_{HH}$ = 15.0 Hz, 2 H, NH_2, for **1a**), 6.67–6.74 (m), 6.88–7.38 (m), 7.49 (s), 7.51 (s), 7.59 (t, $^2J_{HH}$ = 10.0 Hz), 7.70 (t, $^2J_{HH}$ = 10.0 Hz), 7.94 (t, $^2J_{HH}$ = 10.0 Hz) (58 H, C_6H_4 and C_6H_5). ^{13}C{^{1}H} NMR (125 MHz, $CDCl_3$, 298 k, ppm): δ = 125.60 (d, J_{PC} = 5.3 Hz), 125.84 (d, J_{PC} = 5.1 Hz), 126.57 (d, J_{PC} = 9.0 Hz), 126.68 (d, J_{PC} = 9.9 Hz), 126.72 (J_{PC} = 9.6 Hz), 127.05, 127.10 (d, J_{PC} = 3.8 Hz), 127.17 (d, J_{PC} = 2.4 Hz), 127.25 (d, J_{PC} = 2.5 Hz), 128.24 (d, J_{PC} = 5.0 Hz), 128.61, 128.86, 129.94 (d, J_{PC} = 12.6 Hz), 132.40 (d, J_{PC} = 9.0 Hz), 132.59, 132.77 (d, J_{PC} = 9.1 Hz), 132.99, 133.15, 133.15, 133.27 (d, J_{PC} = 9.3 Hz), 133.45 (d, J_{PC} = 9.1 Hz), 133.72 (d, J_{PC} = 9.1 Hz), 134.45, 134.72 (d, J_{PC} = 17.8 Hz), 134.80 (d, J_{PC} = 9.1 Hz), 134.99, 135.13 (d, J_{PC} = 12.5 Hz), 135.47 (d, J_{PC} = 8.9 Hz), 136.19, 136.56, 151. 82, 151.96 (C_6H_4 and C_6H_5). ^{31}P{^{1}H} NMR (202 MHz, in $CDCl_3$, 298 k, ppm): δ = 57.46 (d, $^2J_{PP}$ = 36.4 Hz, for **1a**), 57.57 (d, $^2J_{PP}$ = 36.4 Hz, for **1**), 62.98 (d, $^2J_{PP}$ = 36.4 Hz, for **1**), 64.68 (d, $^2J_{PP}$ = 36.4 Hz, for **1a**). ^{31}P NMR (162 MHz, for solid state of **1**, 298 k, ppm): δ = 57.07 (br), 63.16 (br). IR (Nujol mull, KBr, cm^{-1}): ν = 3046, 3110, 3137, 3258 (NH_2). Anal. Calcd (%) for $Ru_2Cl_4C_{79}H_{70}N_2P_4$ (**1**·toluene, M_r = 1515.26): C 62.61, N 1.85, H 4.66; found: C 62.09, N 1.76, H 4.65. After the NMR data collection, the solution was top-layered with *n*-hexane (0.4 mL) and then kept at room temperature. Two days later, orange crystals of **1**·2 $CDCl_3$ were formed.

(*o*-$Ph_2PC_6H_4NH_2$)$_2RuCl_2$ (2) A mixture of $(PPh_3)_3RuCl_2$ (0.48 g, 0.5 mmol) and *o*-$PPh_2C_6H_4NH_2$ (0.28 g, 1.0 mmol) in toluene (40 mL) was stirred and allowed to heat to 100 °C. After 48 h, the reaction mixture was slowly cooled to room temperature; a large amount of green-yellow solid of **2** was precipitated, collected, and washed with *n*-hexane (2 mL). Yield: 0.33 g, 92%. ^{1}H NMR (500 MHz, $CDCl_3$, 298 k, ppm): δ = 3.23 (br, 2 H, NH_2), 5.89 (br, 2 H, NH_2), 6.16–7.65 (m), 7.85 (m), 8.16 (m) (28 H, C_6H_4 and C_6H_5). ^{13}C{^{1}H} NMR (125 MHz, $CDCl_3$, 298 k, ppm): δ = 125.28, 125.92 (d, J_{PC} = 3.9 Hz), 126.31 (d, J_{PC} = 5.5 Hz), 127.11 (d, J_{PC} = 9.6 Hz), 127.36 (d, J_{PC} = 9.3 Hz), 127.39 (d, J_{PC} = 9.9 Hz), 128.06 (d, J_{PC} = 8.9 Hz), 128.20, 128.31, 128.75, 128.99 (d, J_{PC} = 5.0 Hz), 130.26, 130.53, 131.29 (d, J_{PC} = 9.1 Hz), 131.62 (d, J_{PC} = 9.9 Hz), 132.17, 132.52, 132.73, 133.05, 133.14, 133.51, 133.86, 134.31 (d, J_{PC} = 9.1 Hz), 135.36, 135.67, 137.22, 137.58, 137.84, 148.89 (d, J_{PC} = 16.5 Hz), 151.95 (d, J_{PC} = 19.5 Hz) (C_6H_4 and C_6H_5). ^{31}P{^{1}H} NMR (202 MHz, $CDCl_3$, 298 k, ppm): δ = 60.22 (d, $^2J_{PP}$ = 34.1 Hz), 69.17 (d, $^2J_{PP}$ = 34.1 Hz). IR (Nujol mull, KBr, cm^{-1}): ν = 3041, 3112, 3158, 3289 (NH_2). Anal. Calcd (%) for $RuCl_2C_{36}H_{32}N_2P_2$ (M_r = 726.7): C 59.50, N 3.85, H 4.44; found: C 59.35, N 3.66, H 4.41. Yellow crystals of **2**·$CHCl_3$ were obtained by recrystallization in $CHCl_3$/*n*-hexane at –20 °C for 2 d.

[(*o*-$Ph_2PC_6H_4NH_2$)$_2$(*o*-$PPh_2C_6H_4NH$)Ru]$^+$Cl$^-$ (3) $(PPh_3)_3RuHCl$ (0.46 g, 0.5 mmol) and *o*-$Ph_2PC_6H_4NH_2$ (0.42 g, 1.5 mmol) were placed in a flask connected with a bubbler-equipped coiling

condenser and to it toluene (40 mL) was added. The mixture was stirred and allowed to heat to 100 °C. During the reaction, an evolution of H_2 gas was observed. After 24 h, the reaction mixture was cooled to room temperature; a large amount of orange solid of **3** was precipitated, collected, and washed with *n*-hexane (2 mL). Yield: 0.37 g for **3**·toluene, 77%. ^{1}H NMR (500 MHz, CD_2Cl_2, 298 k, ppm): δ = 3.11 (s, 1 H, N*H*), 3.34 (d, $^2J_{HH}$ = 12.5 Hz, 2 H, NH_2), 4.02 (d, $^2J_{HH}$ = 12.5 Hz, 2 H, NH_2), 6.00 (m), 6.08 (m), 8.28 (m), 6.41–7.76 (m), 8.19 (m), 8.28 (m) (42 H, C_6H_4 and C_6H_5). ^{13}C{^{1}H} NMR (125 MHz, CD_2Cl_2, 298 k, ppm): δ = 110.68, 113.27 (d, J_{PC} = 54.8 Hz), 117.15 (d, J_{PC} = 9.0 Hz), 126.43 (d, J_{PC} = 24.5 Hz), 126.88, 127.19, 127.91, 128.34 (d, J_{PC} = 7.9 Hz), 128.94, 129.23, 129.96 (d, J_{PC} = 54.5 Hz), 130.12 (d, J_{PC} = 44.4 Hz), 131.03, 131.57, 131.71, 132.16 (d, J_{PC} = 6.4 Hz), 132.23, 132.38 (d, J_{PC} = 5.6 Hz), 132.60, 132.93, 133.44 (d, J_{PC} = 55.3 Hz), 133.59 (d, J_{PC} = 6.8 Hz), 134.02 (d, J_{PC} = 10.3 Hz), 134.26 (d, J_{PC} = 8.5 Hz), 134.73, 135.62 (d, J_{PC} = 12.6 Hz), 147.83 (d, J_{PC} = 18.8 Hz), 148.18 (d, J_{PC} = 17.3 Hz), 149.47 (C_6H_4 and C_6H_5). ^{31}P{^{1}H} NMR (202 MHz, CD_2Cl_2, 298 k, ppm): δ = 55.02 (dd, $^2J_{PP}$ = 23.2, 22.8 Hz), 62.10 (t, $^2J_{PP}$ = 22.6 Hz), 63.02 (dd, $^2J_{PP}$ = 23.2, 22.6 Hz). IR (Nujol, mull, KBr, cm^{-1}): ν = 2911, 2962, 3048, 3261, 3284 (NH and NH_2). Anal. Calcd (%) for $RuClC_{54}H_{47}N_3P_3$ (**3**·toluene, M_r = 967.5): C 67.04, N 4.34, H 4.90; found: C 66.73, N 4.07, H 5.22.

$Ph_3P(\eta^2\text{-}H_2)Ru(\mu\text{-}H)(\mu\text{-}o\text{-}PPh_2C_6H_4NH)_2RuH(PPh_3)$ (4) At –75 °C, K[HB*s*Bu$_3$] (0.8 mmol, 0.8 mL 1 M THF solution) was added to a suspension of **1** (0.14 g, 0.2 mmol) in THF (10 mL). The mixture was stirred and warmed naturally to room temperature, during which a clear yellow solution was formed. After additional stirring for 9 h, the KCl salt was formed and filtered off. The filtrate was concentrated to ca. 1 mL, and to it *n*-hexane (5 mL) was added. A yellow precipitate of **4** was quickly formed, which was collected and washed with *n*-hexane (2 mL). Yield: 0.11 g for **4**·*n*-hexane, 85%. ^{1}H NMR (500 MHz, C_6D_6, 298 k, ppm): δ = –12.27 (m, 1 H, Ru-μ-*H*), –8.38 (br, 2 H, Ru-η^2-H_2), –8.22 (m, 1 H, Ru*H*), 2.58 (br, 1 H, N*H*), 4.46 (br, 1 H, N*H*), 5.92 (br), 6.45–7.50 (m), 7.97 (m), 8.04(m) (58 H, C_6H_4 and C_6H_5). ^{13}C{^{1}H} NMR (125 MHz, C_6D_6, 298 k, ppm): δ = 120.41 (d, J_{PC} = 5.0 Hz), 121.22 (d, J_{PC} = 8.8 Hz), 121.93 (d, J_{PC} = 5.0 Hz), 127.02, 127.10, 127.06 (d, J_{PC} = 27.5 Hz), 125.58 (d, J_{PC} = 8.8 Hz), 129.98, 130.68, 131.18 (d, J_{PC} = 10.0 Hz), 132.23 (d, J_{PC} = 11.3 Hz), 132.30 (d, J_{PC} = 7.5 Hz), 132.89, 133.60 (d, J_{PC} = 11.3 Hz), 134.38 (d, J_{PC} = 11.3 Hz), 134.55, 136.90 (d, J_{PC} = 36.3 Hz), 138.55 (d, J_{PC} = 31.3 Hz), 141.20 (d, J_{PC} = 32.5 Hz), 141.39 (d, J_{PC} = 32.5 Hz), 141.58 (d, J_{PC} = 37.5 Hz) (C_6H_4 and C_6H_5). ^{31}P{^{1}H} NMR (202 MHz, C_6D_6, 298 k, ppm): δ = 59.01 (m), 69.60 (d, $^2J_{PP}$ = 12.3 Hz), 71.94 (d, $^2J_{PP}$ = 29.9 Hz), 80.47 (d, $^2J_{PP}$ = 29.9 Hz). IR (Nujol mull, KBr, cm^{-1}): ν = 3041, 3112, 3158, 3289 (NH), 2113, 1956, 1901 (RuH). Anal. Calcd (%) for $RuCl_2C_{36}H_{32}N_2P_2$ (**4**·*n*-hexane, M_r = 726.7): C 67.38, N 2.18, H 5.04; found: C 66.92, N 2.32, H 4.87. After the NMR data collection, the solution was top-layered with *n*-hexane (0.4 mL) and kept at room temperature. Two days later, yellow crystals of **4**·2.5 C_6D_6 were formed.

(o-$Ph_2PC_6H_4NH_2$)(o-$PPh_2C_6H_4NH$)RuCl(CO) (5) $(PPh_3)_3RuHCl(CO)$ (0.48 g, 0.5 mmol) and *o*-$Ph_2PC_6H_4NH_2$ (0.28 g, 1.0 mmol) were placed in a flask connected with a bubbler-equipped coiling condenser, and to it toluene (40 mL) was added. The mixture was stirred and allowed to heat to 100 °C. During the reaction, an evolution of H_2 gas was observed. After 12 h, the reaction mixture was cooled to room temperature; a large amount of yellow solid of **5** was precipitated, collected, and washed with *n*-hexane (2 mL). Yield: 0.31 g, 86%. Compound **5** is insoluble in organic solvent, and the solution NMR data was not obtained. ^{31}P NMR (162 MHz, in solid, 298 k, ppm): δ = 56.97 (br), 64.20 (br). IR (Nujol mull, KBr, cm^{-1}): ν = 1933 (CO), 3048, 3308 (NH and NH_2). Anal. Calcd (%) for $RuClC_{37}H_{31}N_2P_2O$ (M_r = 718.1): C 61.88, N 3.90, H 4.31; found: C 61.89, N 3.62, H 4.14. Yellow

crystals of **5** were formed from an NMR-tube reaction of $RuHCl(CO)(PPh_3)_3$ and 2 equivalents of *o*-$Ph_2PC_6H_4NH_2$ in toluene at 100 °C for 24 h without any stirring.

(*o*-$Ph_2PC_6H_4NH_2$)(*o*-$PPh_2C_6H_4NH$)RuH(CO) (6) and [(*o*-$PPh_2C_6H_4NH)_2Ru(CO)]_2$ (7) At –75 °C, K[HB*s*Bu_3] (0.05 mmol, 0.05 mL 1 M THF solution) was added to a suspension of **5** (0.036 g, 0.05 mmol) in THF (10 mL). The mixture was stirred and warmed naturally to room temperature. After additional stirring for 12 h, the KCl salt was formed and filtered off. All the volatiles were removed under reduced pressure, and the residue was washed with *n*-hexane (2 mL) to give a yellow solid. The ^1H and ^{31}P NMR analysis showed two sets of the data, indicative of a mixture of **6** and **7**. By heat treatment of this mixture in toluene (10 mL) at 70 °C for 5 h pure compound **7** was obtained as a yellow solid after removal of all volatiles. Yield: 0.024 g for **7**·1.5 *n*-hexane, 73%. ^1H NMR (500 MHz, $CDCl_3$, 298 k, ppm): δ = 2.25 (br, 1 H, N*H*), 2.55 (br, 1 H, N*H*), 4.40 (br, 1 H, N*H*), 5.40 (m, 1 H, N*H*), 5.97 (m), 6.07 (m), 6.32–7.41 (m), 8.05 (m), 8.26 (m) (56 H, C_6H_4 and C_6H_5). $^{13}C\{^1H\}$ NMR (125 MHz, $CDCl_3$, 298 k, ppm): δ = 108.54 (d, J_{PC} = 5.2 Hz), 109.24 (d, J_{PC} = 7.8 Hz), 115.83 (d, J_{PC} = 7.1 Hz), 116.65 (d, J_{PC} = 12.3 Hz), 118.82 (d, J_{PC} = 6.1 Hz), 122.59 (d, J_{PC} = 6.9 Hz), 125.00 (d, J_{PC} = 12.0 Hz), 126.08 (d, J_{PC} = 11.6 Hz), 127.26, 127.36 (d, J_{PC} = 4.3 Hz), 127.45, 127.54 (d, J_{PC} = 3.8 Hz), 127.64, 127.81, 127.92 (d, J_{PC} = 9.8 Hz), 128.34 (d, J_{PC} = 9.4 Hz), 128.60 (d, J_{PC} = 17.1 Hz), 128.75 (d, J_{PC} = 21.5 Hz), 128.86 (d, J_{PC} = 23.0 Hz), 129.05 (d, J_{PC} = 8.9 Hz), 129.30, 130.10, 130.72, 130.94 (d, J_{PC} = 10.0 Hz), 131.09, 131.51, 131.70 (d, J_{PC} = 10.0 Hz), 136.83, 137.26, 137.38, 137.71, 138.16 (d, J_{PC} = 9.9 Hz), 138.38, 138.61 (d, J_{PC} = 7.3 Hz), 162.90 (d, J_{PC} = 15.4 Hz) (C_6H_4 and C_6H_5), 167.76 (d, J_{PC} = 29.0 Hz), 168.70 (d, J_{PC} = 22.4 Hz) (*C*O). $^{31}P\{^1H\}$ NMR (202 MHz, $CDCl_3$, 298 k, ppm): δ = 53.25 (d, $^2J_{PP}$ = 20.2 Hz), 55.20 (d, $^2J_{PP}$ = 20.2 Hz), 58.48 (d, $^2J_{PP}$ = 18.2 Hz), 59.65 (d, $^2J_{PP}$ = 18.2 Hz). IR (Nujol mull, KBr, cm^{-1}): ν = 1905 (CO), 2916, 2958, 2999, 3041 (NH). Anal. Calcd (%) for $Ru_2C_{74}H_{60}N_4P_4O_2$ (**7**·1.5 *n*-hexane, M_r = 1363.4): C 65.04, N 4.10, H 4.39; found: C 64.32, N 4.06, H 4.51. Yellow crystals of **7**·2.5 toluene were obtained by recrystallization in toluene/*n*-hexane at –20 °C for 4 d.

Reaction of 7 and H_2 to 6 In an NMR tube was added **7** (6 mg, 4.3 μmol) followed by 0.5 mL C_6D_6. The atmosphere inside the tube was quickly exchanged from Ar into H_2. The tube was kept at 10 °C with occasionally shaking. The ^1H and $^{31}P\{^1H\}$ NMR spectra were recorded. After ca. 56 h, the ^1H and $^{31}P\{^1H\}$ NMR data indicated a complete conversion of **7** into **6**. ^1H NMR (500 MHz, C_6D_6, 298 k, ppm): δ = -12.14 (t, $^2J_{HH}$ = 20.0 Hz, 1 H, Ru*H*), 2.77 (br, 1 H, N*H*), 3.21 (br, 2 H, NH_2), 6.09–7.25 (m), 7.80 (m), 8.20 (br) (28 H, C_6H_4 and C_6H_5). $^{31}P\{^1H\}$ NMR (202 MHz, C_6D_6, 298 k, ppm): δ = 53.2 (d, $^2J_{PP}$ = 263.0 Hz), 64.0 (d, $^2J_{PP}$ = 263.0 Hz). The $^{13}C\{^1H\}$ NMR data acquired was not clear probably because of a low concentration. IR (Nujol mull, KBr, cm^{-1}): ν = 3056, 2962, 2919, 2844 (NH), 2190 (RuH), 1897 (CO). Yellow crystals of **6** were obtained by exposing an NMR-tube THF/*n*-hexane solution of **7** to H_2 at 10 °C for 2 d.

Reaction of 7 and D_2 The reaction of **7** and D_2 was treated in a similar manner to that of **7** and H_2. The related ^1H and $^{31}P\{^1H\}$ NMR spectra were recorded to witness a processing of the reaction (see S9, *vide infra*).

(*o*-$PPh_2C_6H_4NMe_2)_2RuCl_2$ (9) A mixture of $(PPh_3)_3RuCl_2$ (0.29 g, 0.3 mmol) and *o*-$PPh_2C_6H_4NMe_2$ (0.23 g, 0.75 mmol) in toluene (40 mL) was stirred and allowed to heat to 100 °C. After 48 h, the reaction mixture was cooled to room temperature. By concentration (to ca. 1 mL), *n*-hexane (5 mL) was added to it; a large amount of brown-green solid was precipitated. The solid was collected and

subjected to recrystallization in THF/*n*-hexane (5 mL/2 mL) solvent mixture, giving brown crystals of **9** after 3 d at 10 °C. Yield: 0.16 g, 68%. ^{1}H NMR (500 MHz, $CDCl_3$, 298 k, ppm): δ = 3.25 (s, 12 H, NMe_2), 7.04-7.19 (m), 7.26 (m), 7.46 (m), 7.76 (d, $^{2}J_{HH}$ = 10.0 Hz) (28 H, C_6H_4 and C_6H_5). ^{13}C{^{1}H} NMR (125 MHz, $CDCl_3$, 298 k, ppm): δ = 53.68 (CH_3), 121.07 (d, J_{PC} = 5.0 Hz), 121.11 (d, J_{PC} = 5.0 Hz), 125.58 (d, J_{PC} = 2.5 Hz), 126.98 (d, J_{PC} = 5.0 Hz), 127.02 (d, J_{PC} = 5.0 Hz), 129.09, 131.08, 133.21, 134.72 (d, J_{PC} = 5.0 Hz), 134.76 (d, J_{PC} = 5.0 Hz), 134.83, 135.03 (d, J_{PC} = 2.5 Hz), 135.21, 136.27, 136.44, 136.61, 161.72 (d, J_{PC} = 6.5 Hz), 161.76 (d, J_{PC} = 6.5 Hz) (C_6H_4 and C_6H_5). ^{31}P{^{1}H} NMR (202 MHz, $CDCl_3$, 298 k, ppm): δ = 59.03. Anal. Calcd (%) for $RuCl_2C_{40}H_{40}N_2P_2$ (M_r = 782.7): C 61.33, N 3.56, H 5.11; found: C 61.23, N 3.40, H 5.69.

S3. X-Ray Crystallographic Analysis and Structure

I. X-ray Crystallographic Analysis

Crystallographic data for crystals of **1**·2 $CDCl_3$, **2**·$CHCl_3$, **4**·2.5 C_6D_6, **5**, **6**, and **7**·2.5 toluene were collected on an Oxford Gemini S Ultra system. During measurement a Cu-K_α radiation (λ = 1.54178 Å) was used for **1**·2 $CDCl_3$ and **2**·$CHCl_3$ and a graphite-monochromatic Mo-K_α radiation (λ = 0.71073 Å) for **4**·2.5 C_6D_6, **5**, **6**, and **7**·2.5 toluene. Absorption correction was applied using the spherical harmonics program (multi-scan type). All structures of the crystals were solved by direct methods (SHELXS-96)[11] and refined against F^2 using SHELXL-97 program.[12] In general, the non-hydrogen atoms were located from different Fourier synthesis and refined anisotropically, and hydrogen atoms were included using a riding model with U_{iso} tied to the U_{iso} of the parent atoms unless otherwise specified. In **1**·2 $CDCl_3$, one half moiety of **1** was disclosed and the whole molecule was obtained by symmetric operation. The NH_2 protons in **1** were located from different Fourier synthesis. In **2**·$CHCl_3$, the NH_2 protons were located from different Fourier synthesis. The $CHCl_3$ were disordered and treated in two parts with the respective occupations refined into 0.7829 and 0.2171. In **4**·2.5 C_6D_6, the C(56) atom was refined isotropically as the U_{eq}(max)/U_{eq}(min) value of this atom appeared at the A alert level once refined anisotropically even by means of the ShelX restraining. The H atoms at the respective Ru and N atoms were located from different Fourier synthesis. In **5**, the NH_2 protons were located from the different Fourier synthesis. In **6**, the H atoms at the respective Ru and N atoms were located from different Fourier synthesis. In **7**·2.5 toluene, the H(1) at N(1) and H(3) at N(3) were located by different Fourier synthesis. One toluene molecule was seriously disordered and the H atoms were not able to be included. Cell parameters, data collection, and structure solution and refinement are given in Tables S1 and S2.

II. Crystal Data Collection and Structural Refinement Details

Table S1 For compounds **1**·2 $CDCl_3$, **2**·$CHCl_3$, and **4**·2.5 C_6D_6.[a]

	1·2 $CDCl_3$	**2**·$CHCl_3$	**4**·2.5 C_6D_6
formula	$C_{74}H_{62}Cl_{10}N_2P_4Ru_2$[b]	$C_{37}H_{33}Cl_5N_2P_2Ru$	$C_{87}H_{79}N_2P_4Ru_2$[b]
fw	1661.79	845.91	1478.54
cryst syst	Monoclinic	Triclinic	Monoclinic
space group	*C*2/*c*	*P*–1	*P*2(1)/*n*
a/Å	28.1421(11)	10.9600(5)	18.146(3)
b/Å	15.5660(5)	12.5092(5)	23.863(2)
c/Å	16.7390(9)	14.3745(7)	18.672(2)
α/deg		77.162(4)	
β/deg	105.027(5)	70.923(4)	117.597(17)
γ/deg		87.593(4)	
V/Å^3	7081.9(5)	1814.96(14)	7165.2(15)
Z	4	2	4
ρ_{calcd}/g·cm^{-3}	1.557	1.548	1.371
μ/mm^{-1}	8.131	7.951	0.559
F(000)	3360	856	3052
crystal size/mm^3	0.20 × 0.05 × 0.05	0.30 × 0.30 × 0.10	0.40 × 0.10 × 0.05
θ range/deg	3.27–62.07	3.34–65.60	2.87–25.00
index ranges	$-32 \le h \le 23$ $-17 \le k \le 15$ $-19 \le l \le 19$	$-10 \le h \le 12$ $-14 \le k \le 14$ $-12 \le l \le 16$	$-21 \le h \le 21$ $-25 \le k \le 28$ $-22 \le l \le 22$
collected data	11208	11400	35010
unique data	5517 (R_{int} = 0.0324)	6063 (R_{int} = 0.0209)	12600 (R_{int} = 0.1611)
completeness to *θ* (%)	98.5	97.1	99.8
data/restraints/params	5517/186/461	6063/141/472	12600/225/869
GOF on F^2	1.031	1.030	0.914
final *R* indices [$I > 2(I)$]	R_1 = 0.0384 wR_2 = 0.0947	R_1 = 0.0360 wR_2 = 0.0949	R_1 = 0.0813 wR_2 = 0.1076
R indices (all data)	R_1 = 0.0498 wR_2 = 0.1010	R_1 = 0.0369 wR_2 = 0.0957	R_1 = 0.1663 wR_2 = 0.1325
Largest diff peak/hole (e·Å^{-3})	0.968/–0.677	1.904/–1.531	0.688/–0.687

[a] All data were collected at 173(2) K. $R_1 = \sum(||F_o| - |F_c||)/\sum|F_o|$, $wR_2 = [\sum w(F_o^2 - F_c^2)^2/\sum w(F_o^2)]^{1/2}$, GOF = $[\sum w(F_o^2 - F_c^2)^2/(N_o - N_p)]^{1/2}$. [b] In the structural analysis, only H atom rather D atom was able to be included.

Table S2 For compounds **5, 6**, and **7**·2.5 toluene. [a]

	5	**6**	**7**·2.5 toluene
formula	$C_{37}H_{31}ClN_2OP_2Ru$	$C_{37}H_{32}N_2OP_2Ru$	$C_{91.50}H_{80}N_4O_2P_4Ru_2$
fw	718.10	683.66	1593.62
cryst syst	Monoclinic	Triclinic	Monoclinic
space group	*P*2(1)/*n*	*P*–1	*P*2(1)/*n*
a/Å	9.6626(2)	9.4756(5)	14.0553(4)
b/Å	18.7669(3)	12.3693(6)	21.4168(6)
c/Å	17.4652(3)	15.0544(8)	25.5830(7)
α/deg		102.681(4)	
β/deg	92.018(2)	104.014(5)	99.946(2)
γ/deg		106.027(5)	
V/Å^3	3165.12(10)	1565.89(14)	7585.2(4)
Z	4	2	4
ρ_{calcd}/g·cm^{-3}	1.507	1.450	1.395
μ/mm^{-1}	0.715	0.636	0.536
F(000)	1464	700	3284
crystal size/mm^3	0.25 × 0.20 × 0.15	0.40 × 0.20 × 0.10	0.20 × 0.10 × 0.10
θ range/deg	3.03–26.00	3.43–26.00	3.07–26.00
index ranges	$-7 \le h \le 11$ $-23 \le k \le 21$ $-20 \le l \le 21$	$-11 \le h \le 10$ $-14 \le k \le 15$ $-18 \le l \le 16$	$-17 \le h \le 17$ $-26 \le k \le 25$ $-31 \le l \le 31$
collected data	13584	12060	40417
unique data	6060 (R_{int} = 0.0271)	6152 (R_{int} = 0.0314)	14900 (R_{int} = 0.0725)
completeness to *θ* (%)	97.6	99.7	99.8
data/restraints/params	6060/0/405	6152/0/392	14900/1285/1065
GOF on F^2	1.070	1.070	1.027
final *R* indices [*I*>2 (*I*)]	R_1 = 0.0305 wR_2 = 0.0619	R_1 = 0.0315 wR_2 = 0.0739	R_1 = 0.0580 wR_2 = 0.1009
R indices (all data)	R_1 = 0.0385 wR_2 = 0.0643	R_1 = 0.0398 wR_2 = 0.0780	R_1 = 0.0924 wR_2 = 0.1114
Largest diff peak/hole (e·Å^{-3})	0.350/–0.354	0.759/–0.415	0.719/–0.651

[a] All data were collected at 173(2) K. $R_1 = \sum(||F_o| - |F_c||)/\sum|F_o|$, $wR_2 = [\sum w(F_o^2 - F_c^2)^2/\sum w(F_o^2)]^{1/2}$, GOF $= [\sum w(F_o^2 - F_c^2)^2/(N_o - N_p)]^{1/2}$.

III. X-Ray Crystal Structure

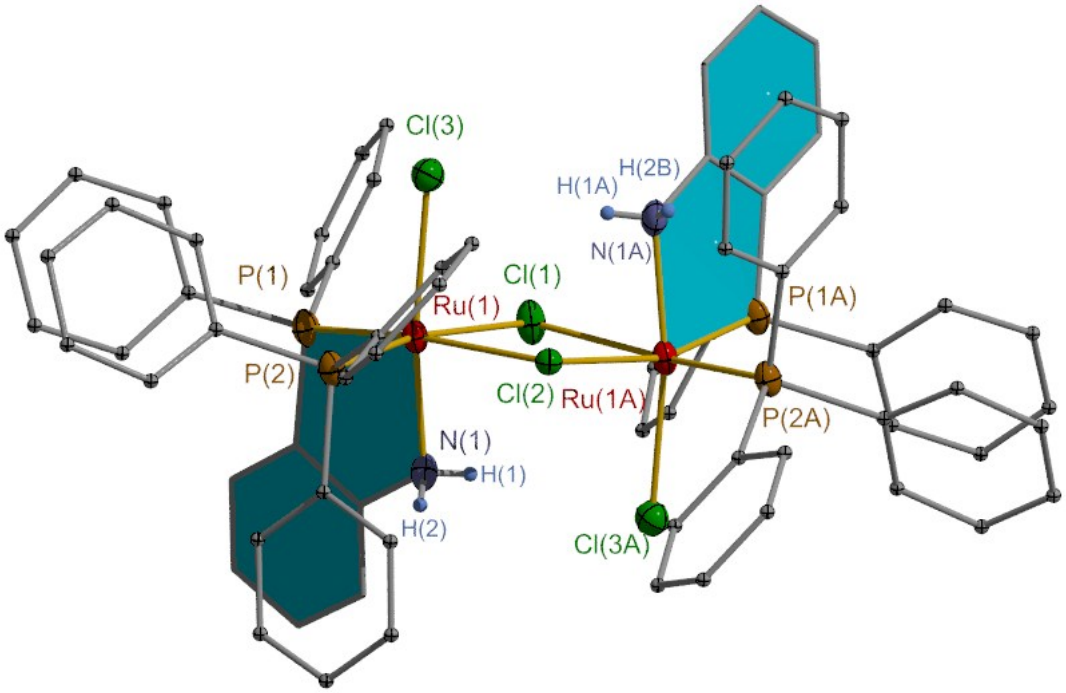

Fig. S1 X-ray crystal structure of **1** with the aryl ring H atoms omitted for clarity. Selected bond lengths [Å] and angles [°]: Ru(1)–P(1) 2.245(1), Ru(1)–P(2) 2.274(1), Ru(1)–N(1) 2.107(4), Ru(1)−Cl(1) 2.500(1), Ru(1)−Cl(2) 2.459(1), Ru(1)−Cl(3) 2.443(1); P(1)–Ru(1)–N(1) 84.40(11). Symmetry code (A): –x+1, y, –z+1/2.

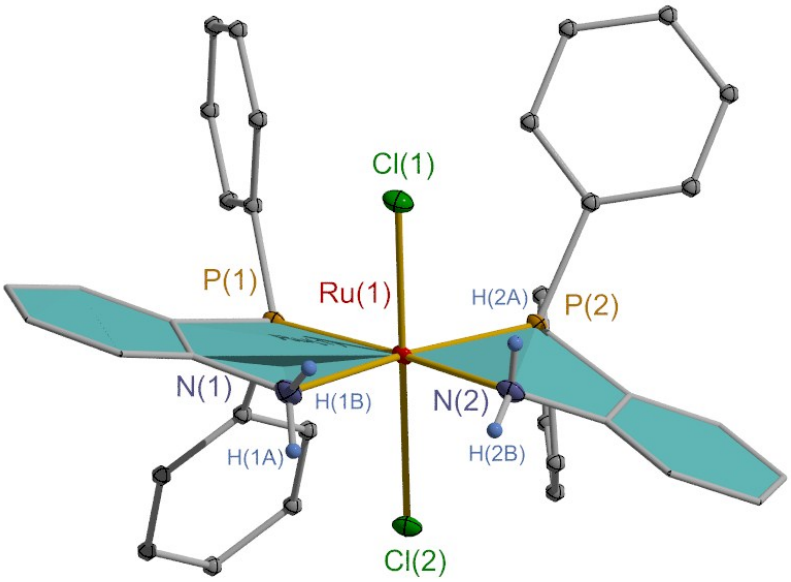

Fig. S2 X-ray crystal structure of **2** with the aryl ring H atoms omitted for clarity. Selected bond lengths [Å] and angles [°]: Ru(1)–P(1) 2.2608(8), Ru(1)–P(2) 2.2483(8), Ru(1)–N(1) 2.172(3),

Ru(1)−N(2) 2.166(3), Ru(1)−Cl(1) 2.3923(8), Ru(1)−Cl(2) 2.4314(7); P(1)–Ru(1)–N(1) 82.83(8), P(2)–Ru(1)–N(2) 81.57(8).

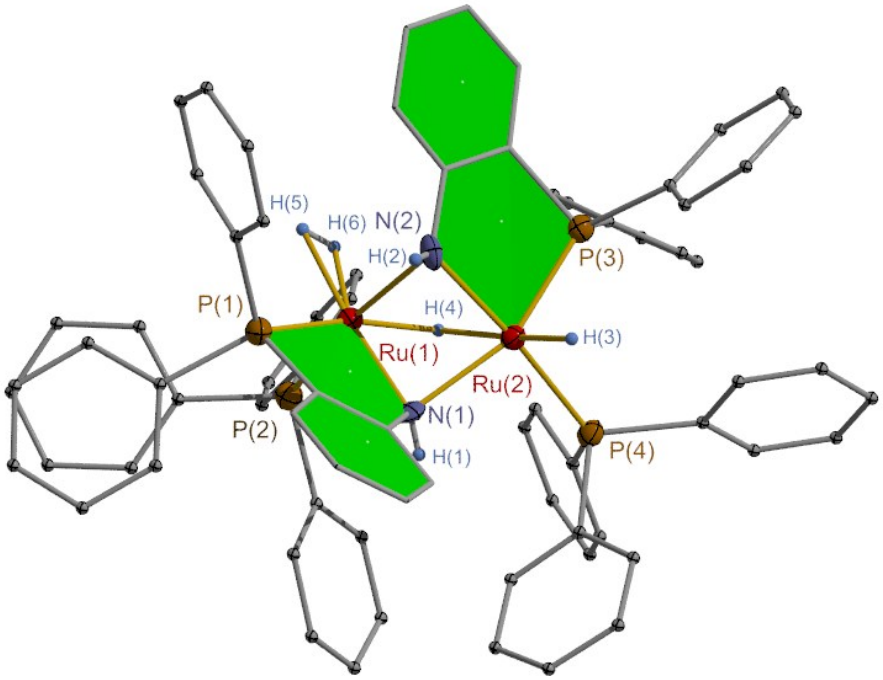

Fig. S3 X-ray crystal structure of **4** with the aryl ring H atoms omitted for clarity. Selected bond lengths [Å] and angles [°]: Ru(1)–P(1) 2.318(2), Ru(1)–P(2) 2.279(2), Ru(1)–N(1) 2.087(7), Ru(1)−N(2) 2.183(7), Ru(1)−H(4) 1.71(5), Ru(1)−H(5) 1.58(7), Ru(1)−H(6) 1.77(7) (Ru(1)···$H_{2(centroid)}$ 1.67(7)), H(5)−H(6) 0.722, Ru(2)–P(3) 2.211(2), Ru(2)–P(4) 2.260(2), Ru(2)–N(1) 2.177(7), Ru(2)−N(2) 2.117(6), Ru(2)−H(4) 1.83(6), Ru(2)−H(3) 1.65(6); P(1)–Ru(1)–N(1) 82.90(18), P(3)–Ru(2)–N(2) 83.95(18).

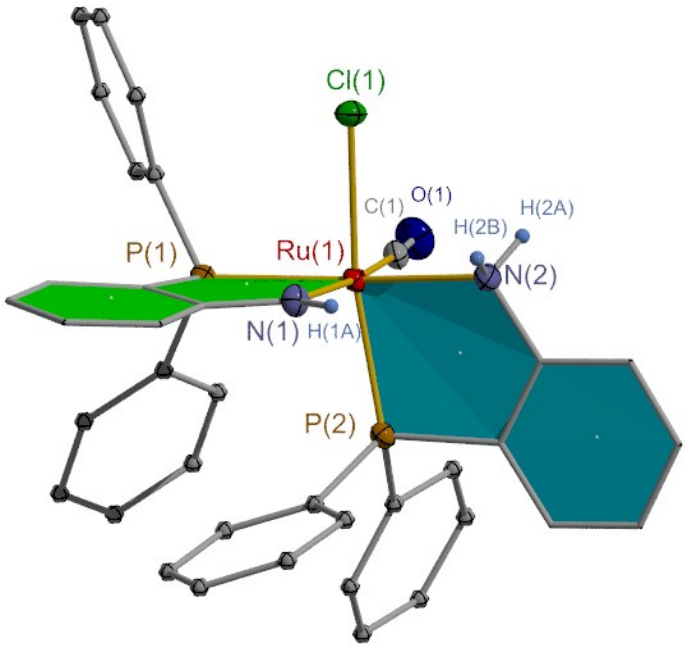

Fig. S4 X-ray crystal structure of **5** with the aryl ring H atoms omitted for clarity. Selected bond lengths [Å] and angles [°]: Ru(1)–P(1) 2.300(1), Ru(1)–P(2) 2.288(1), Ru(1)–N(1) 2.089(2), Ru(1)−N(2) 2.176(2), Ru(1)−C(1) 1.865(2), C(1)−O(1) 1.152(3), Ru(1)−Cl(1) 2.457(1); P(1)–Ru(1)–N(1) 81.68(6), P(2)–Ru(1)–N(2) 82.53(6).

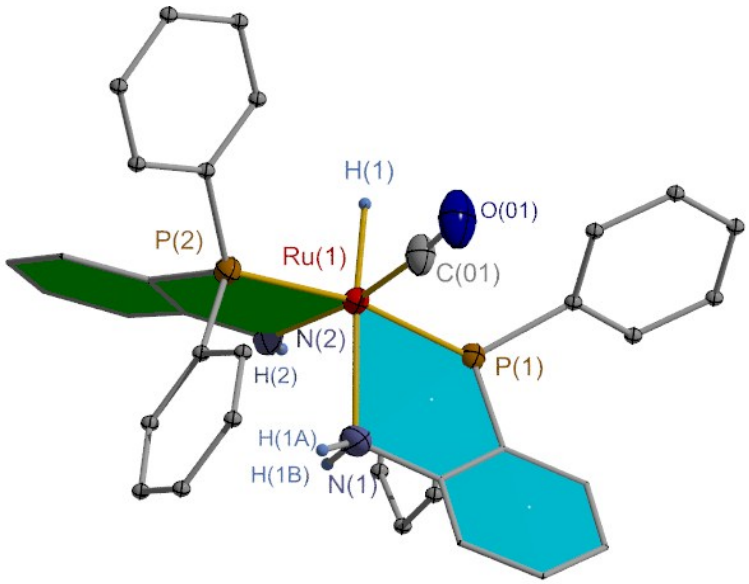

Fig. S5 X-ray crystal structure of **6** with the aryl ring H atoms omitted for clarity. Selected bond lengths [Å] and angles [°]: Ru(1)–P(1) 2.331(1), Ru(1)–P(2) 2.294(1), Ru(1)–N(1) 2.276(2), Ru(1)−N(2) 2.111(2), Ru(1)−C(01) 1.834(3), C(01)−O(01) 1.171(3), Ru(1)−H(1) 1.67(2); P(1)–Ru(1)–N(1) 77.71(6), P(2)–Ru(1)–N(2) 79.74(6).

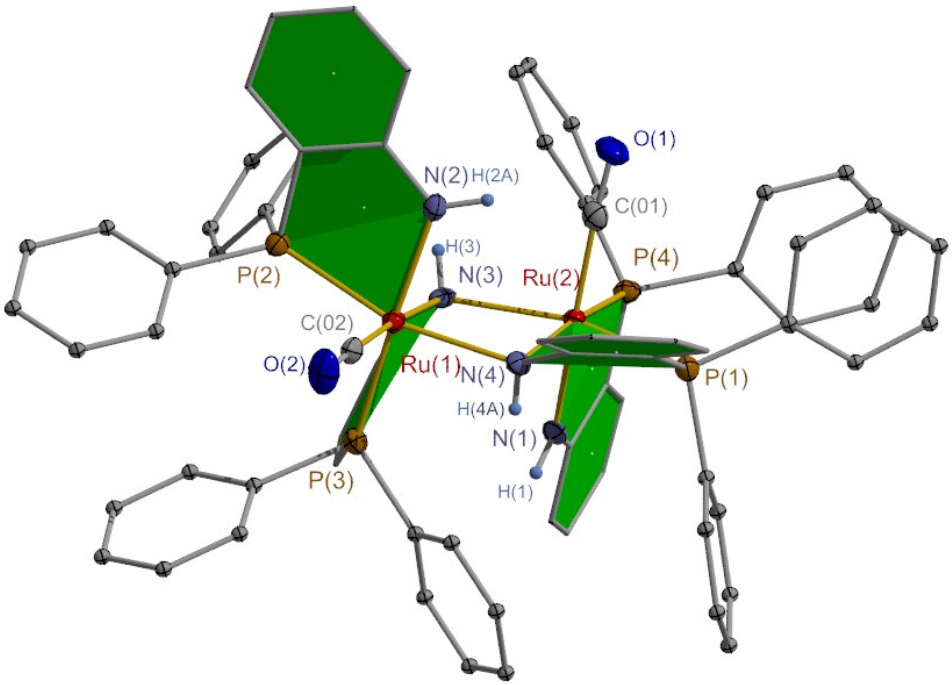

Fig. S6 X-ray crystal structure of **7** with the aryl ring H atoms omitted for clarity. Selected bond lengths [Å] and angles [°]: Ru(1)–P(2) 2.334(1), Ru(1)–P(3) 2.302(1), Ru(1)–N(1) 2.176(3), Ru(1)−N(2) 2.085(3), Ru(1)−N(3) 2.170(4), Ru(1)−C(02) 1.837(5), C(02)−O(2) 1.166(5), Ru(2)–P(1) 2.287(1), Ru(1)–P(4) 2.312(1), Ru(2)–N(1) 2.158(4), Ru(2)−N(3) 2.241(3), Ru(2)−N(4) 2.082(3), Ru(2)−C(01) 1.856(4), C(01)−O(1) 1.164(4); P(2)–Ru(1)–N(2) 80.04(10), P(3)–Ru(1)–N(3) 81.37(9), P(1)–Ru(2)–N(1) 80.16(9), P(4)–Ru(1)–N(4) 81.12(10).

S4. Table of Summarized Important Bond Parameters

Table S3 Summarized Ru–P, Ru–N, and Ru–H bond lengths (Å) for compounds **1**–**2** and **4**–**7**.

Comp.	Ru–P	Ru–N			Ru–H		
		$Ru–N_{NH2}$	$Ru–N_{NH}$	Ru-μ–N_{NH}	Ru–H	Ru-μ–H	Ru–η^2-H_{H2}
1	2.245(1)[c]	2.107(4)					
	2.274(1)[b]						
2	2.2608(8),	2.172(3)					
	2.2483(8)[c]	2.166(3)					
4	2.279(2), 2.260(2)[b]			2.087(7), 2.183(7)	1.65(6)	1.71(5)	1.58(7)[a]
	2.211(2), 2.318(2)[d]			2.177(7), 2.117(6)		1.83(6)	1.77(7)[a]
5	2.288(1)[c]	2.176(2)	2.089(2)				
	2.300(1)[d]						
6	2.331(1)[c]	2.276(2)	2.111(2)		1.67(2)		
	2.294(1)[d]						
7	2.287(1), 2.312(1)[c]		2.082(3)	2.176(3), 2.158(4)			
	2.334(1), 2.302(1)[d]		2.085(3)	2.170(4), 2.241(3)			

[a] $Ru\cdots H_{2(centroid)}$: 1.67(7). [b] $Ru–P_{PPh3}$. [c] $Ru–P_{o\text{-}PPh2C6H4NH2}$. [d] $Ru–P_{o\text{-}PPh2C6H4NH}$.

The coordination geometric bond parameters around the Ru centers of **1**–**2** and **4**–**7** are listed in Table S3. The Ru–P bond lengths for $Ru–P_{PPh3}$ (2.260(2)–2.279(2) Å), $Ru–P_{o\text{-}PPh2C6H4NH2}$ (2.287(1)–2.331(1) Å), and $Ru–P_{o\text{-}PPh2C6H4NH}$ (2.211(2)–2.334(1) Å) are comparable. The Ru–N bond lengths can be divided into three groups. Generally, the $Ru–N_{o\text{-}PPh2C6H4NH2}$ bond lengths (av. 2.170 Å) are longer by ca. 0.08 Å than those of the $Ru–N_{o\text{-}PPh2C6H4NH}$ bond (av. 2.092 Å). The latter bond is thought to have a double bond character with respect to location of a lone pair of electrons at the N atom into an unoccupied orbitals of the Ru atom.[13] The Ru-μ–$N_{o\text{-}PPh2C6H4NH}$ bond lengths (av. 2.164 Å) are close to those of the former one due to a bridged bonding character.

S5. Temperature-dependent Solution $^{31}P\{^{1}H\}$ NMR Study of Complex 1

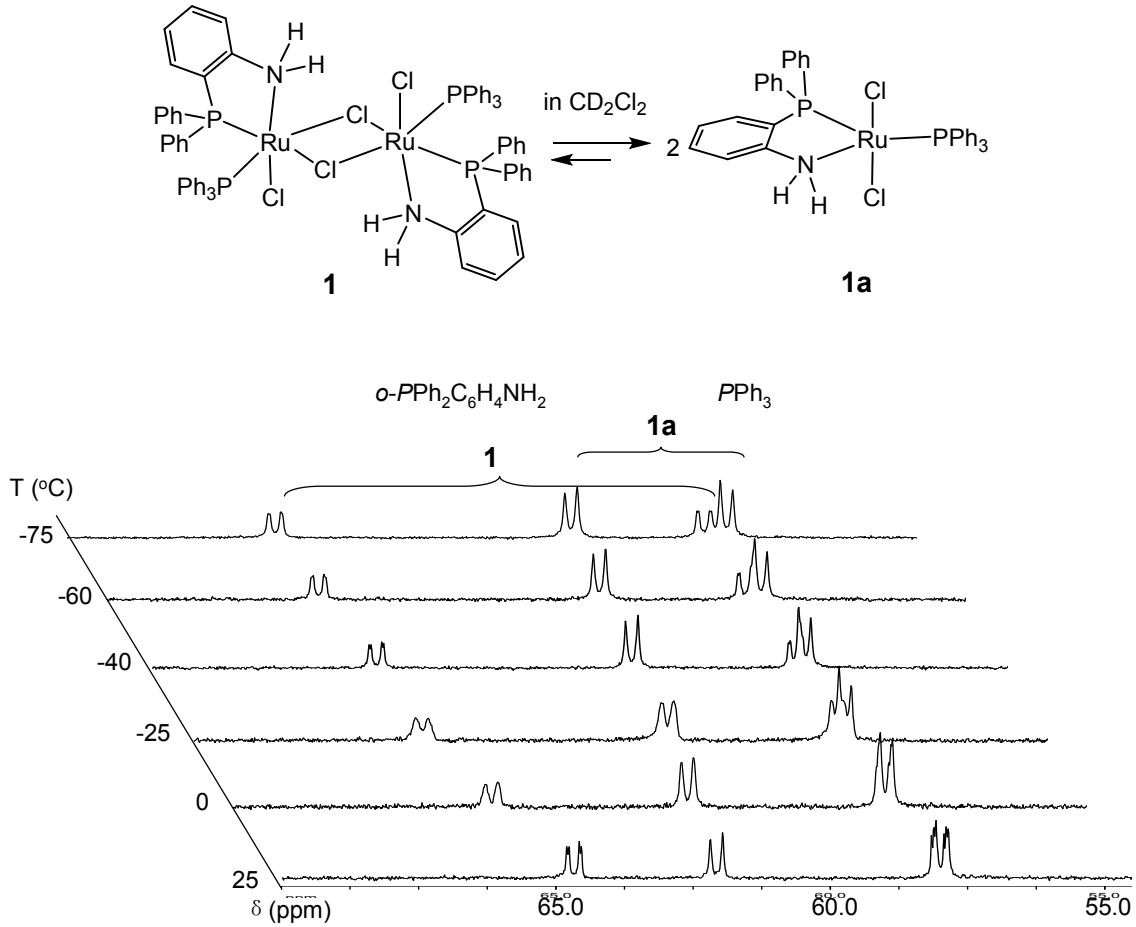

Fig. S7 Variable temperature (25 – –75 °C) $^{13}P\{^{1}H\}$ NMR spectroscopic studies of **1** recorded in CD_2Cl_2.

Liu and coworkers have reported on synthesis of compound (PPh_3)(o-$PPh_2C_6H_4NH_2)RuCl_2$ (**1a**) as a dark-green solid by refluxing a THF solution of $(PPh_3)_3RuCl_2$ and one equivalent o-$PPh_2C_6H_4NH_2$ for 6 h. They obtained a complicated NMR data for this compound probably due to isomeric structures formed with respect to different arrangements for the two Cl^- and one PPh_3 at the Ru towards the C_2NPRu chelate ring in steric.[10] We have proved a solid state dimer structure of **1**. The solid state ^{31}P NMR spectrum gave two broad resonances (57.07 and 63.16 ppm). The solution NMR (^{1}H, $^{13}C\{^{1}H\}$, $^{31}P\{^{1}H\}$ and ^{31}P) spectrum, however, appeared to exhibit two sets of the resonance data. We then performed the variable temperature (25 – –75 °C) $^{13}P\{^{1}H\}$ NMR study and observed a clear splitting of the two sets of the phosphorus resonances. Therefore, we thought that in solution **1** might partially dissociate into **1a** and an equilibrium between **1** and **1a** was then maintained.

S6. The ^{1}H and $^{31}P\{^{1}H\}$ NMR Studies of Reaction of Complex 7 with H_2

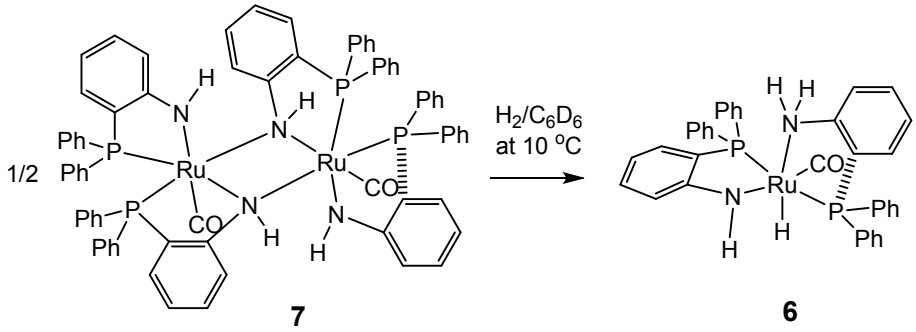

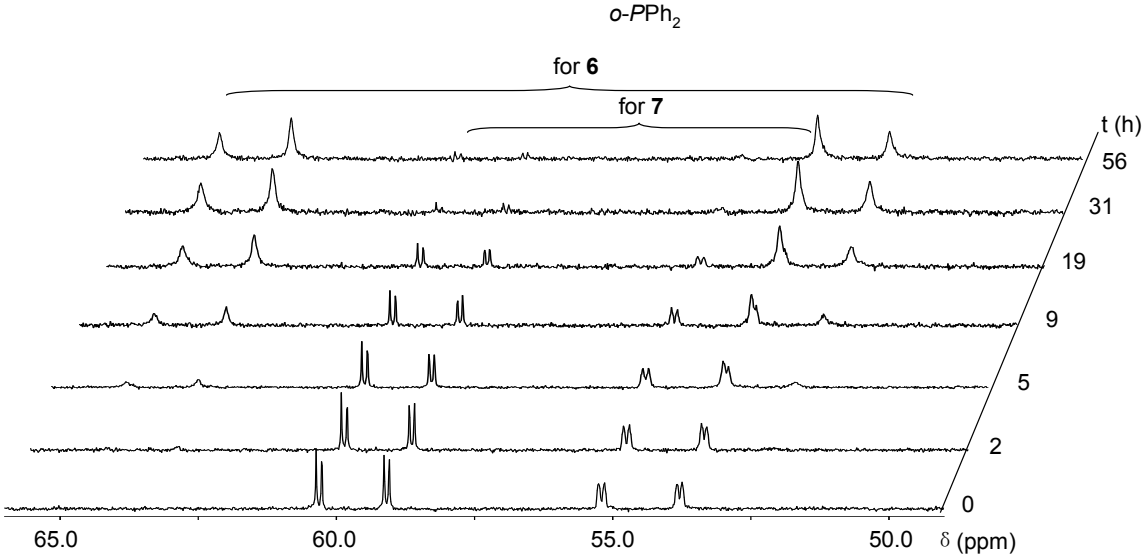

Fig. S8 The $^{13}P\{^{1}H\}$ NMR kinetic studies of reaction of **7** with H_2 to **6** in C_6D_6 at 10 °C.

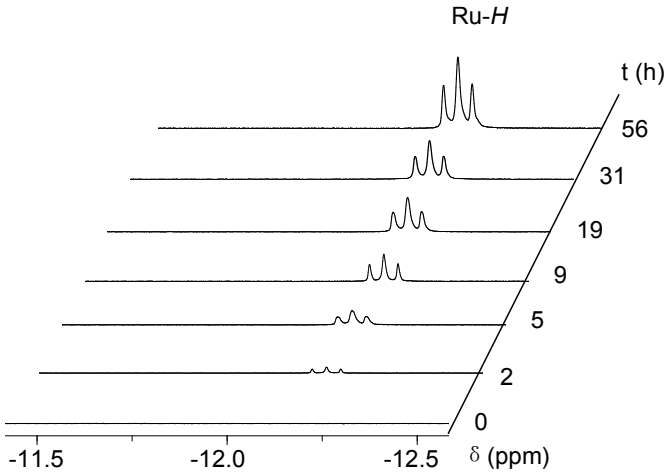

Fig. S9 The ^{1}H NMR kinetic studies of reaction of **7** with H_2 to **6** in C_6D_6 at 10 °C, in which the resonance changes of the Ru*H* were herein enhanced.

S7. Selected ^{1}H NMR Spectral Data of the Reaction Product of 1 and K[HB*s*Bu$_3$] at D$_2$ Atmosphere

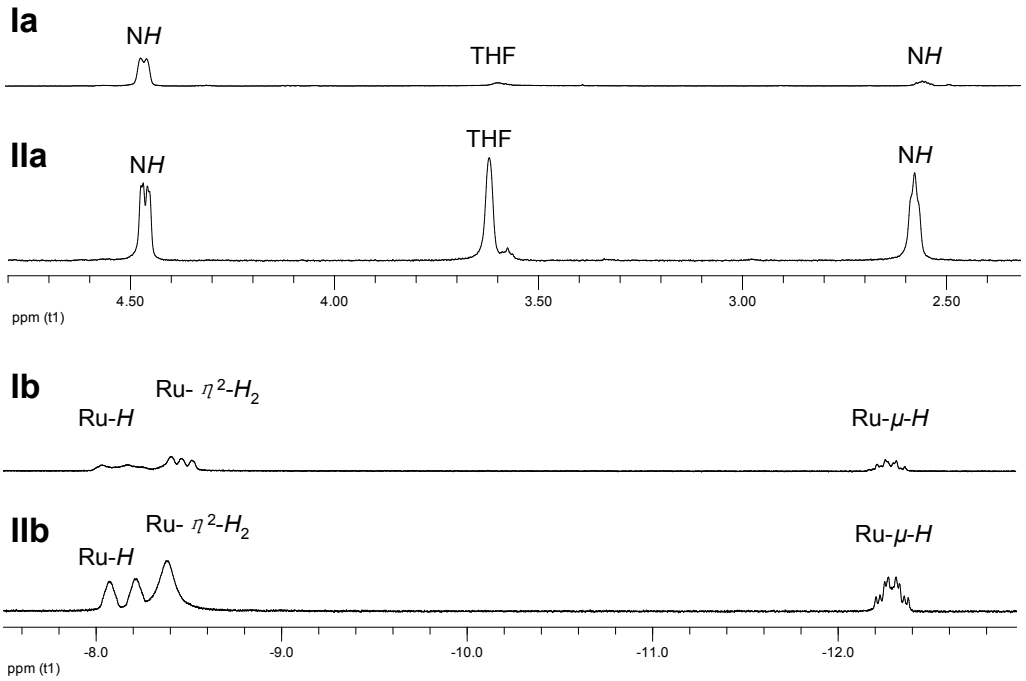

Fig. S10 Comparison of selected ^{1}H NMR spectral data (enhanced proton resonances for the N*H* , Ru-*H* , Ru-μ-*H*, and Ru-η^2-*H*$_2$) for reaction product of **1** and K[HB*s*Bu$_3$] at D$_2$ atmosphere (**Ia** and **Ib**) and **4** (**IIa** and **IIb**).

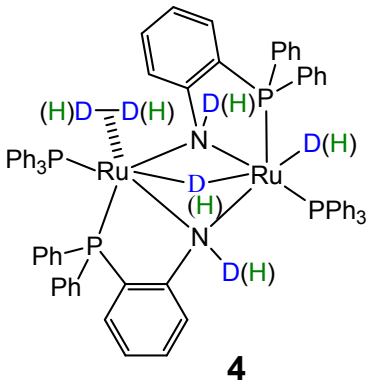

4

Reaction of **1** (0.14 g, 0.2 mmol) and K[HB*s*Bu$_3$] (0.8 mmol, 0.8 mL 1 M THF solution) in THF (10 mL) at D$_2$ atmosphere was conducted from –75 °C to room temperature within 9 h. By removal of KCl, concentration (to ca. 1 mL), and precipitation (with 5 mL *n*-hexane), a yellow solid was formed, collected, and washed (with 2 mL *n*-hexane). After drying under vacuum for 3 h, this solid was subjected to the ^{1}H and ^{31}P{^{1}H} NMR spectral analysis. As shown in Fig. S11 by comparison with the related data of **4**, the proton resonances for the N*H*, Ru-*H*, Ru-η^2-*H*$_2$ and Ru-μ-*H* still present although in a lower integral intensity. This result suggests an occurring of the reaction via an alternative switch between **4** and **4a** under the D$_2$/DH addition/elimination in a similar manner to that for the reaction of **7** and D$_2$ to **6** (Scheme S1, *vide infra*), leading to a partially D/H-exchanged formation of **4**.

S8. Suggested Scheme for Reaction of 7 with D_2 to 6

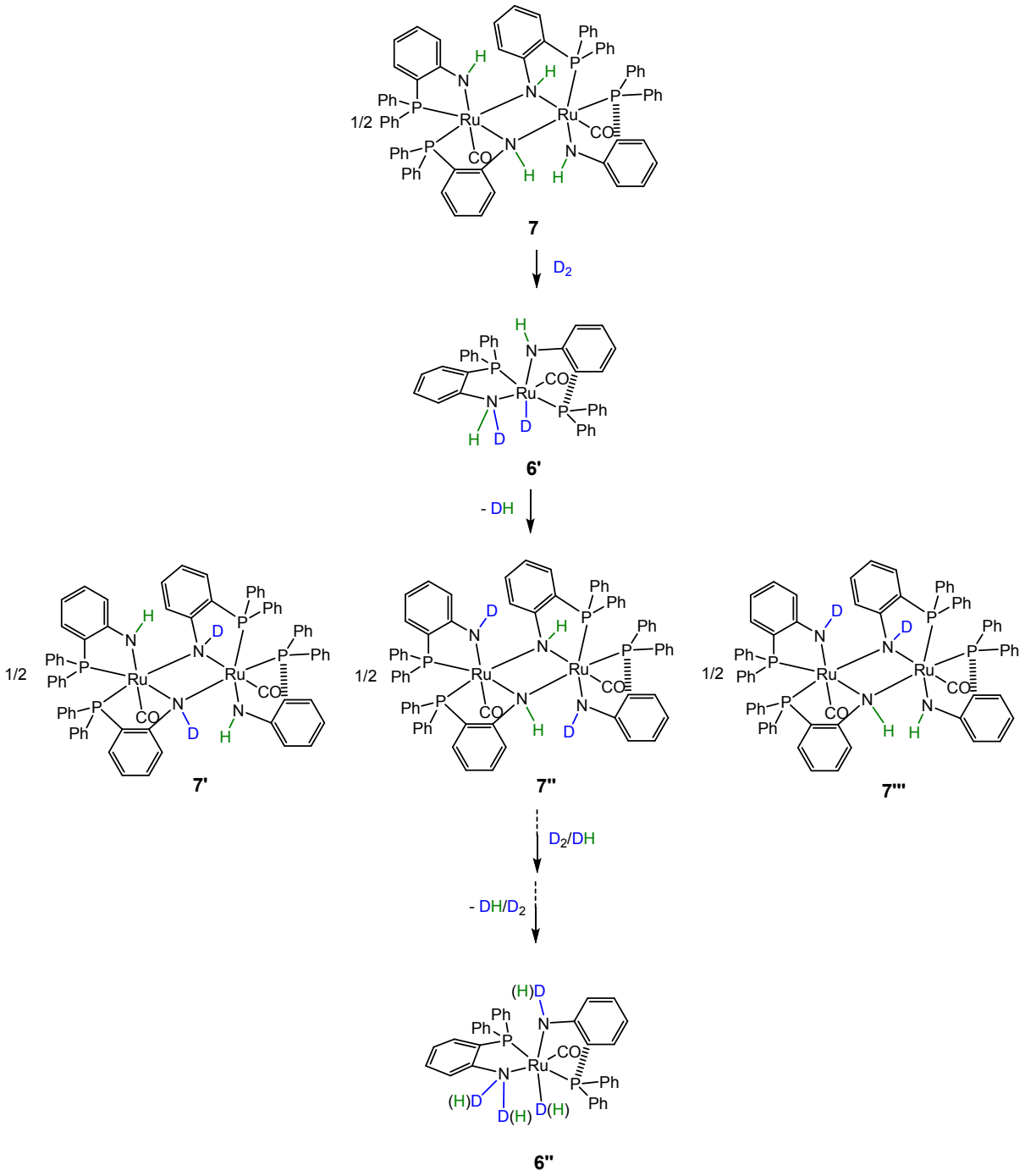

Scheme S1 Suggested functional group transformation reaction switched between **7** and **6** at D_2 resulted from the NMR data shown in Fig. 3 in the text.

S9. NMR Spectra of Compounds

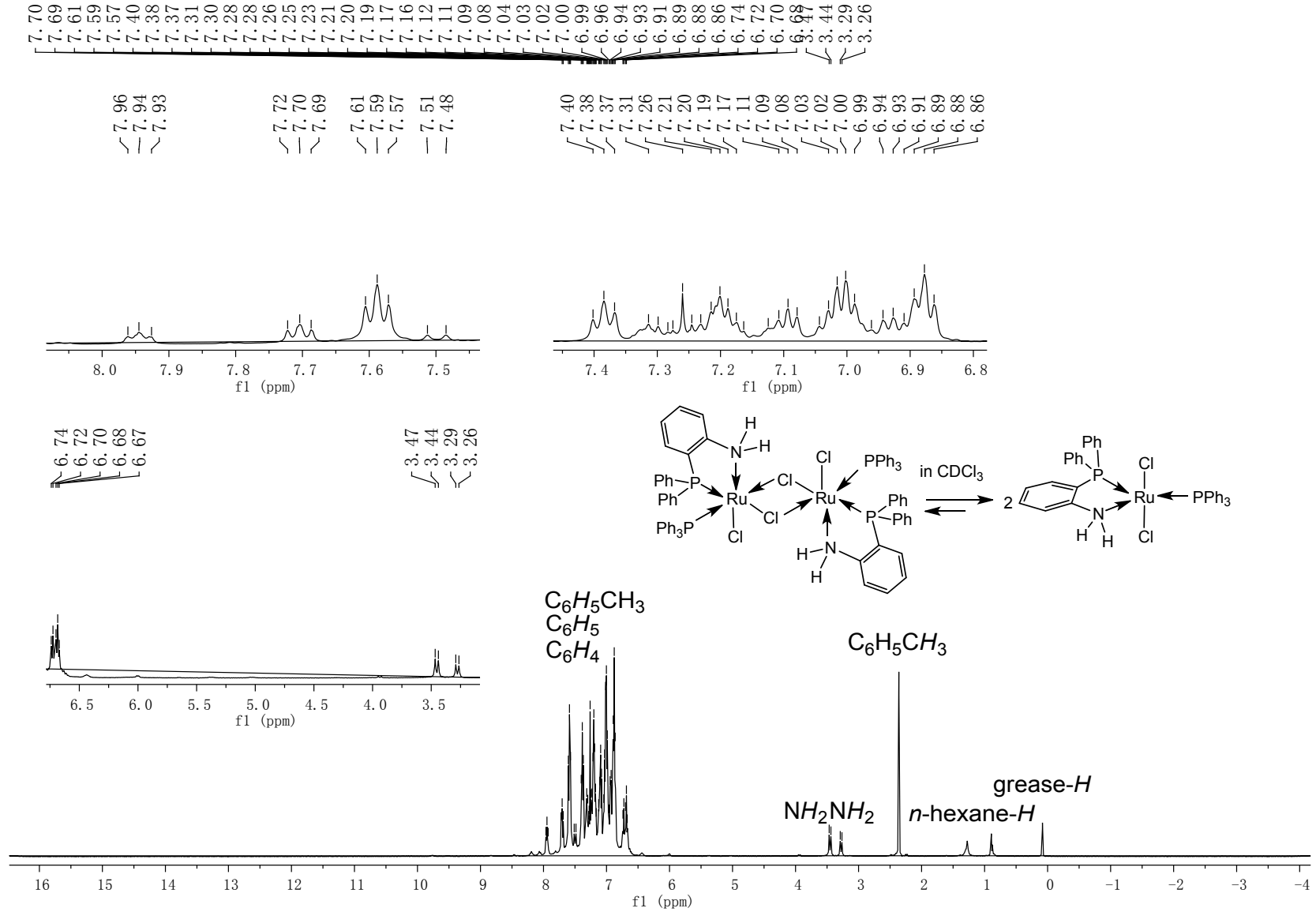

Fig. S11-a ^{1}H NMR spectrum of complex **1** in $CDCl_3$.

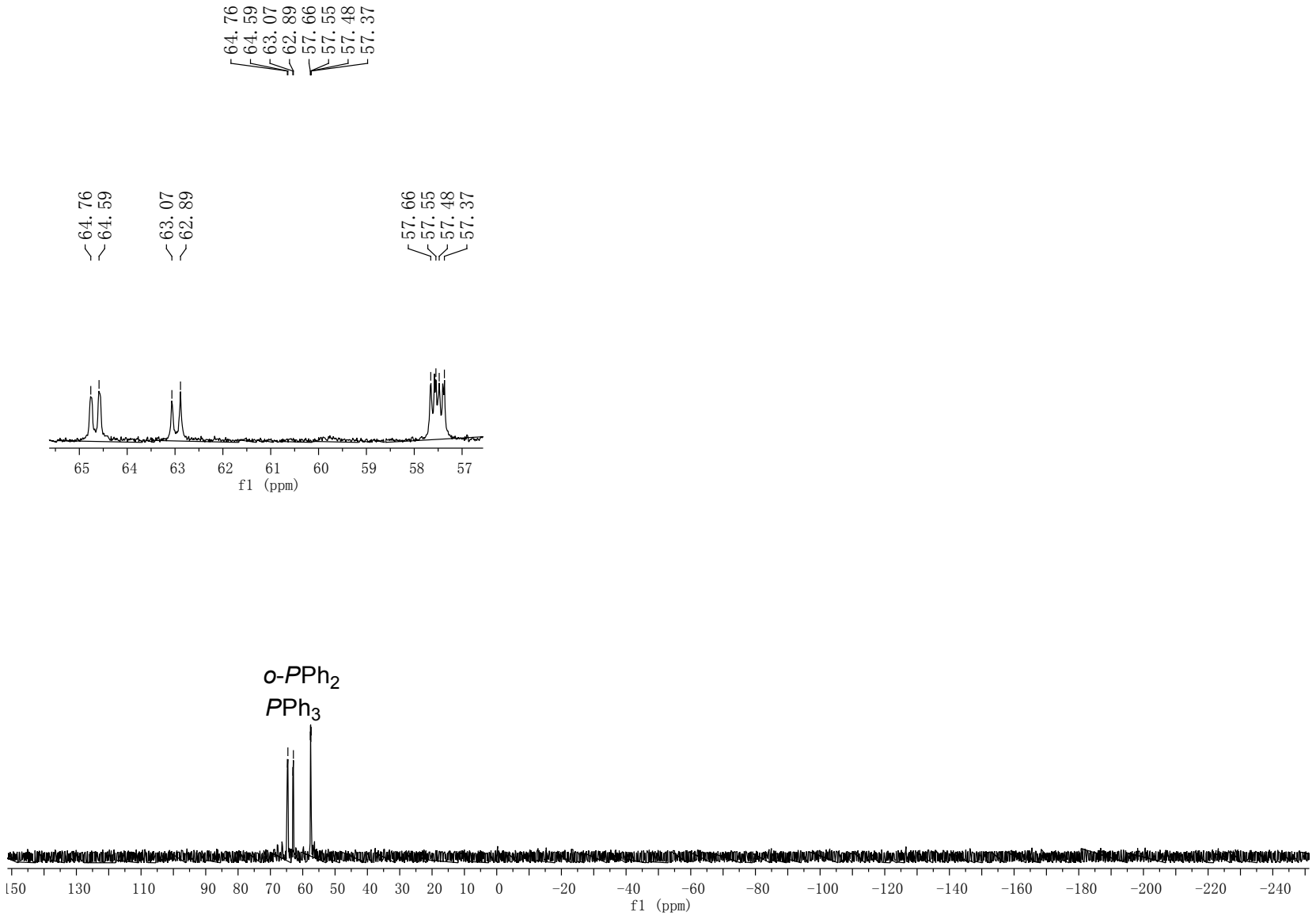

Fig. S11-b $^{31}P\{^{1}H\}$ NMR spectrum of complex **1** in $CDCl_3$.

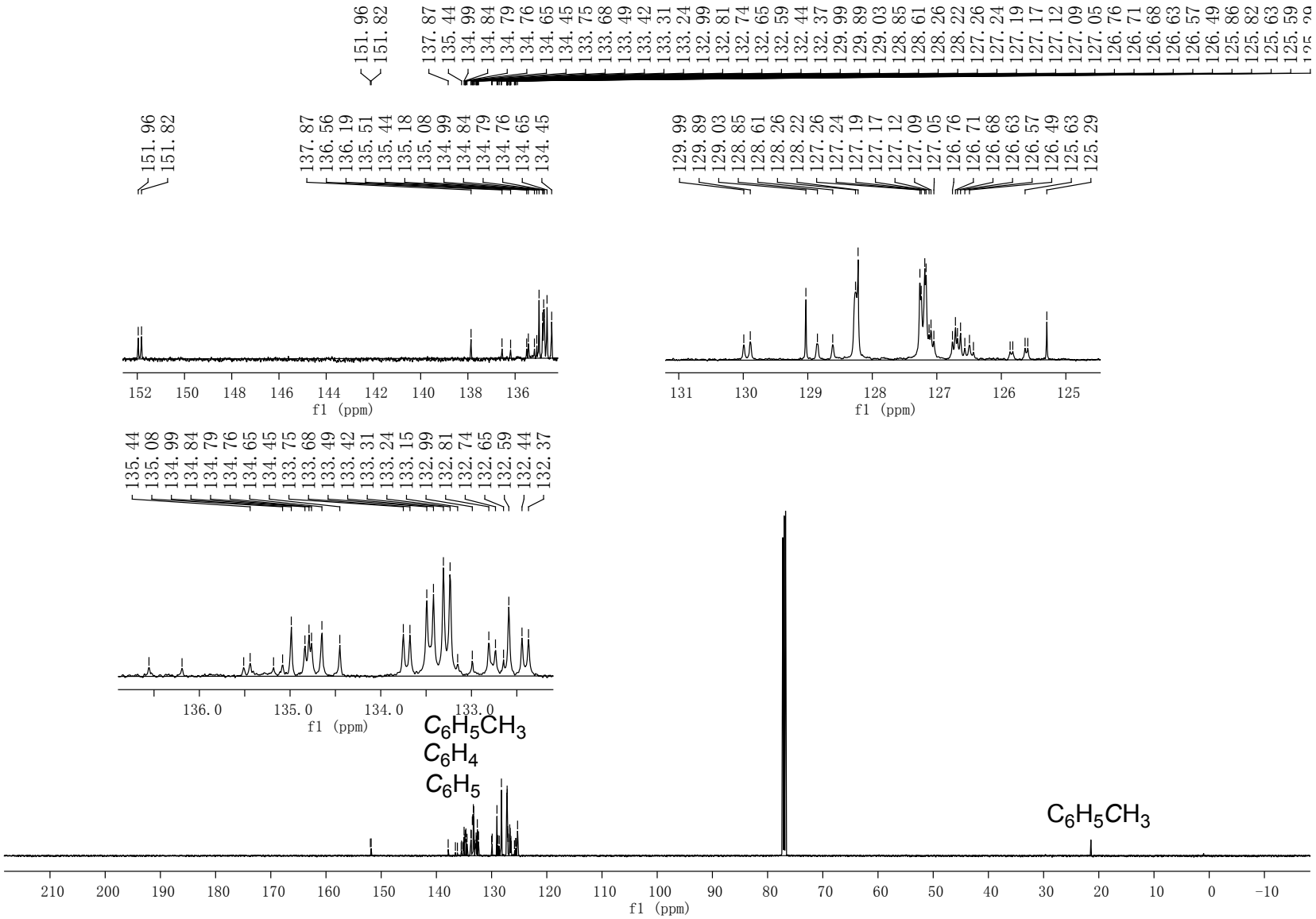

Fig. S11-c $^{13}C\{^1H\}$ NMR spectrum of complex **1** in $CDCl_3$.

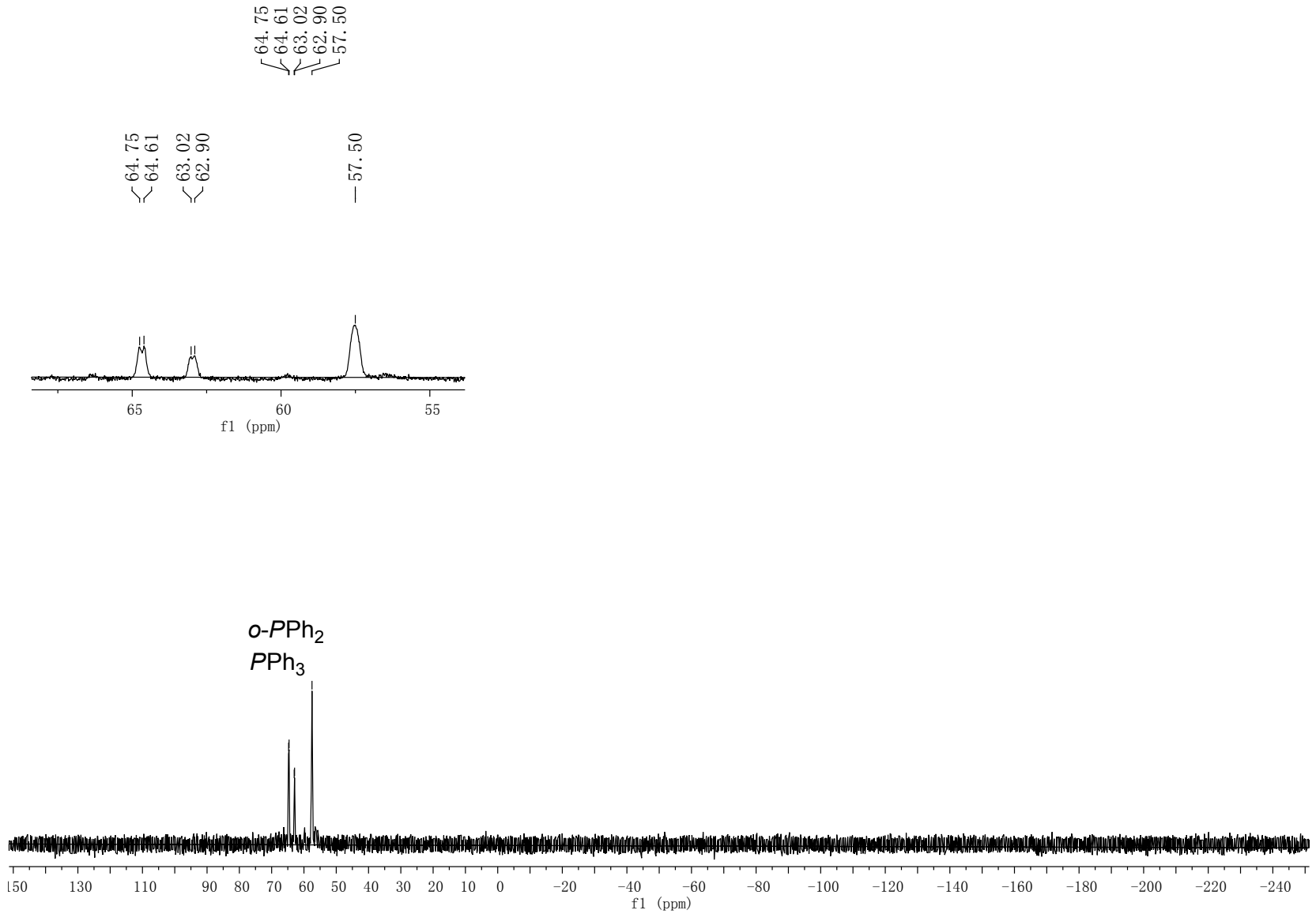

Fig. S11-d ^{31}P NMR spectrum of complex **1** in $CDCl_3$.

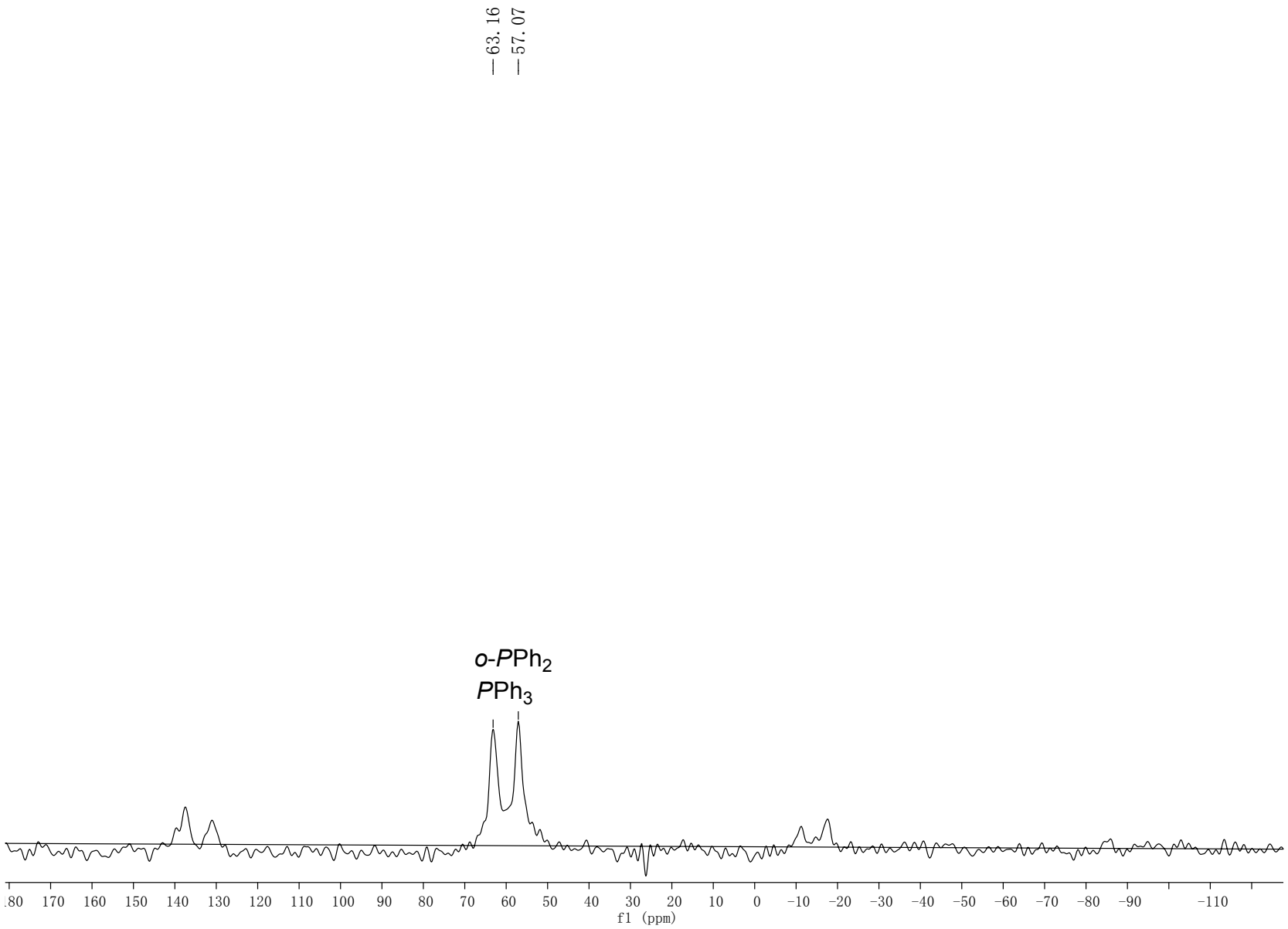

Fig. S11-e Solid state ^{31}P NMR spectrum of complex **1**.

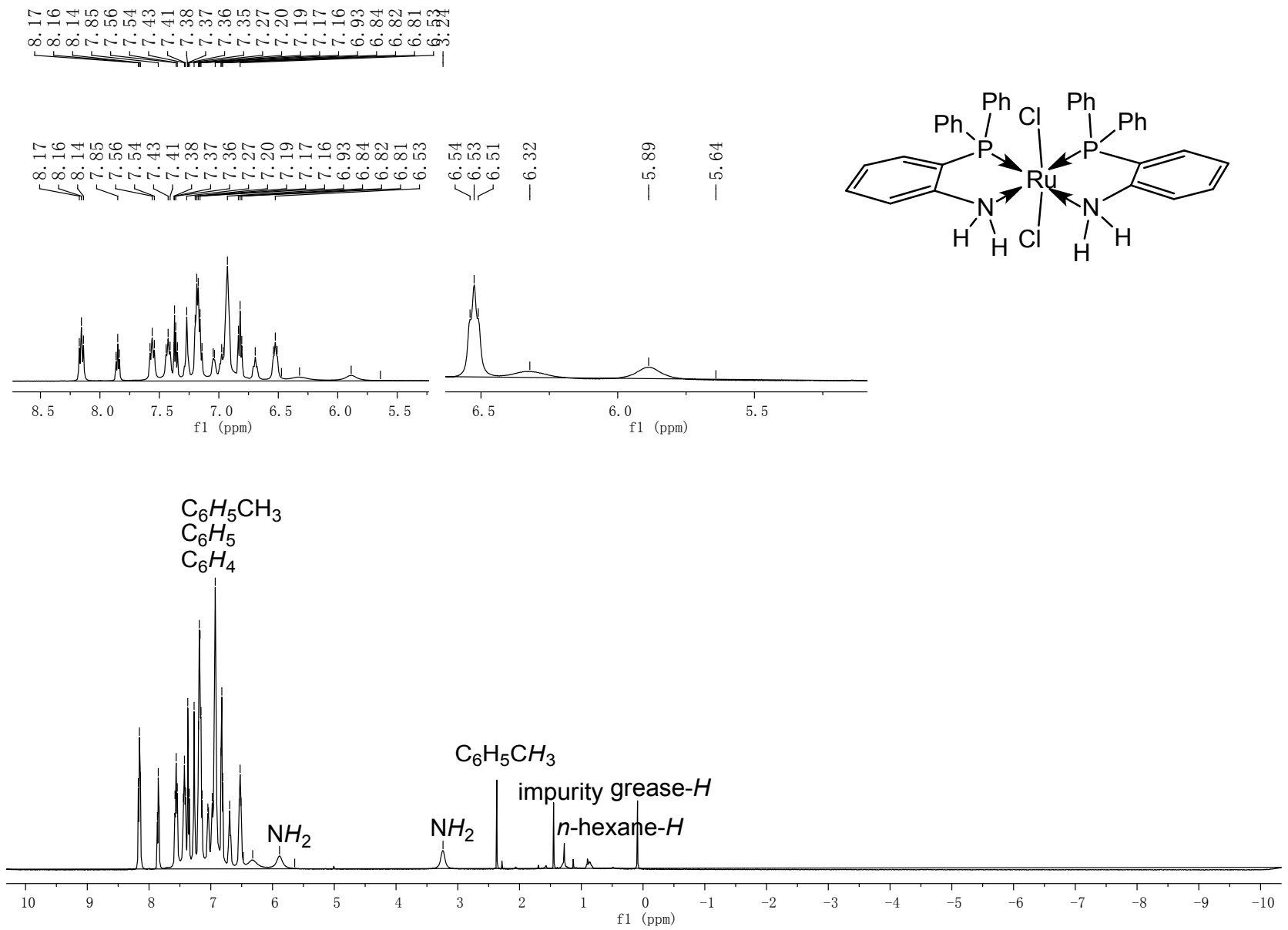

Fig. S12-a ^{1}H NMR spectrum of complex **2** in $CDCl_3$.

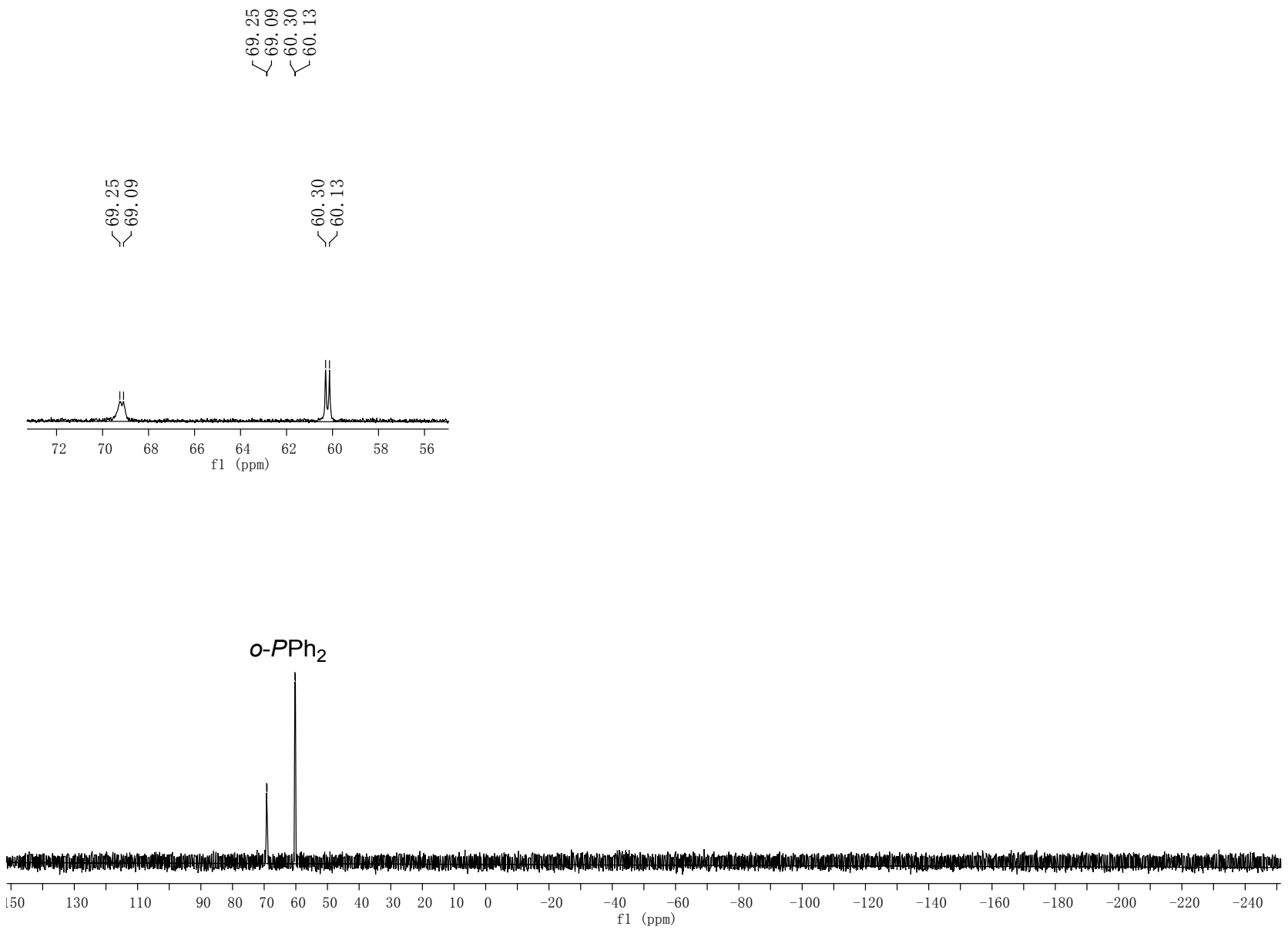

Fig. S12-b $^{31}P\{^{1}H\}$ NMR spectrum of complex **2** in $CDCl_3$.

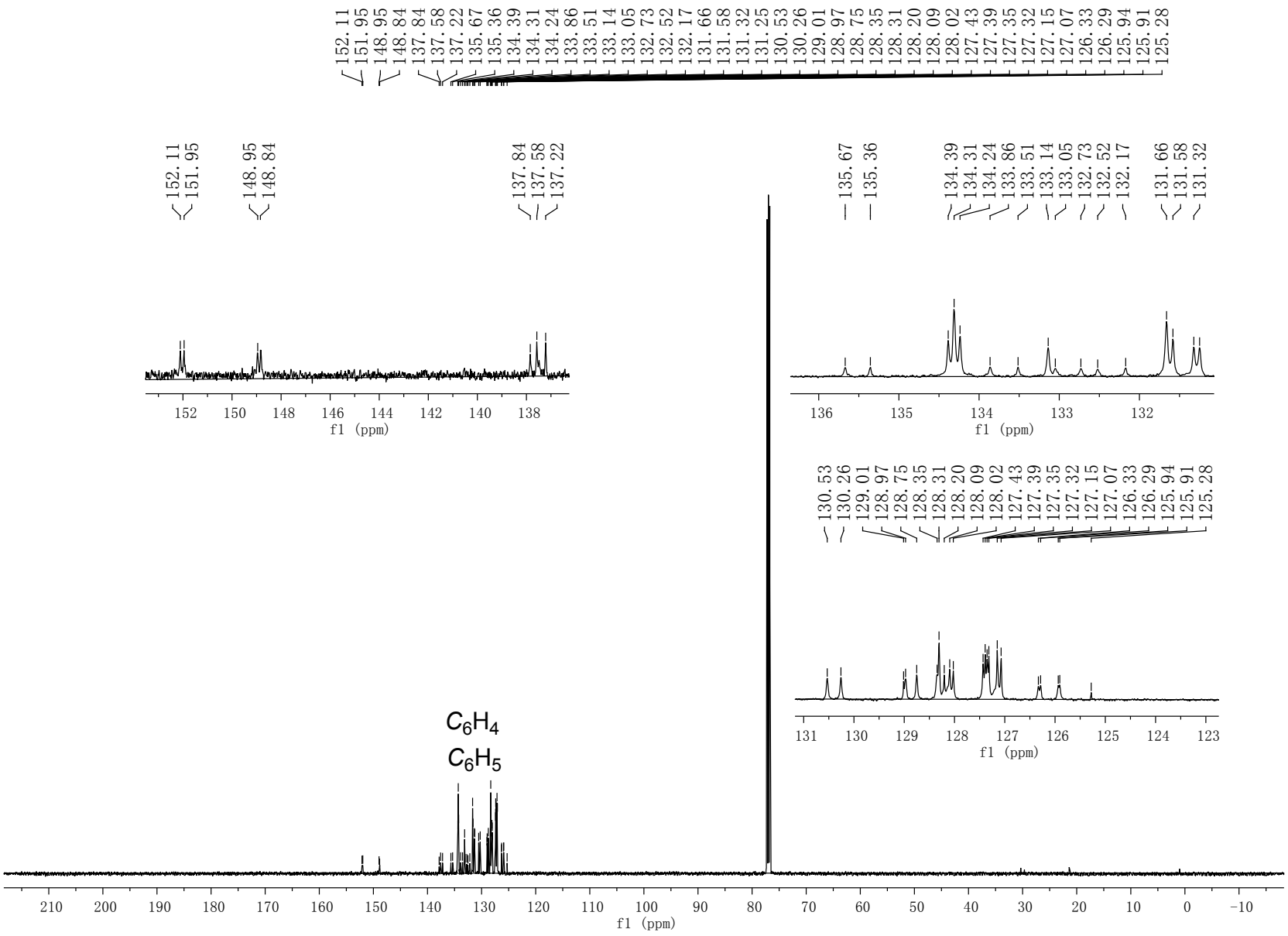

Fig. S12-c $^{13}C\{^{1}H\}$ NMR spectrum of complex **2** in $CDCl_3$.

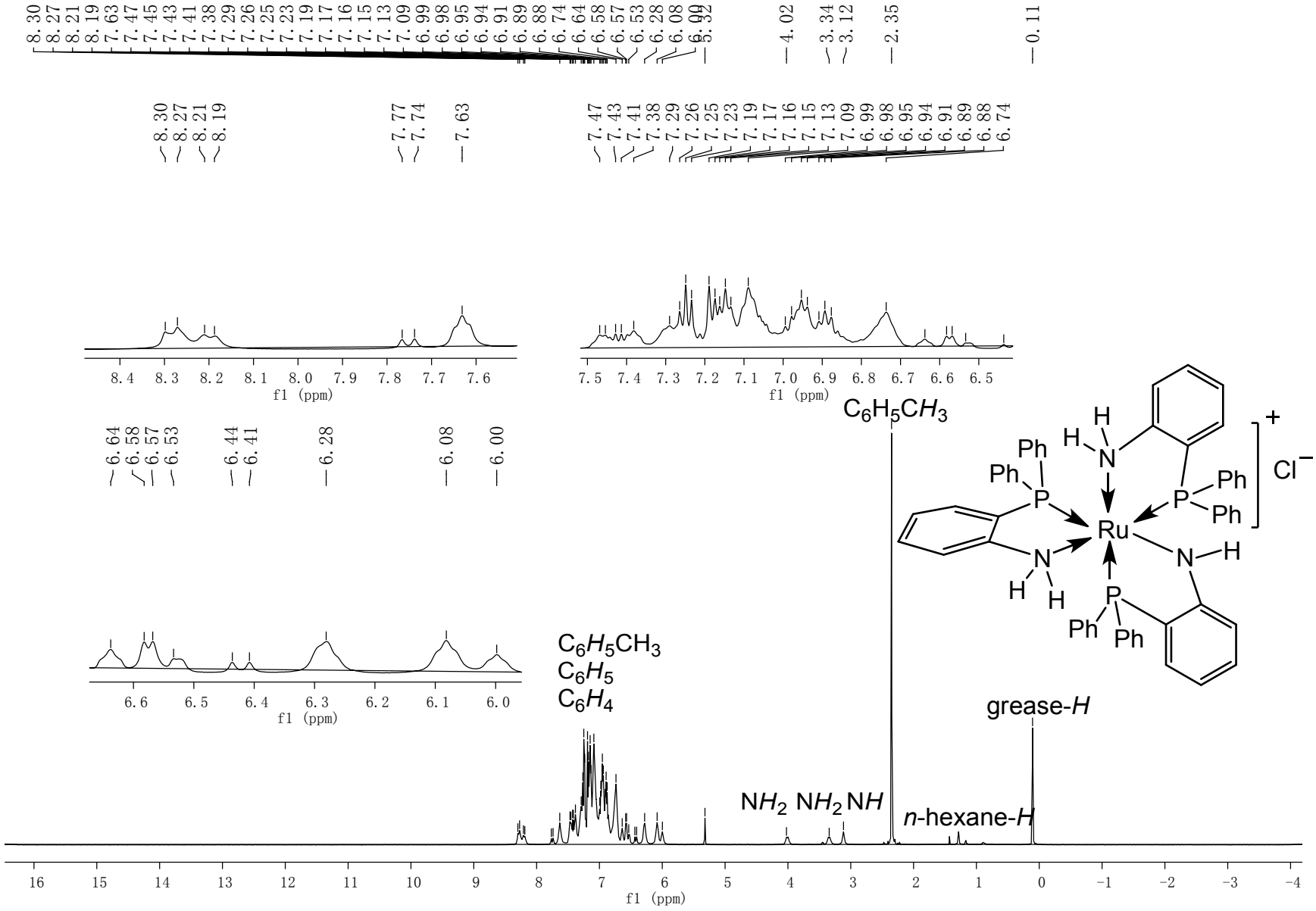

Fig. S13-a ^{1}H NMR spectrum of complex **3** in CD_2Cl_2.

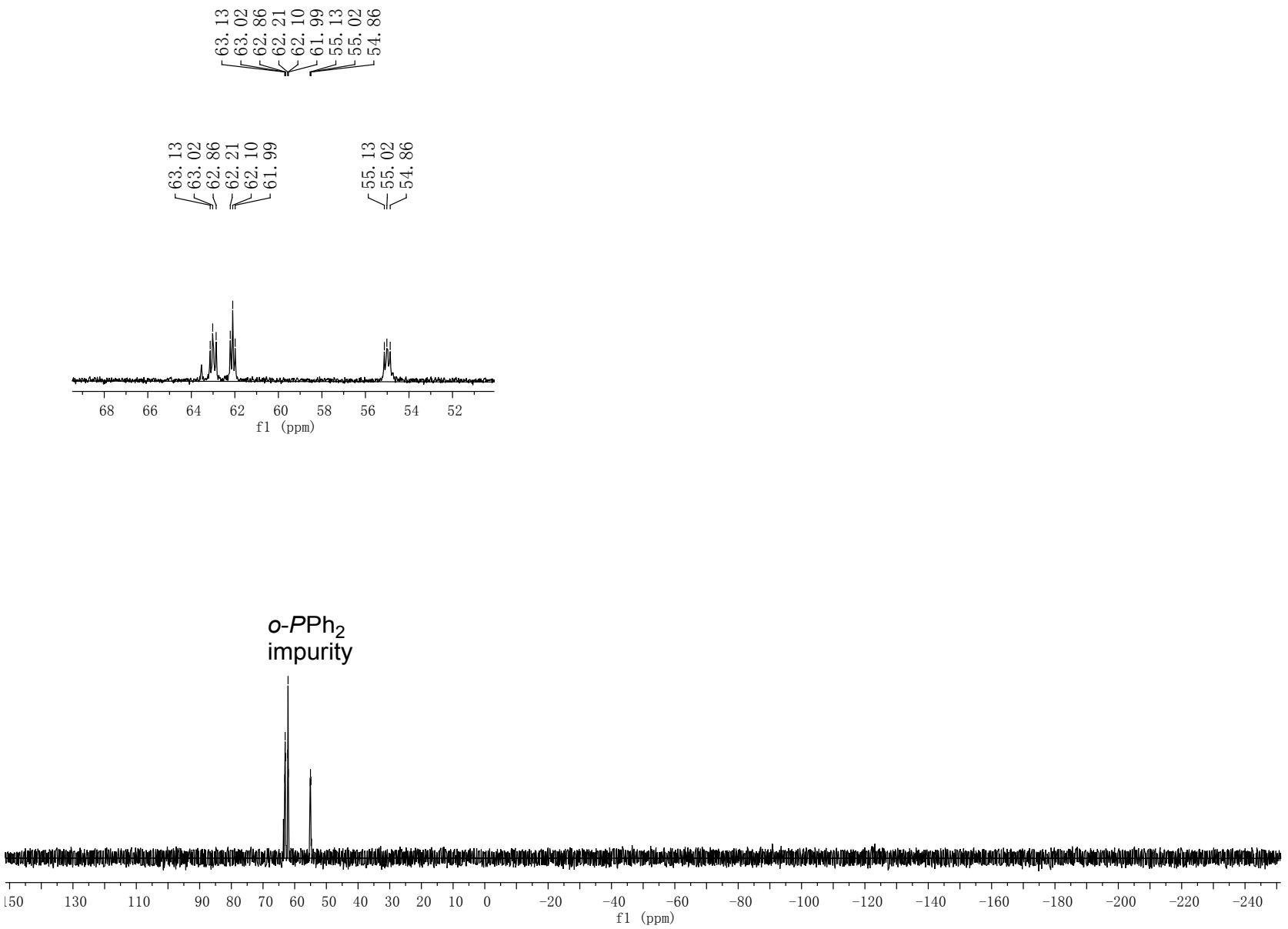

Fig. S13-b $^{31}P\{^{1}H\}$ NMR spectrum of complex **3** in CD_2Cl_2.

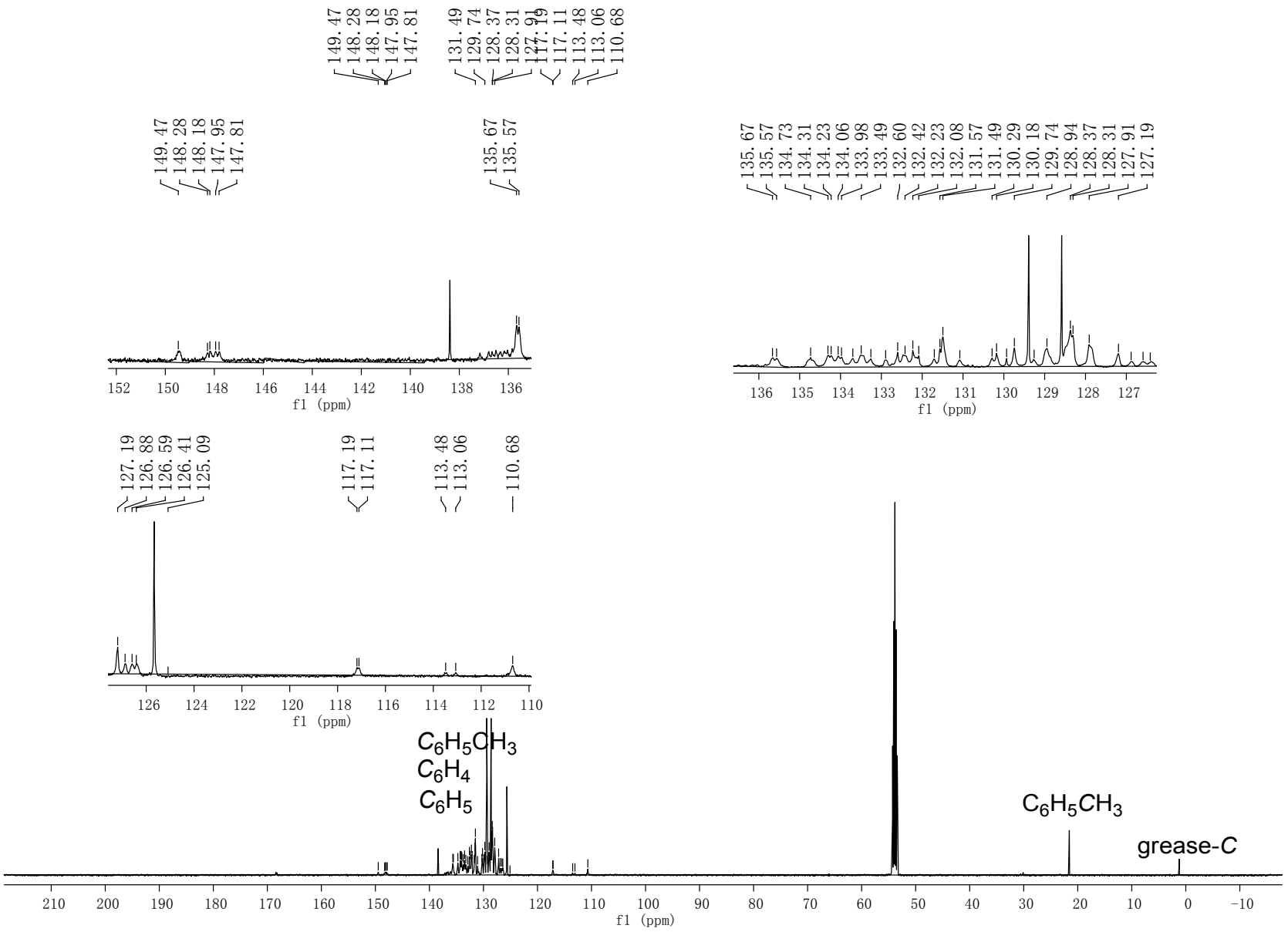

Fig. S13-c $^{13}C\{^{1}H\}$ NMR spectrum of complex **3** in CD_2Cl_2.

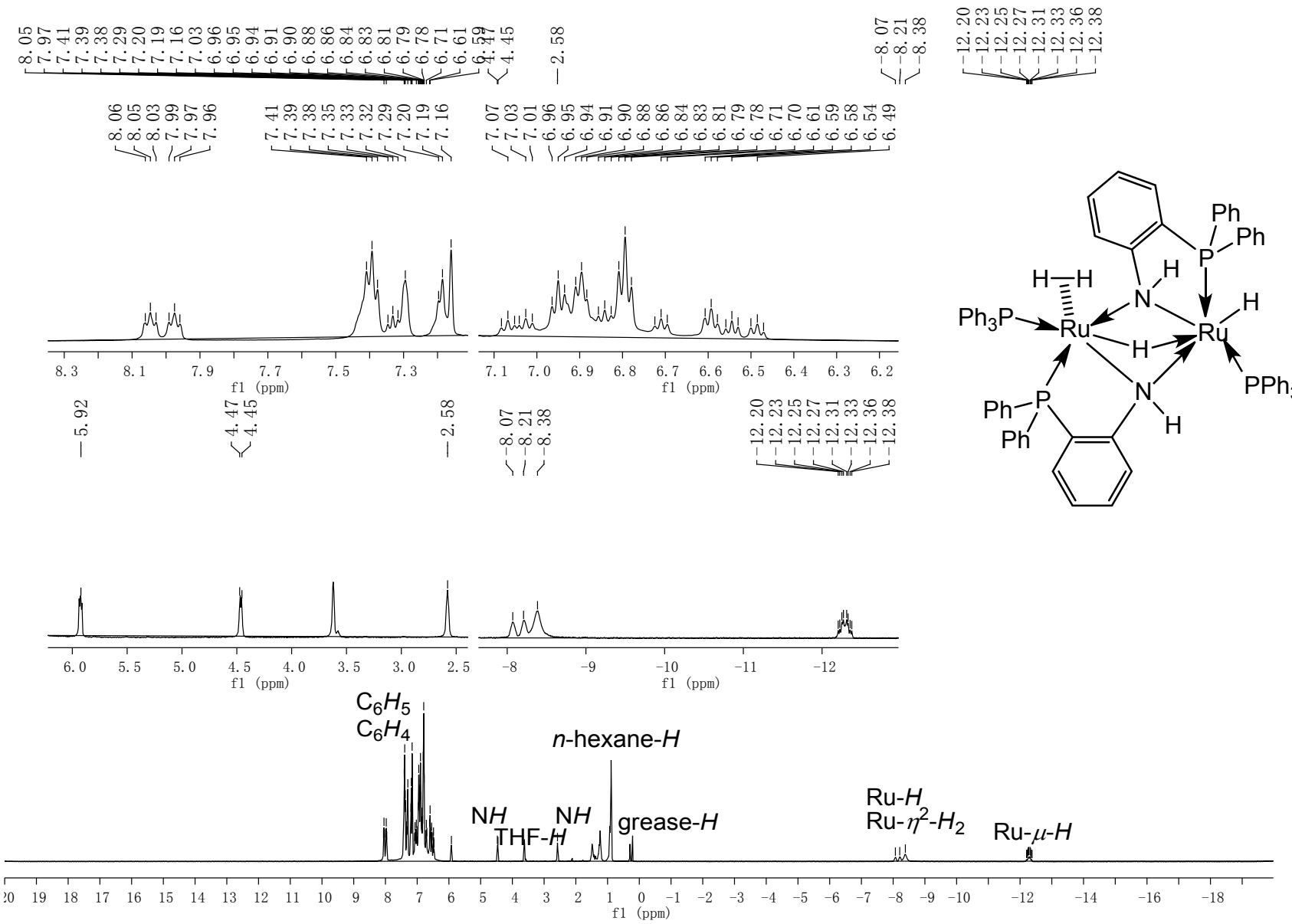

Fig. S14-a ^{1}H NMR spectrum of complex **4** in C_6D_6.

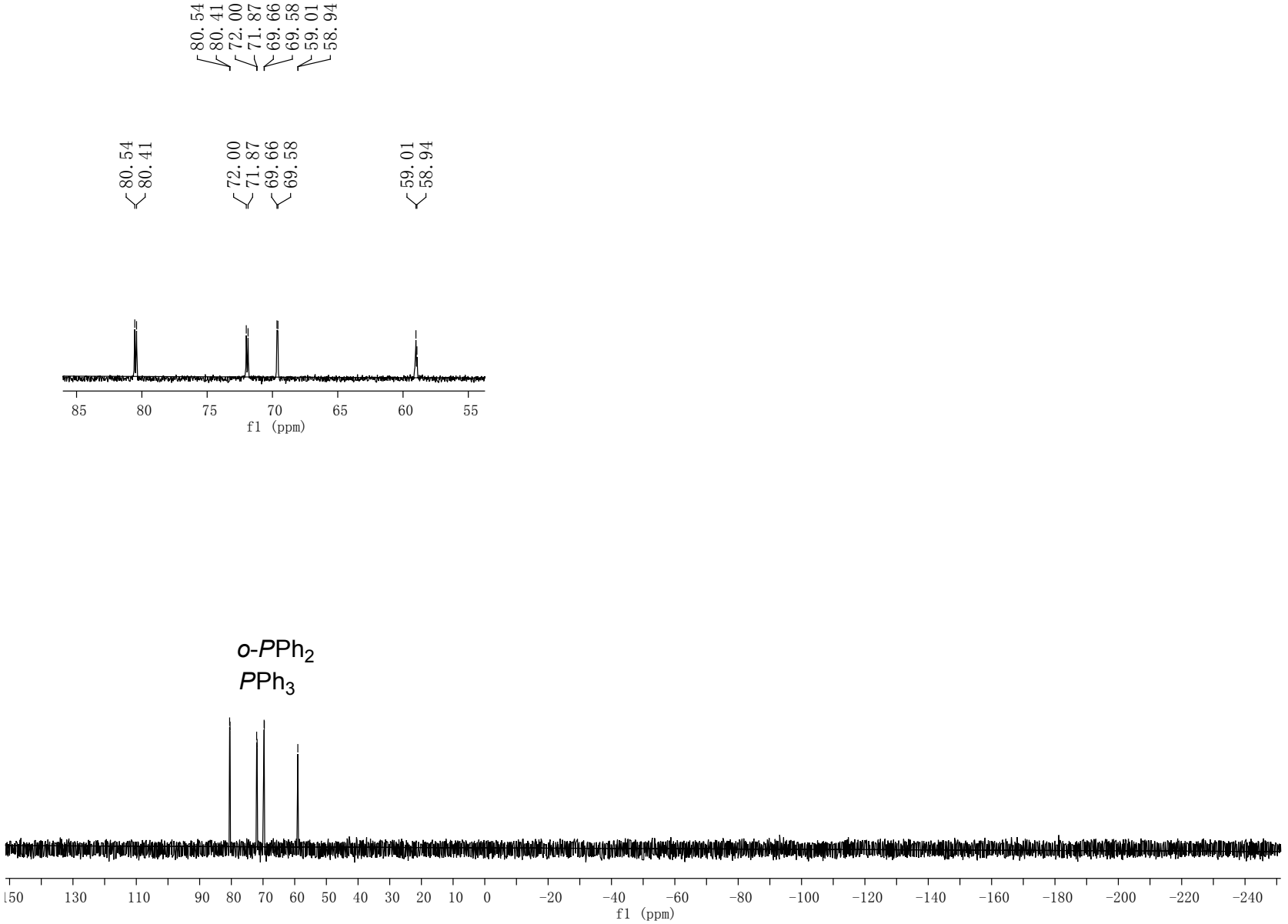

Fig. S14-b $^{31}P\{^{1}H\}$ NMR spectrum of complex **4** in C_6D_6.

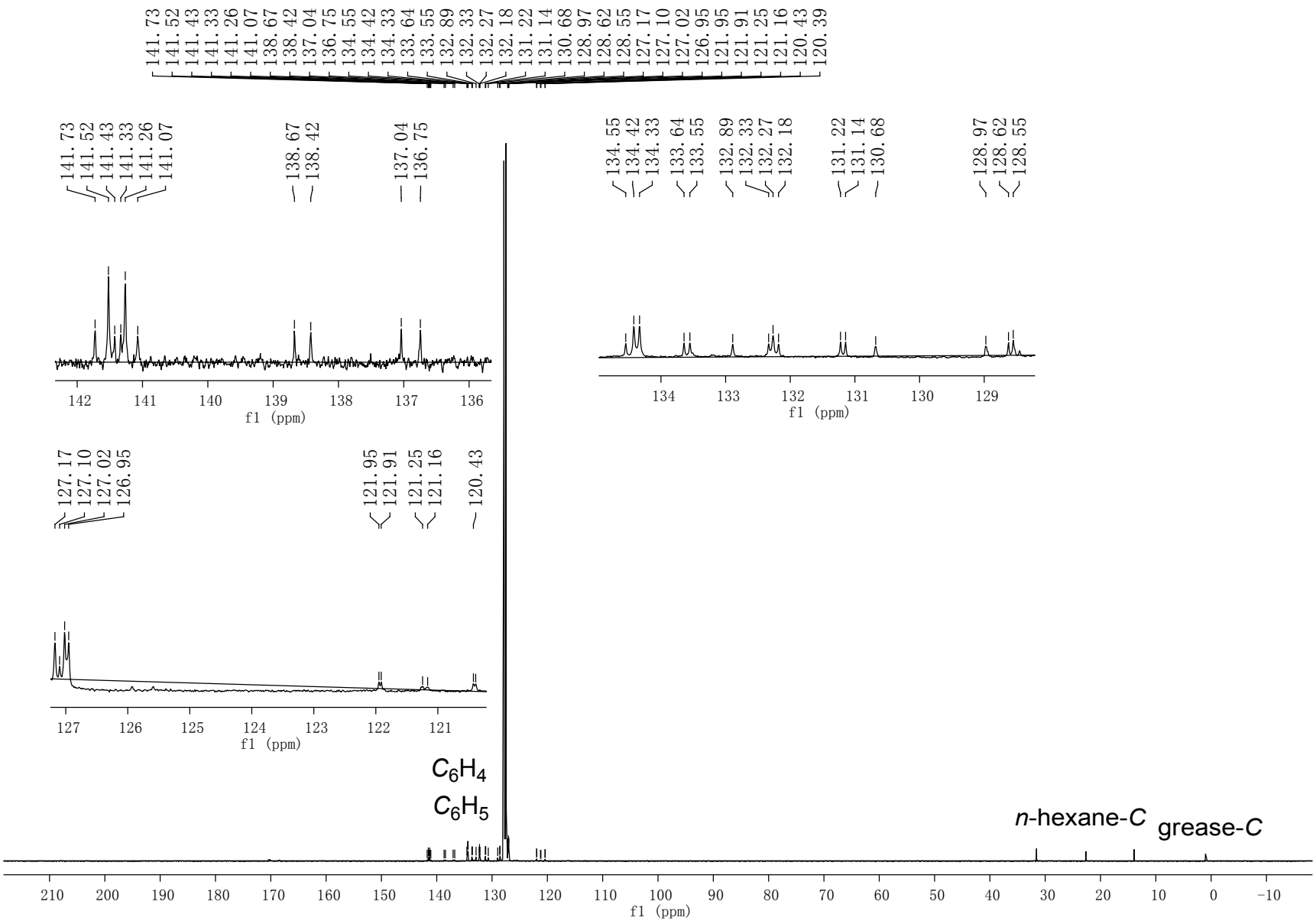

Fig. S14-c $^{13}C\{^{1}H\}$ NMR spectrum of complex **4** in C_6D_6.

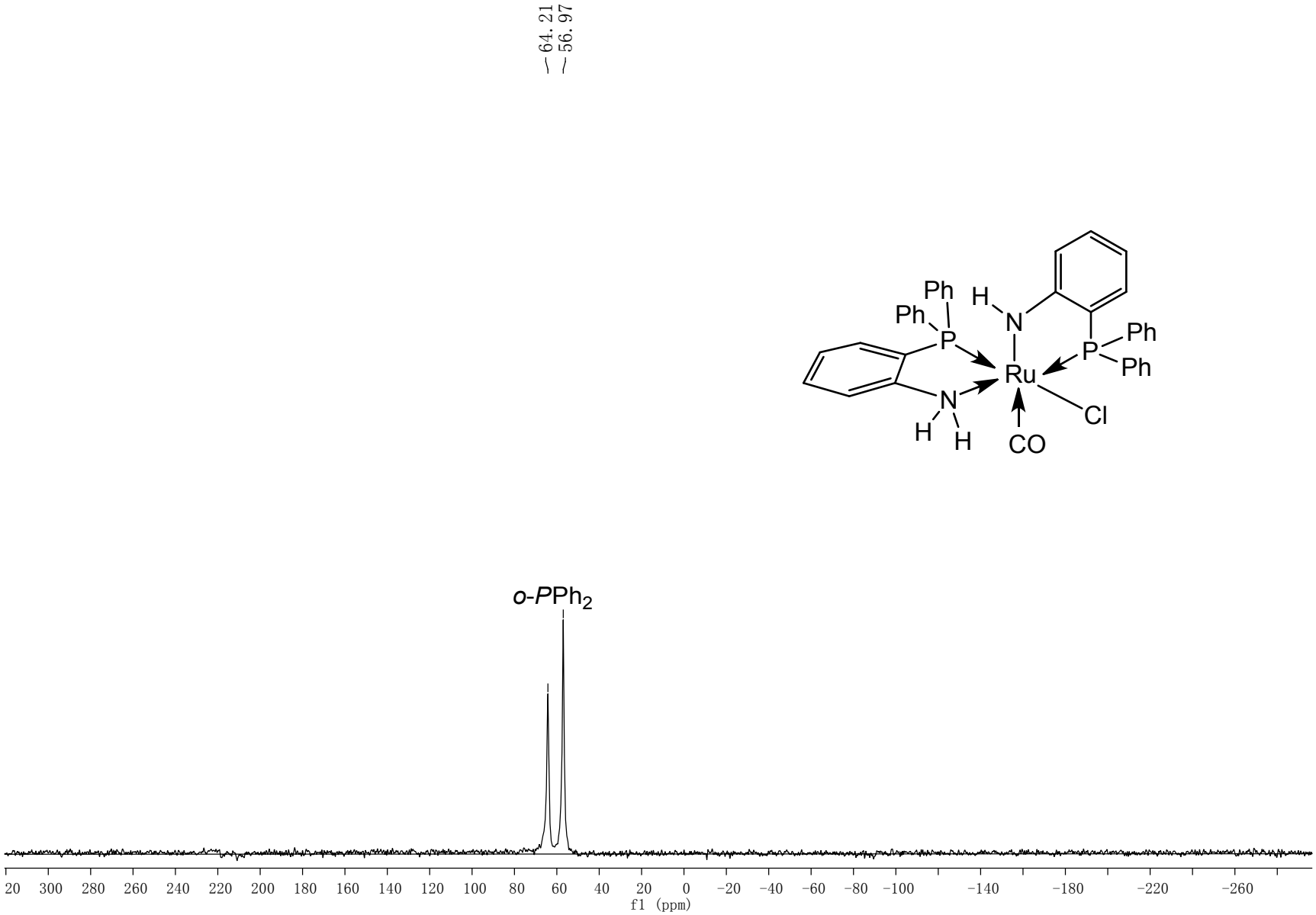

Fig. S15 Solid state ^{31}P NMR spectrum of complex **5**.

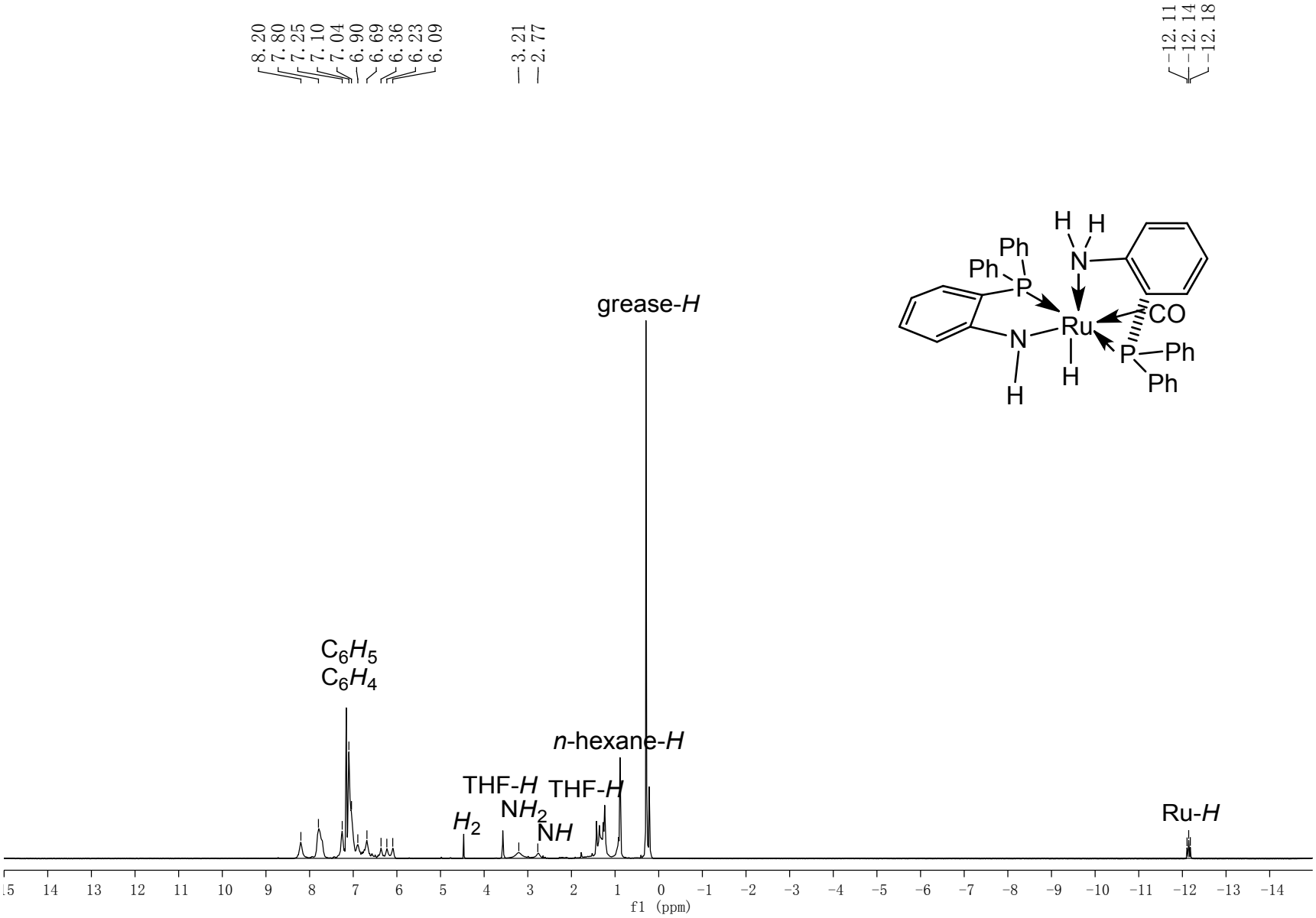

Fig. S16-a ^{1}H NMR spectrum of complex **6** in C_6D_6.

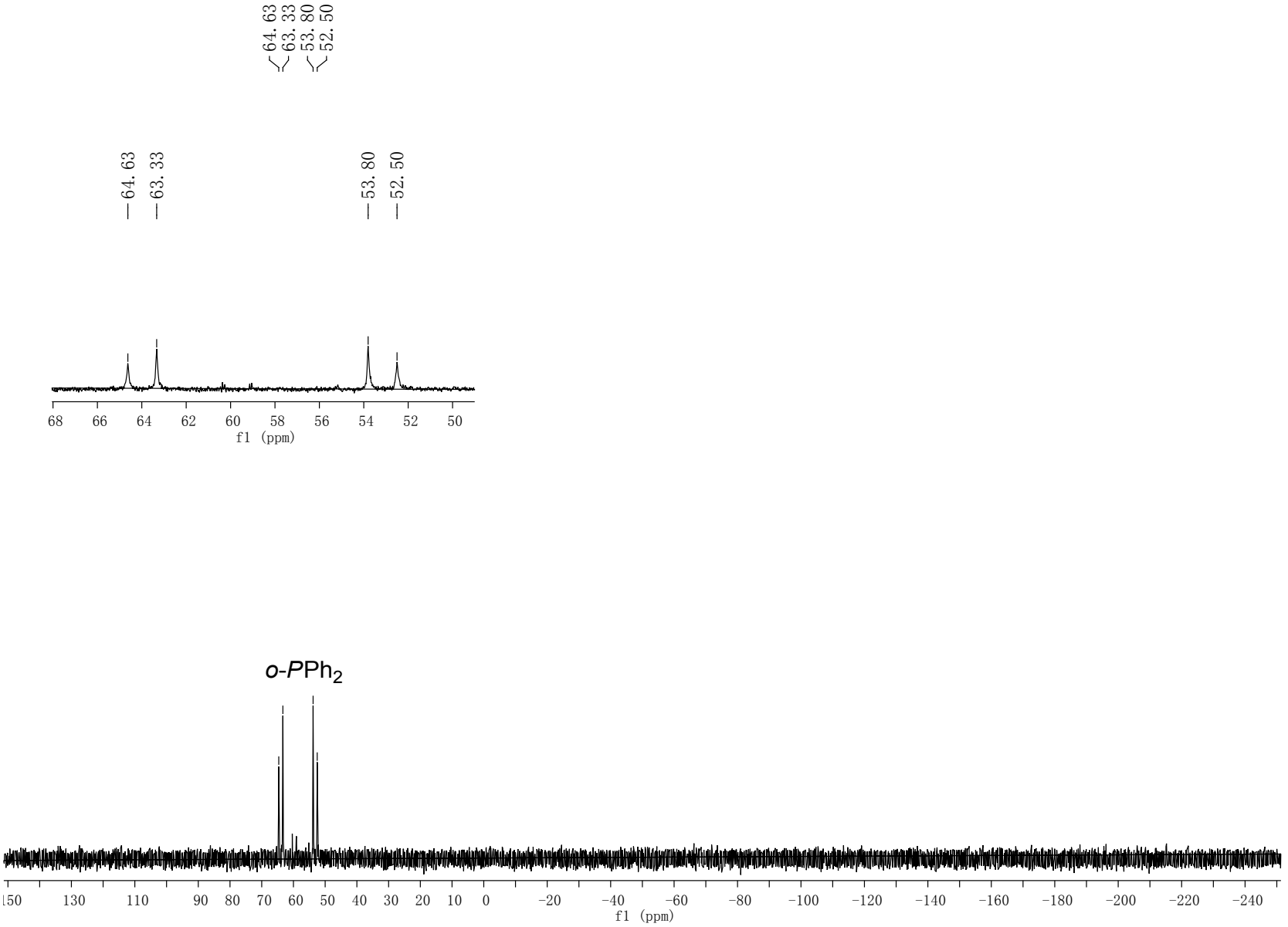

Fig. S16-b $^{31}P\{^{1}H\}$ NMR spectrum of complex **6** in C_6D_6.

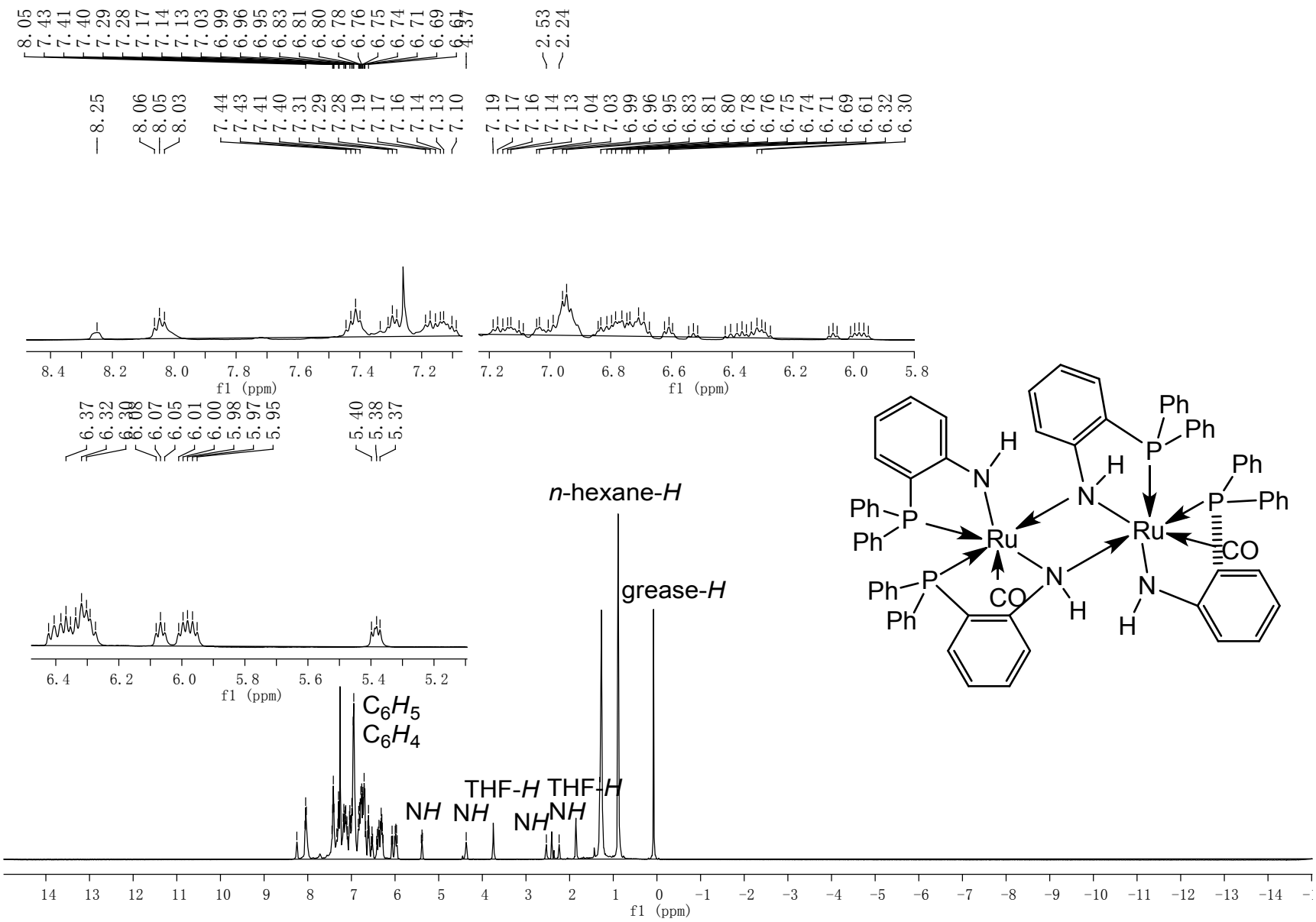

Fig. S17-a ^{1}H NMR spectrum of complex **7** in $CDCl_3$.

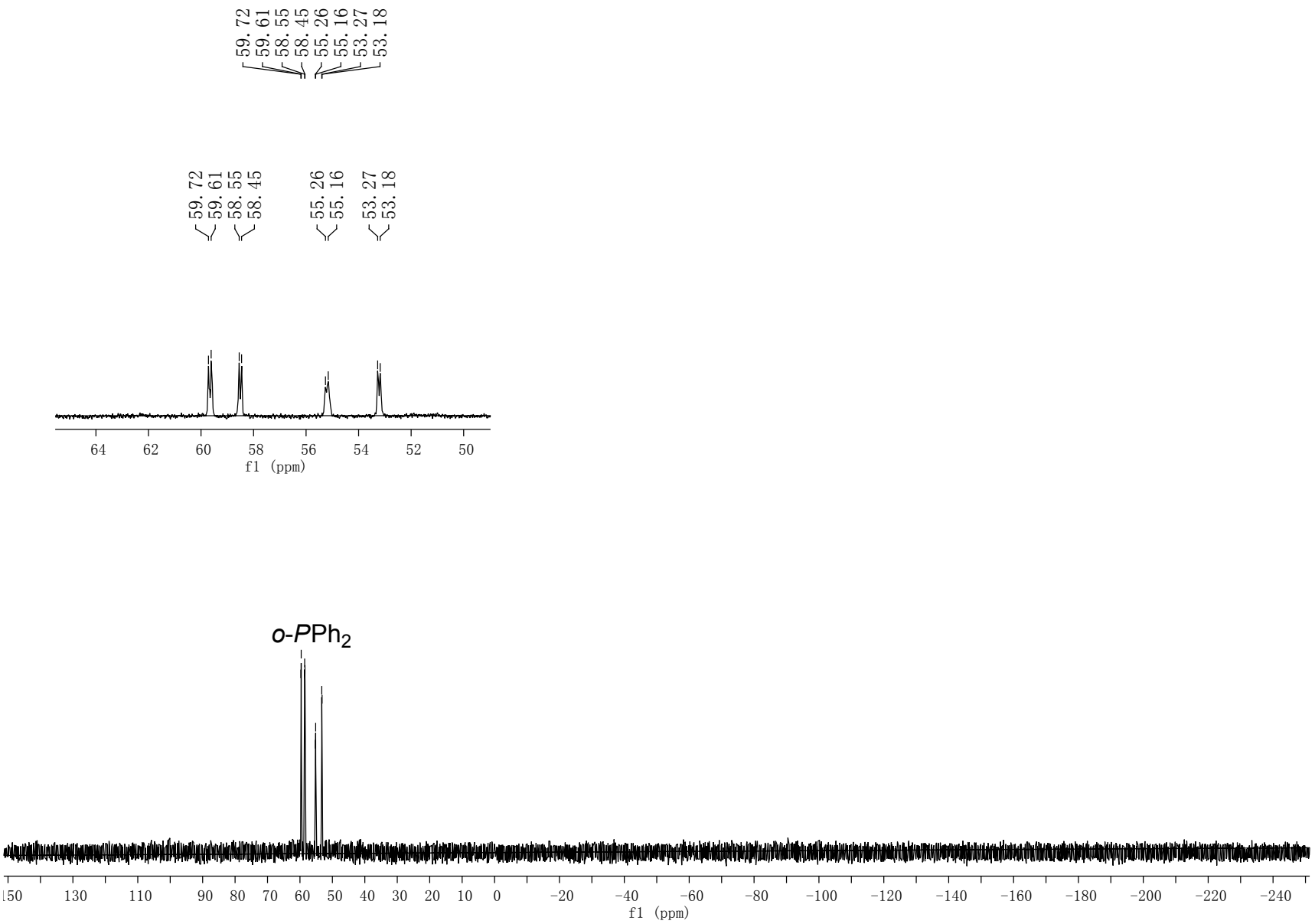

Fig. S17-b $^{31}P\{^{1}H\}$ NMR spectrum of complex **7** in $CDCl_3$.

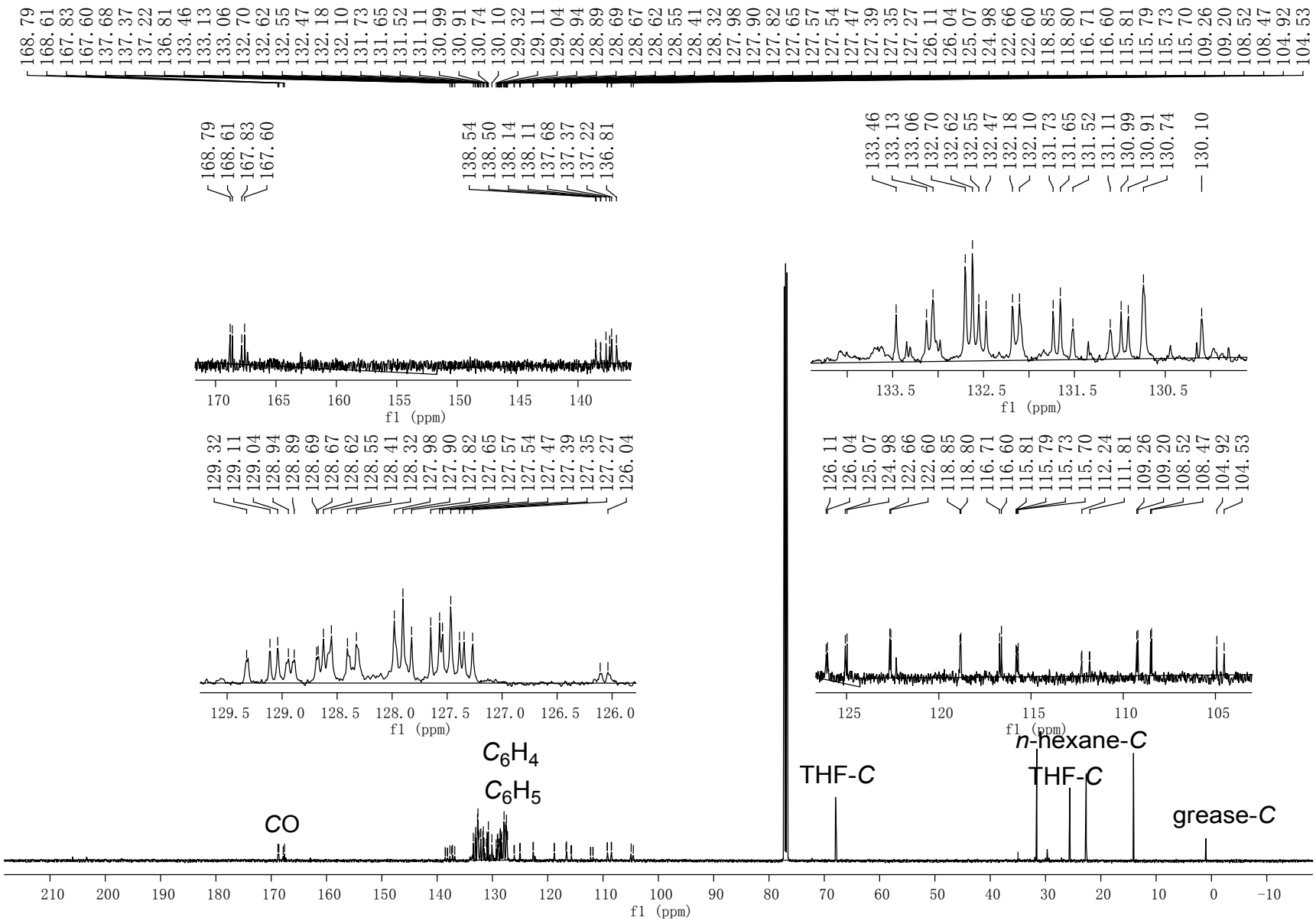

Fig. S17-c $^{13}C\{^{1}H\}$ NMR spectrum of complex **7** in $CDCl_3$.

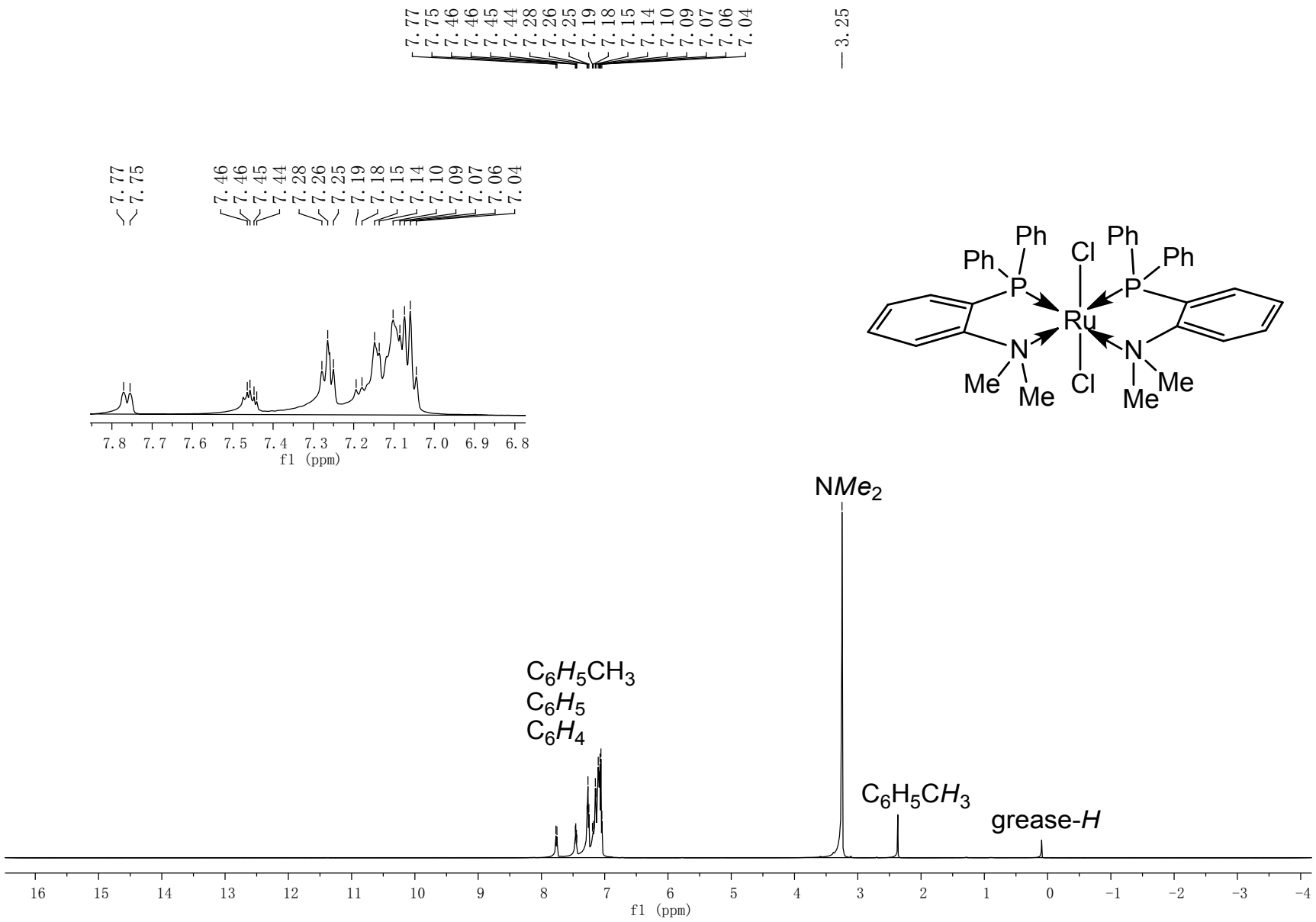

Fig. S18-a ^{1}H NMR spectrum of complex **9** in $CDCl_3$.

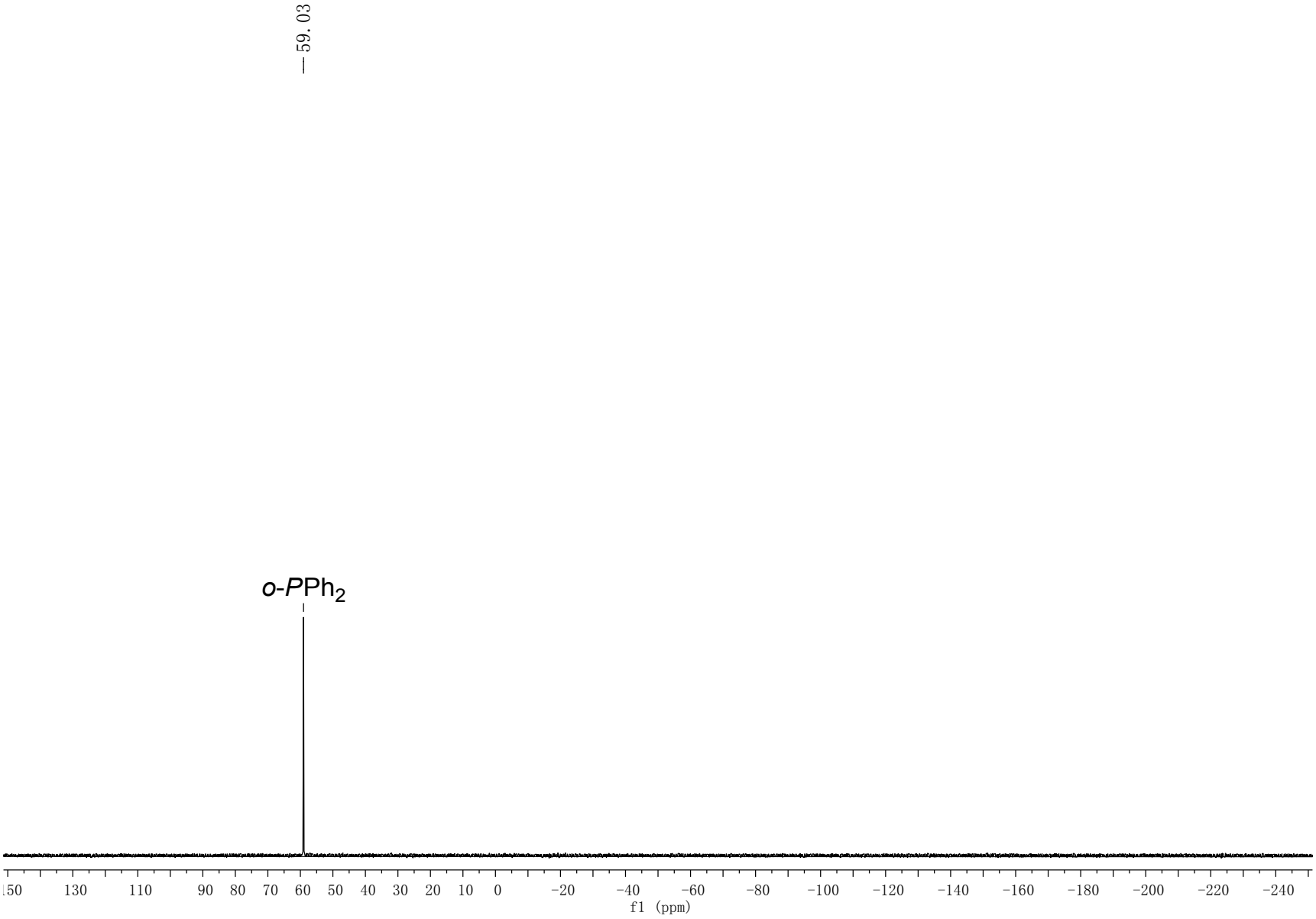

Fig. S18-b $^{31}P\{^{1}H\}$ NMR spectrum of complex **9** in $CDCl_3$.

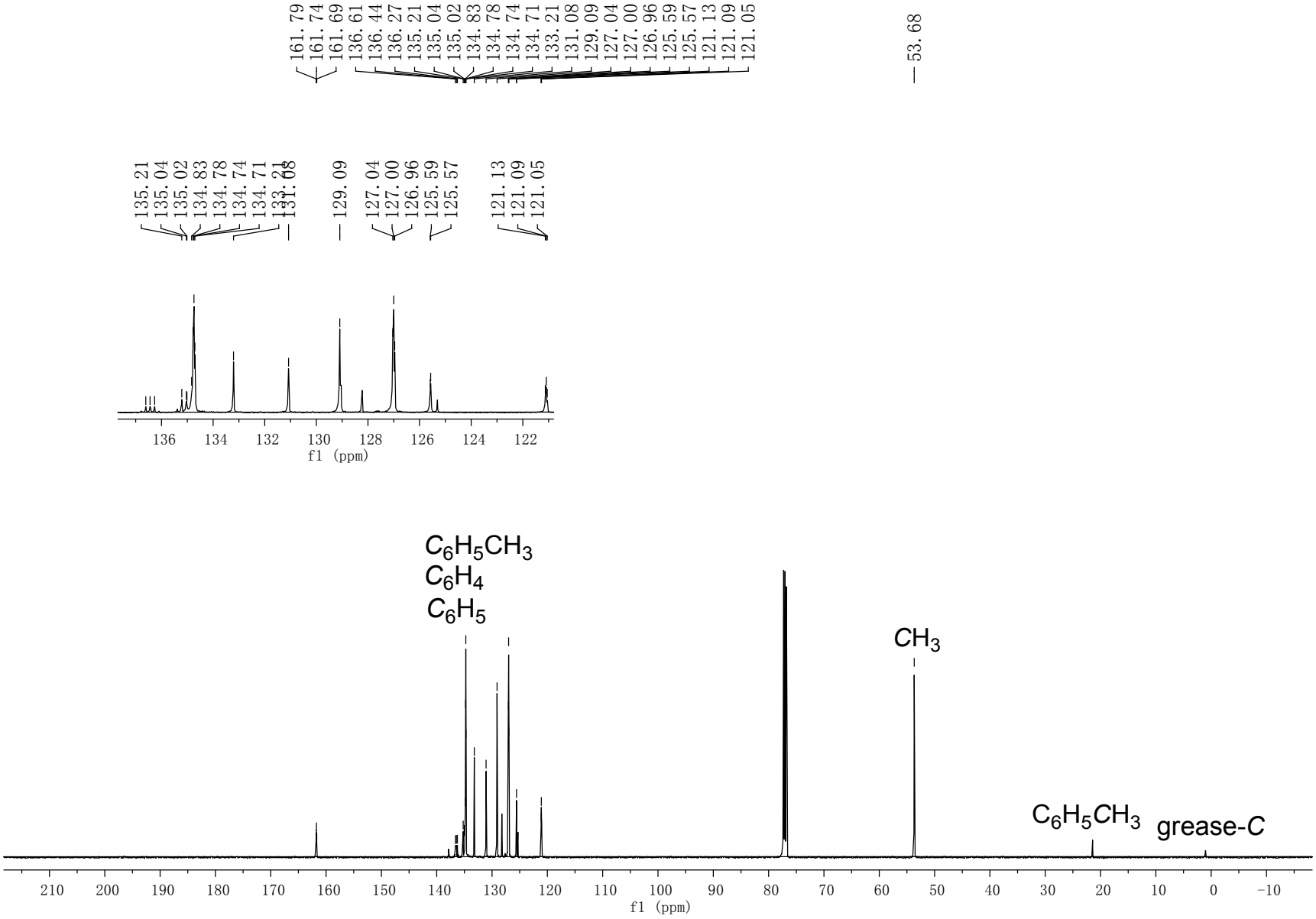

Fig. S18-c $^{13}C\{^{1}H\}$ NMR spectrum of complex **9** in $CDCl_3$.

S10. GC Analytic Figures of the Selected Catalytic Reactions

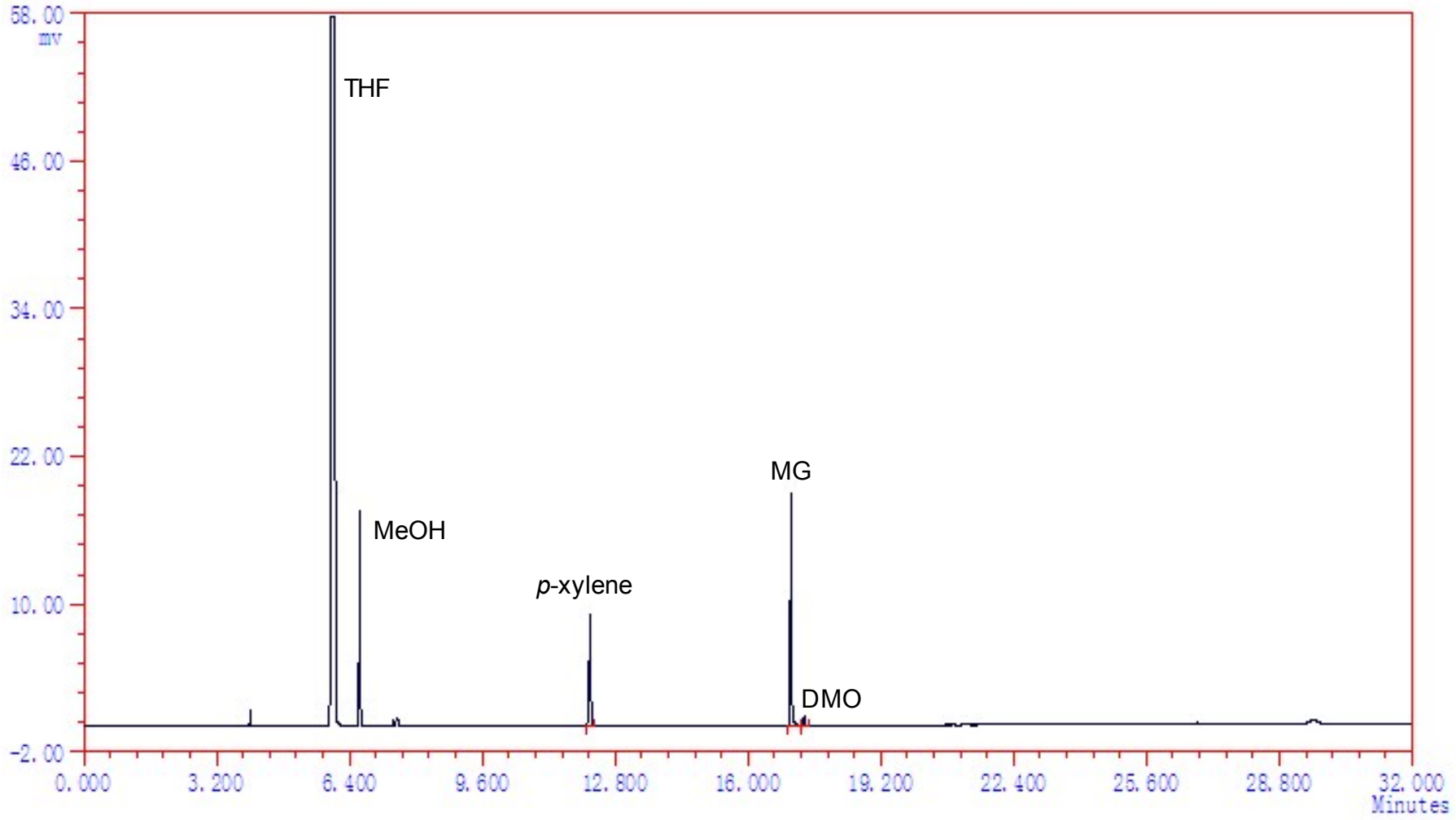

Fig. S19 GC analysis result for H_2-hydrogenation of DMO to MG by **1**/20 NaOMe (entry 1).

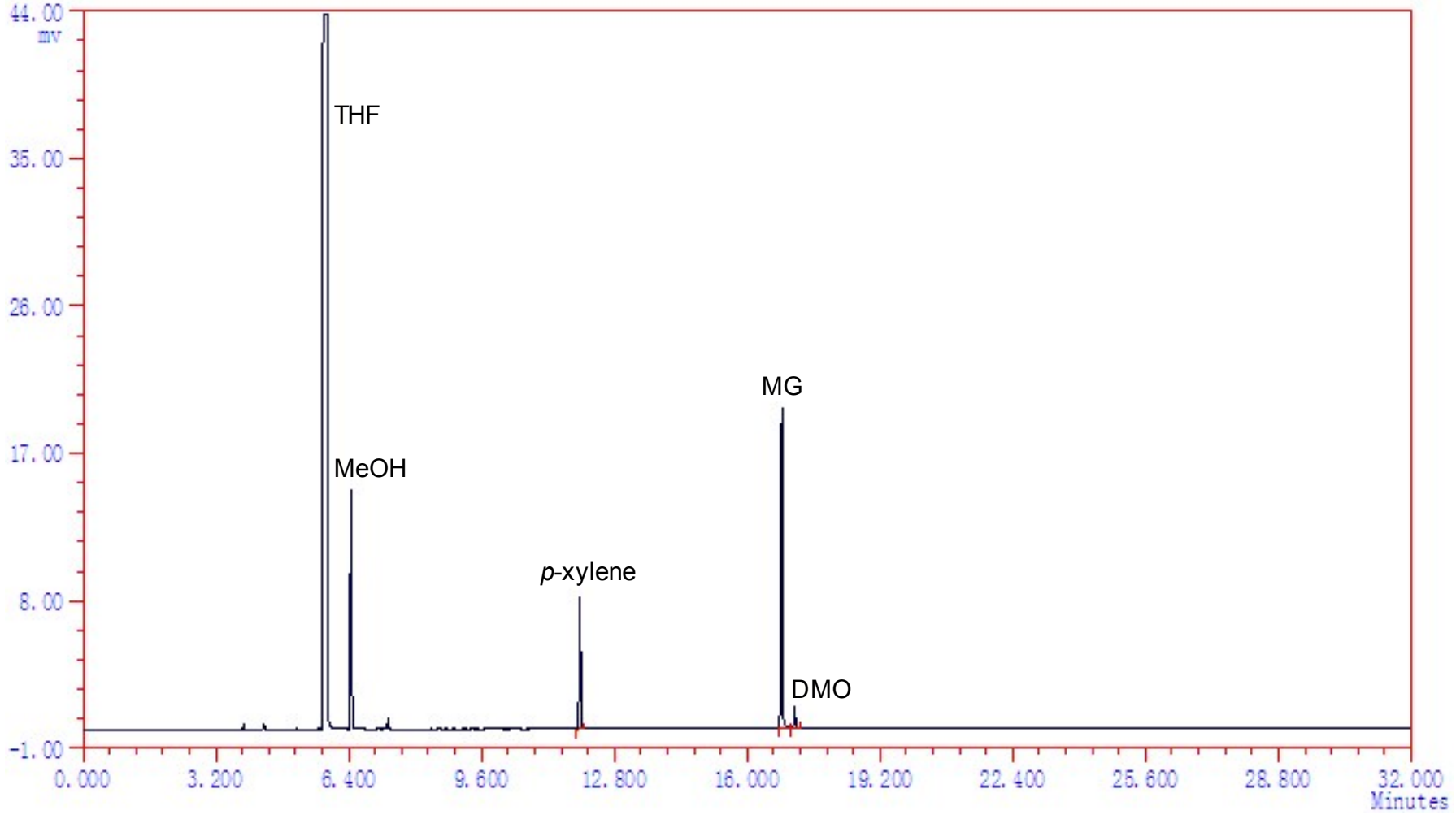

Fig. S20 GC analysis result for H_2-hydrogenation of DMO to MG by **2**/10 NaOMe (entry 2).

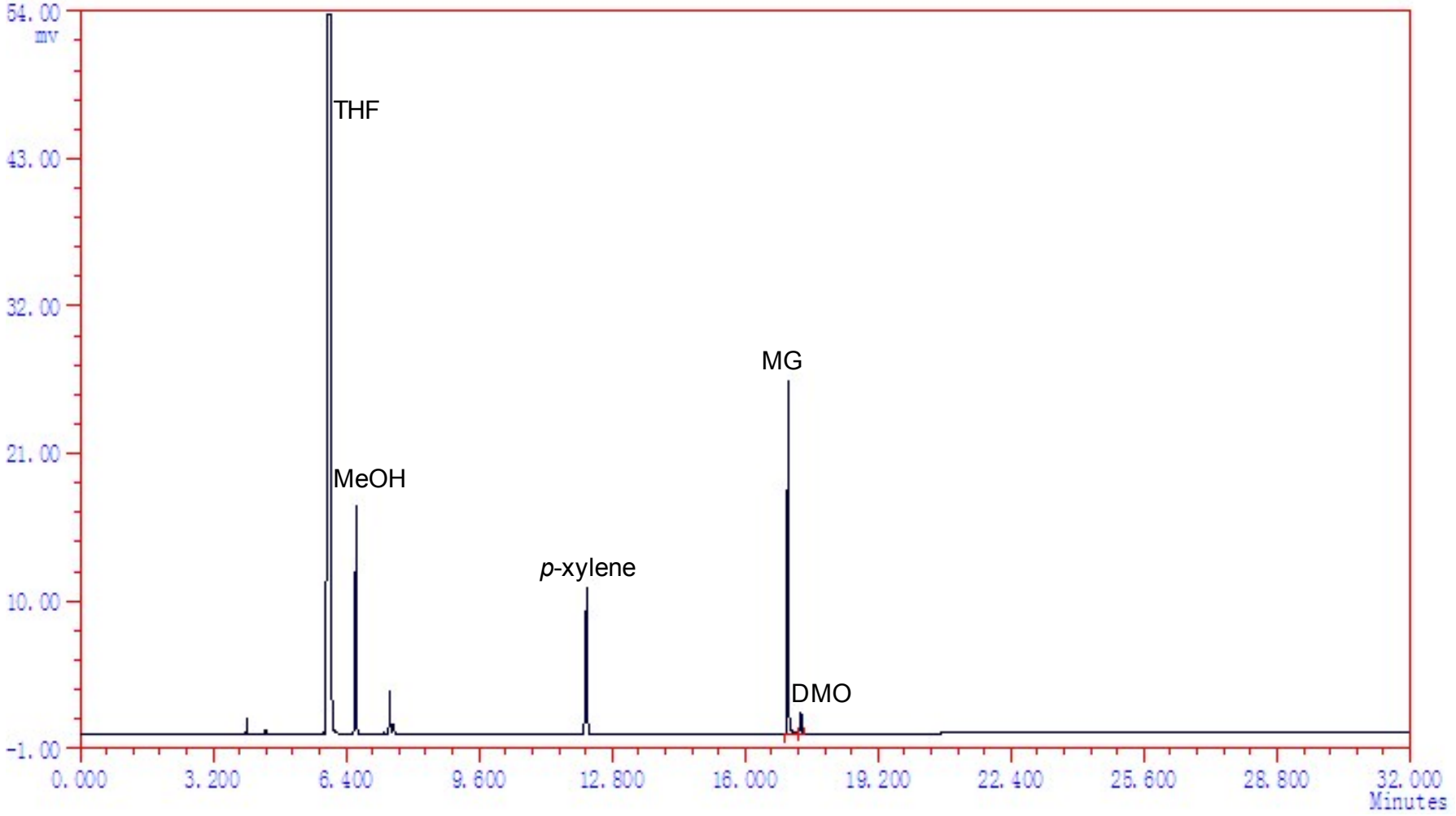

Fig. S21 GC analysis result for H_2-hydrogenation of DMO to MG by **4** (entry 4).

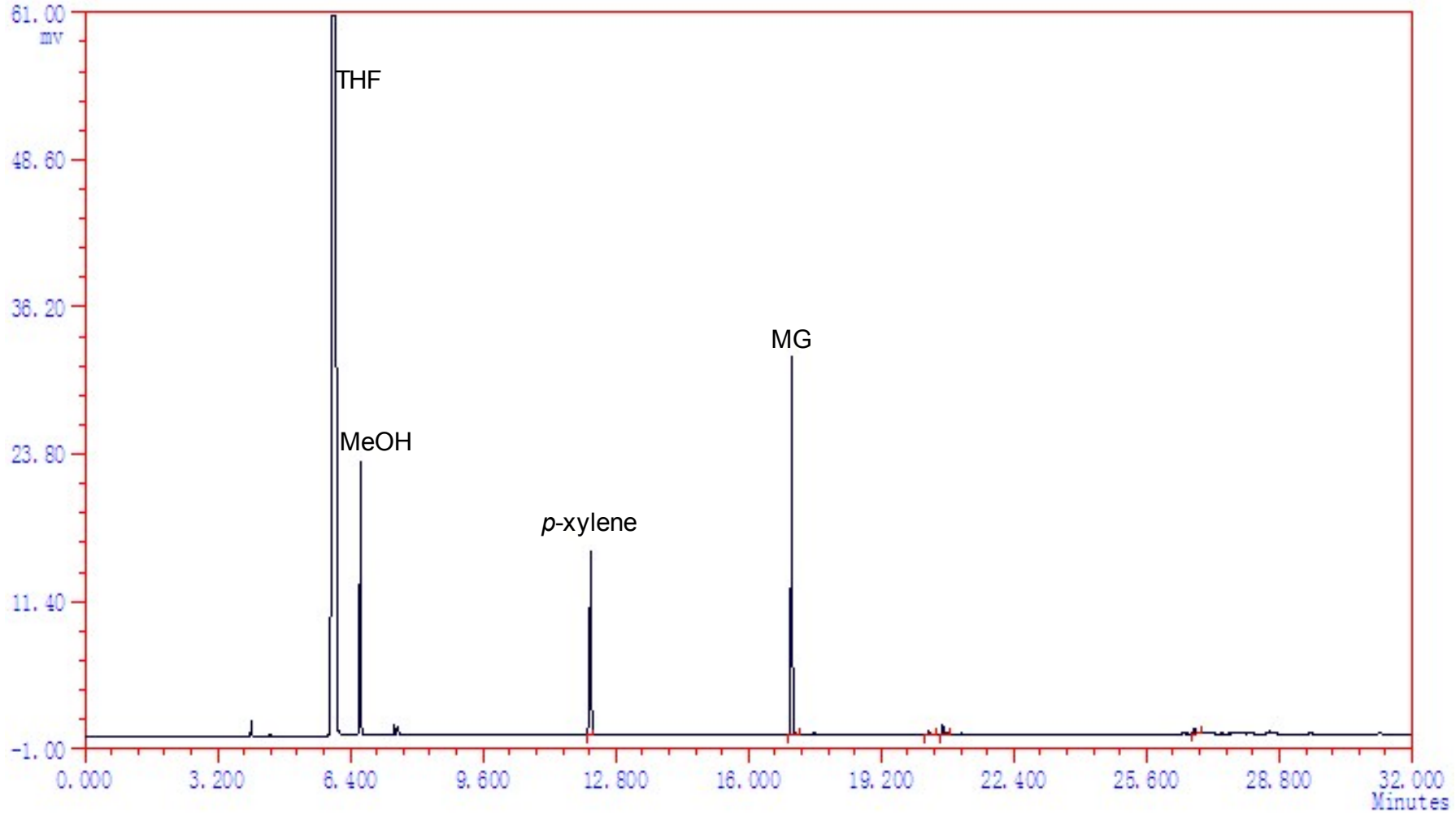

Fig. S22 GC analysis result for H_2-hydrogenation of DMO to MG by **4**/20 NaOMe (entry 5).

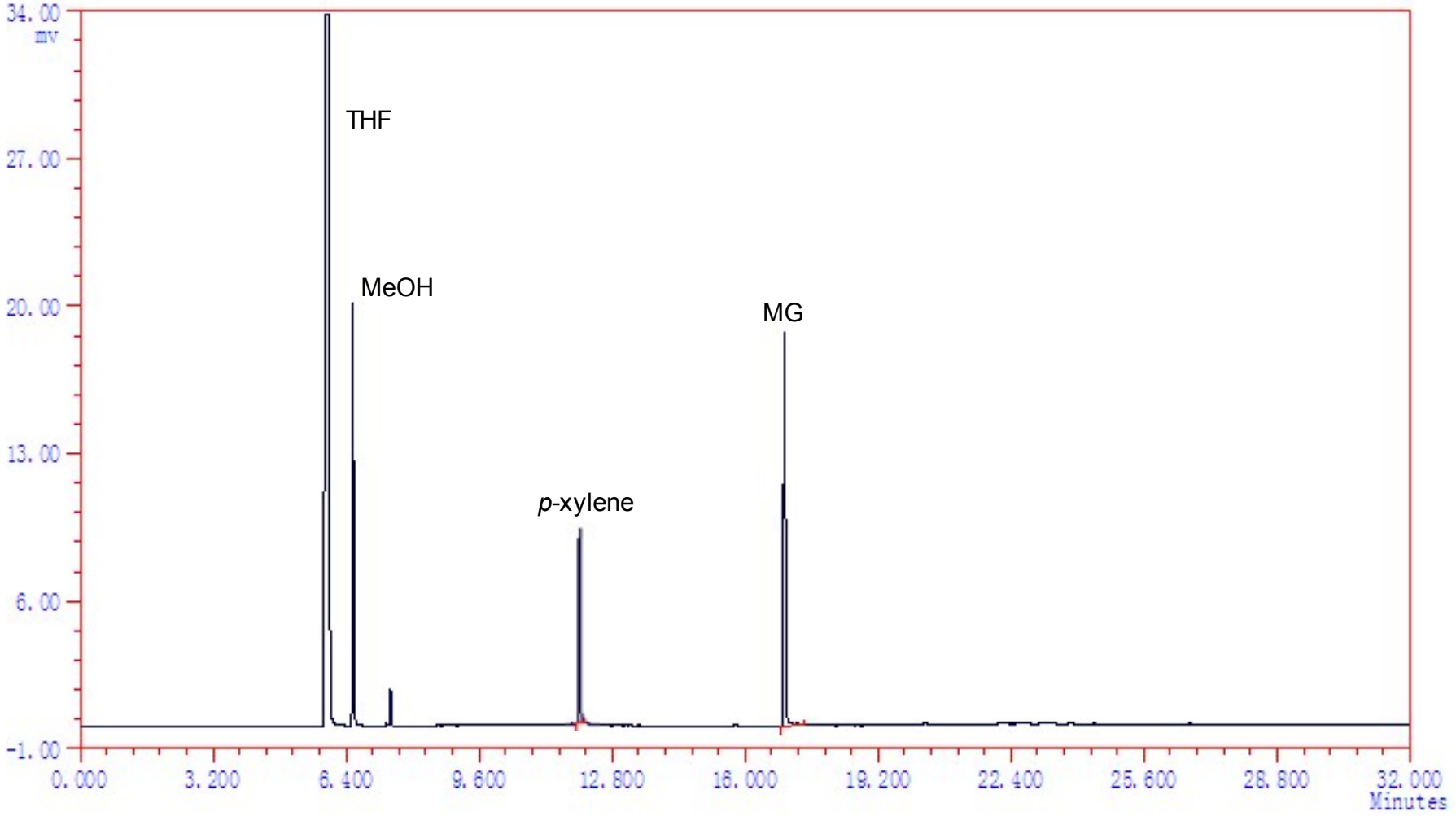

Fig. S23 GC analysis result for H_2-hydrogenation of DMO to MG by **5**/10 NaOMe (entry 6).

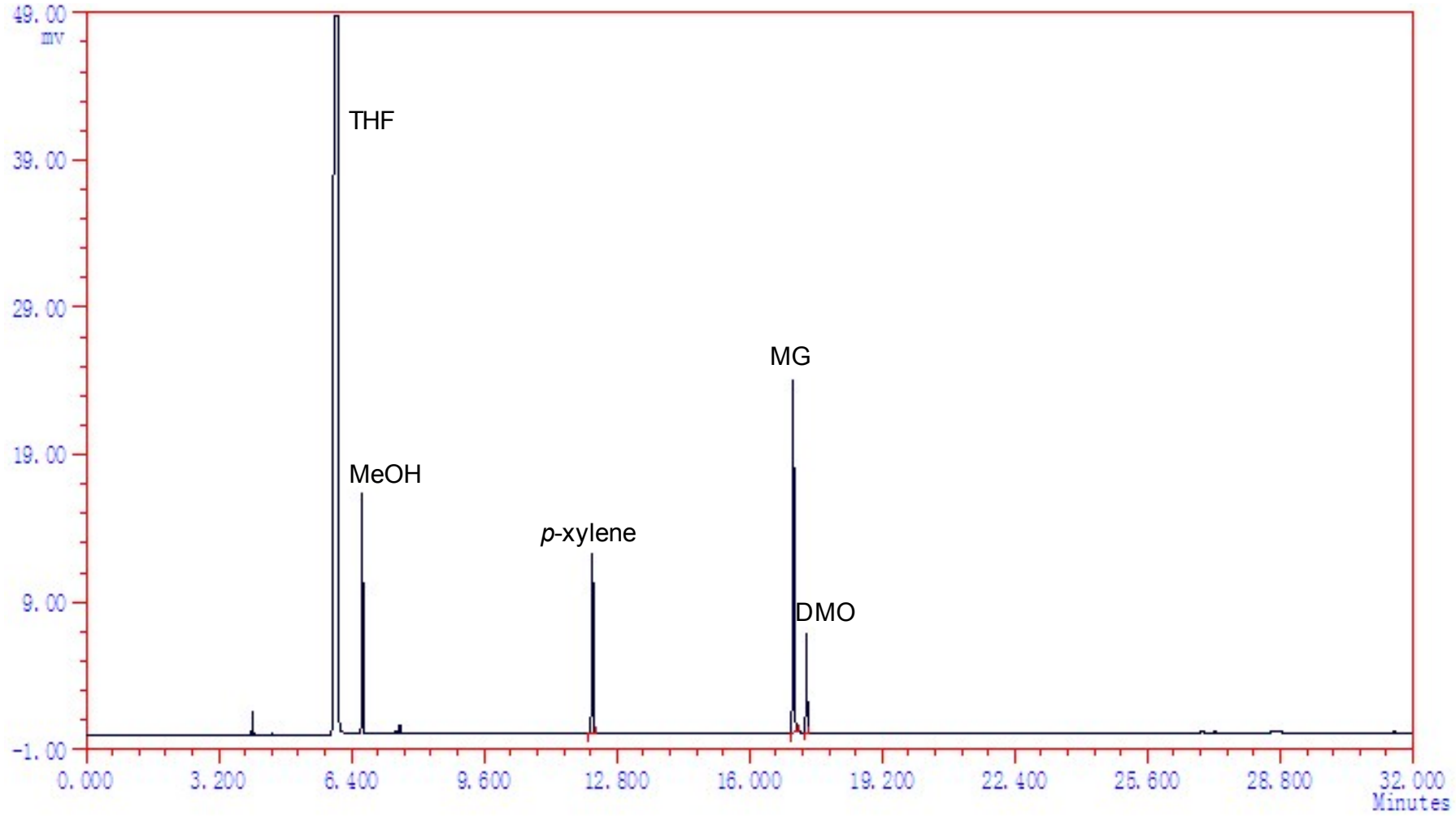

Fig. S24 GC analysis result for H_2-hydrogenation of DMO to MG by **7** (entry 7).

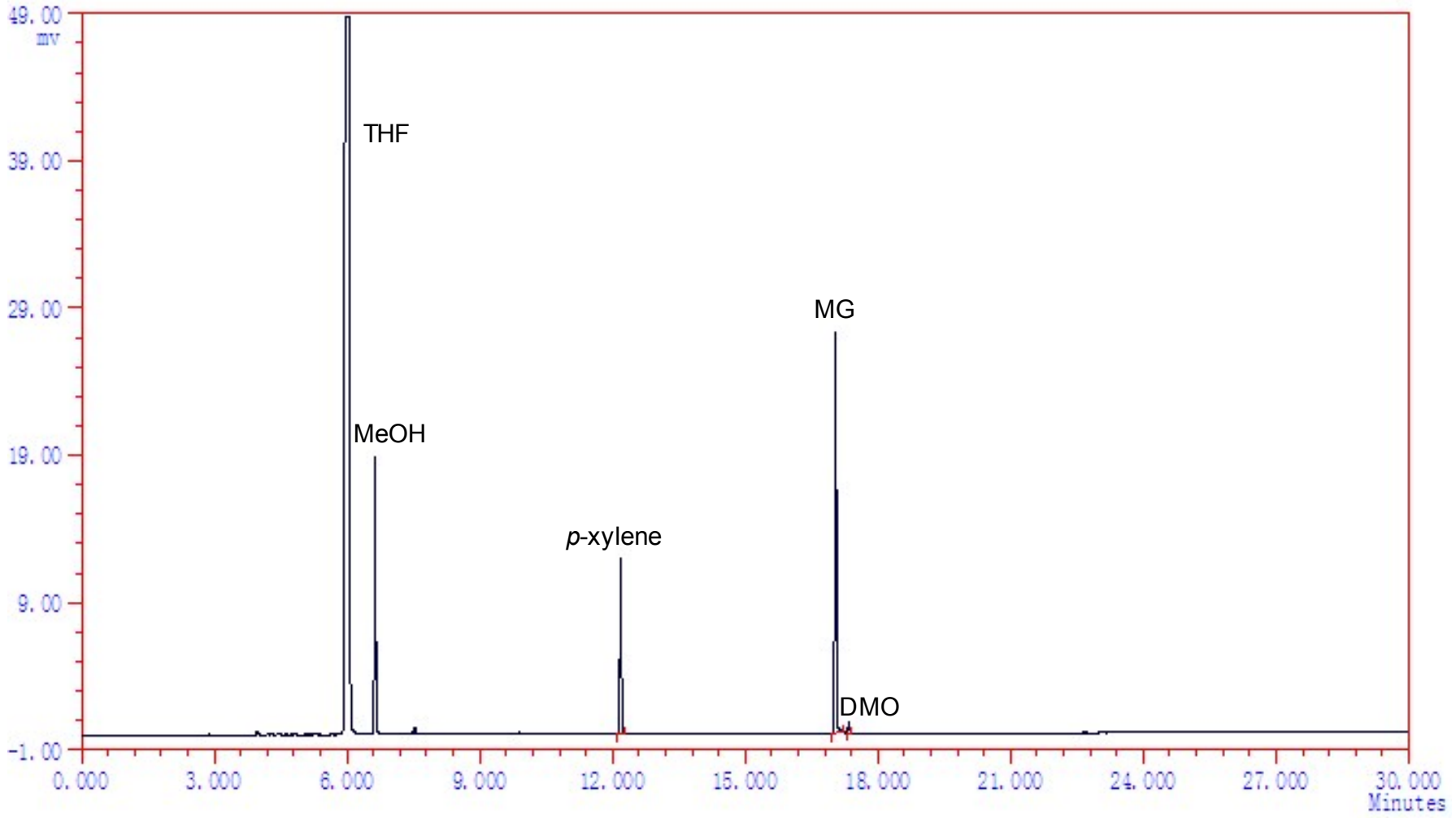

Fig. S25 GC analysis result for H_2-hydrogenation of DMO to MG by **7**/20 NaOMe (entry 8).

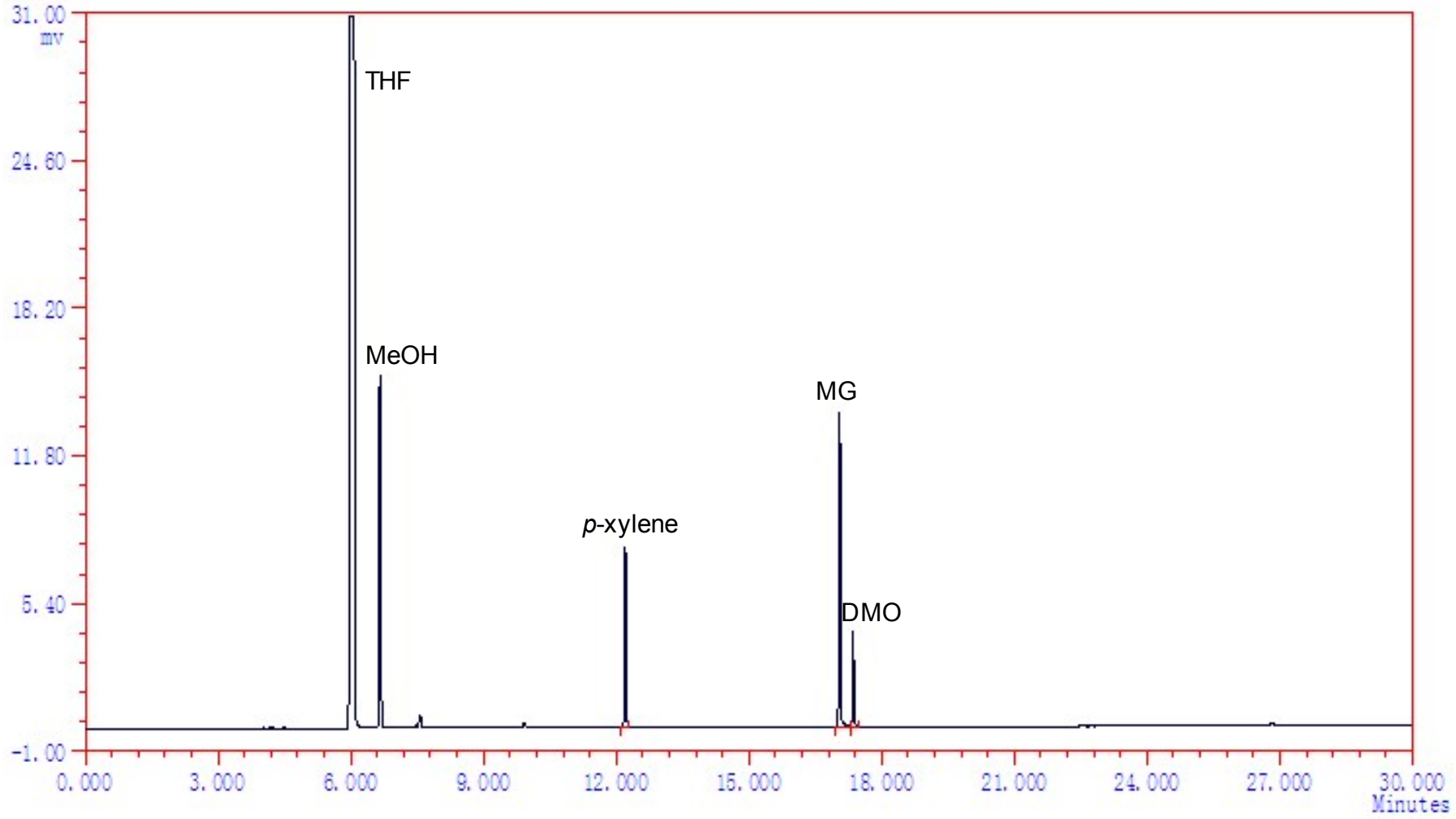

Fig. S26 GC analysis result for H_2-hydrogenation of DMO to MG by **2**/10 NaOMe (entry 12).

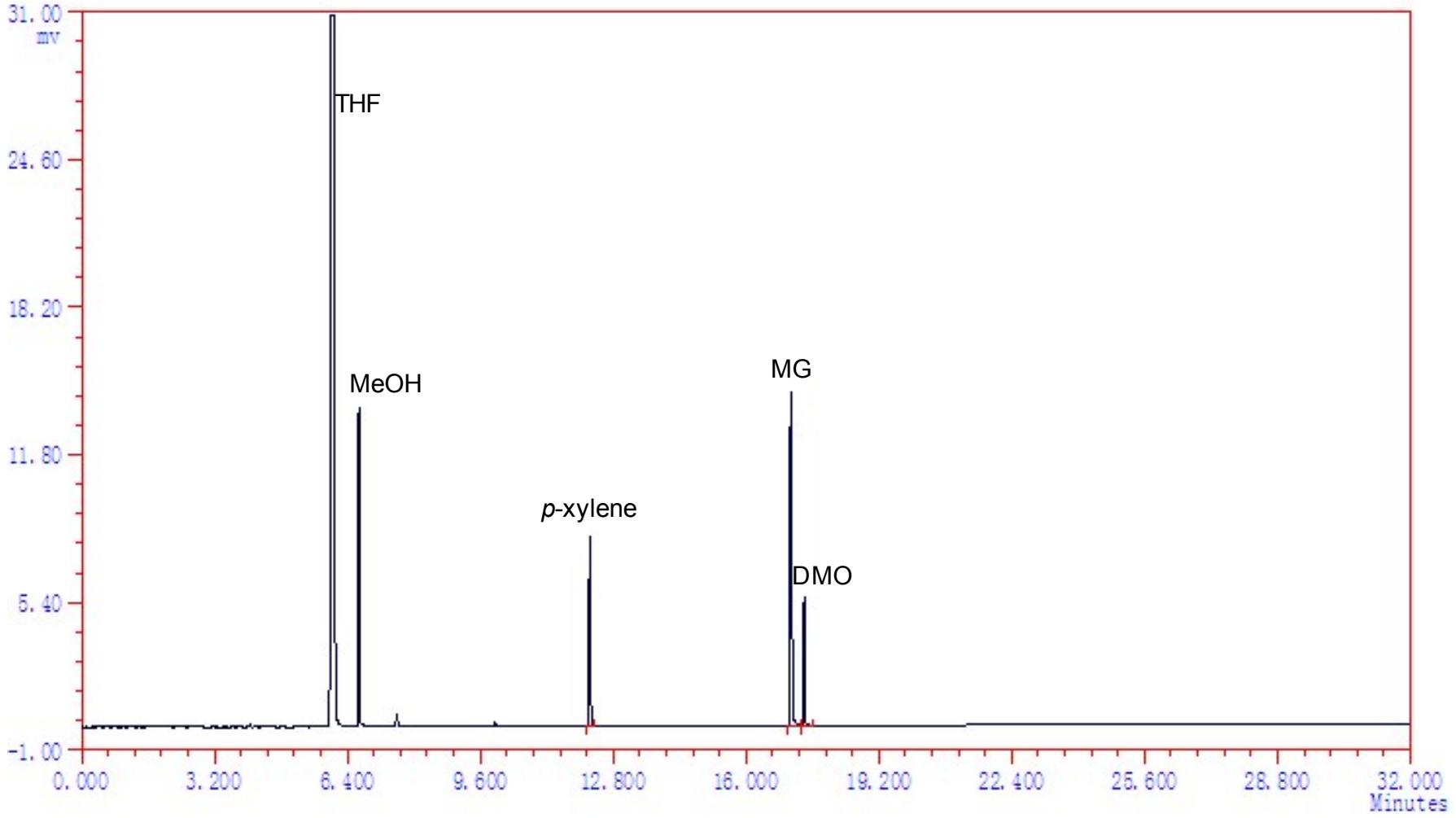

Fig. S27 GC analysis result for H_2-hydrogenation of DMO to MG by **2**/10 NaOMe (entry 14).

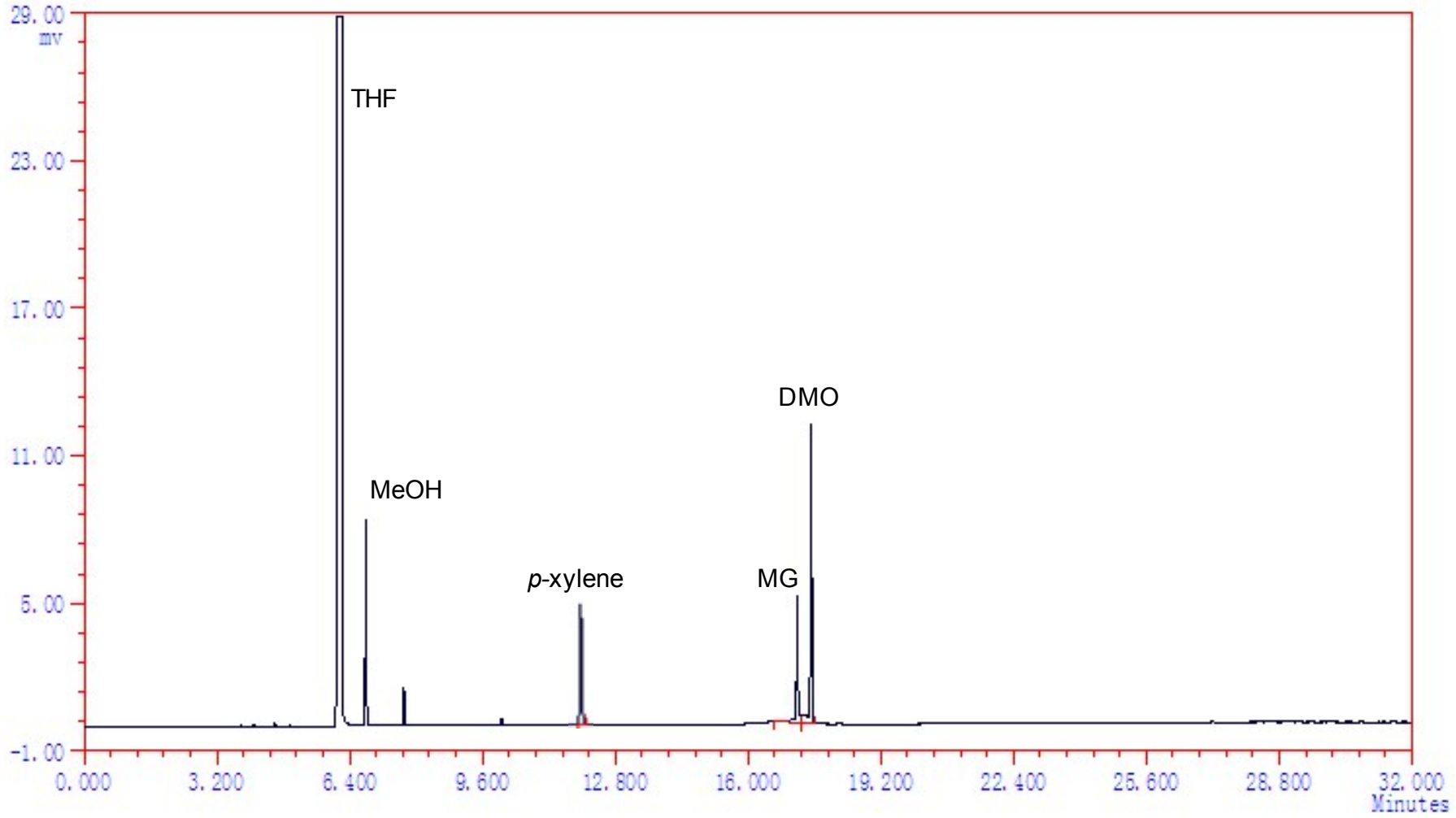

Fig. S28 GC analysis result for H_2-hydrogenation of DMO to MG by **2**/10 NaOMe (entry 17).

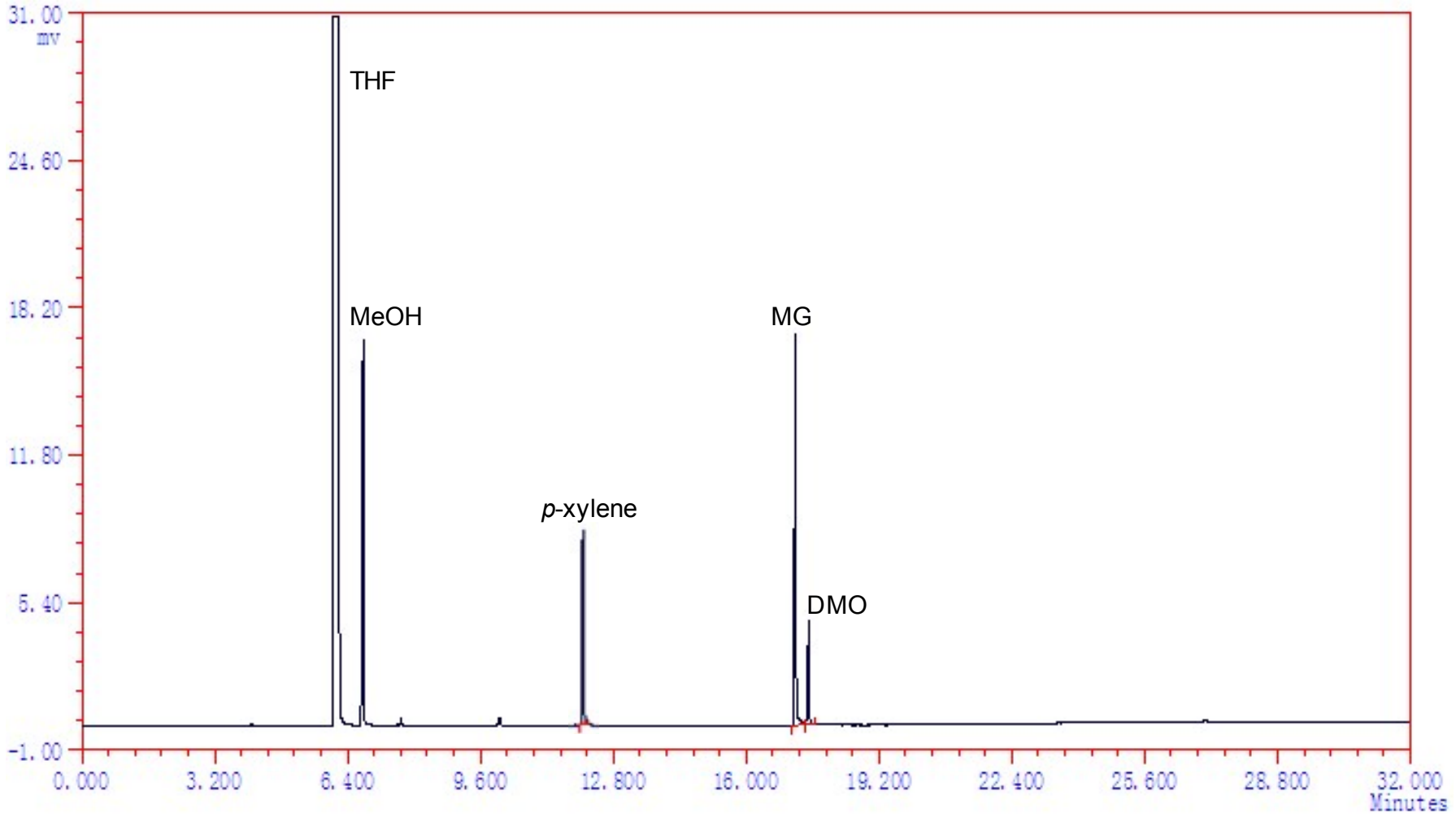

Fig. S29 GC analysis result for H_2-hydrogenation of DMO to MG by **2**/10 NaOMe (entry 21).

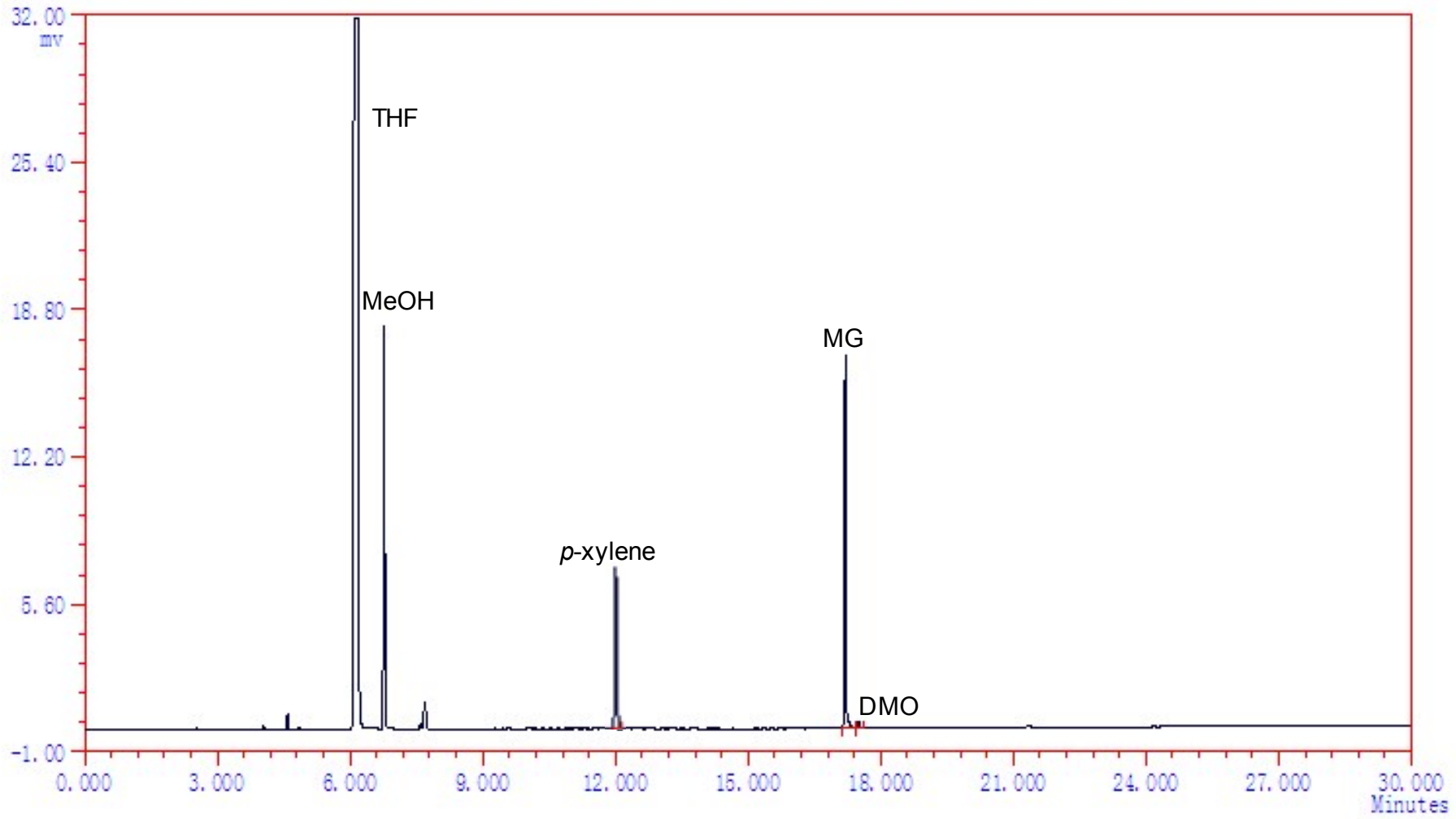

Fig. S30 GC analysis result for H_2-hydrogenation of DMO to MG by **2**/10 NaOMe (entry 22).

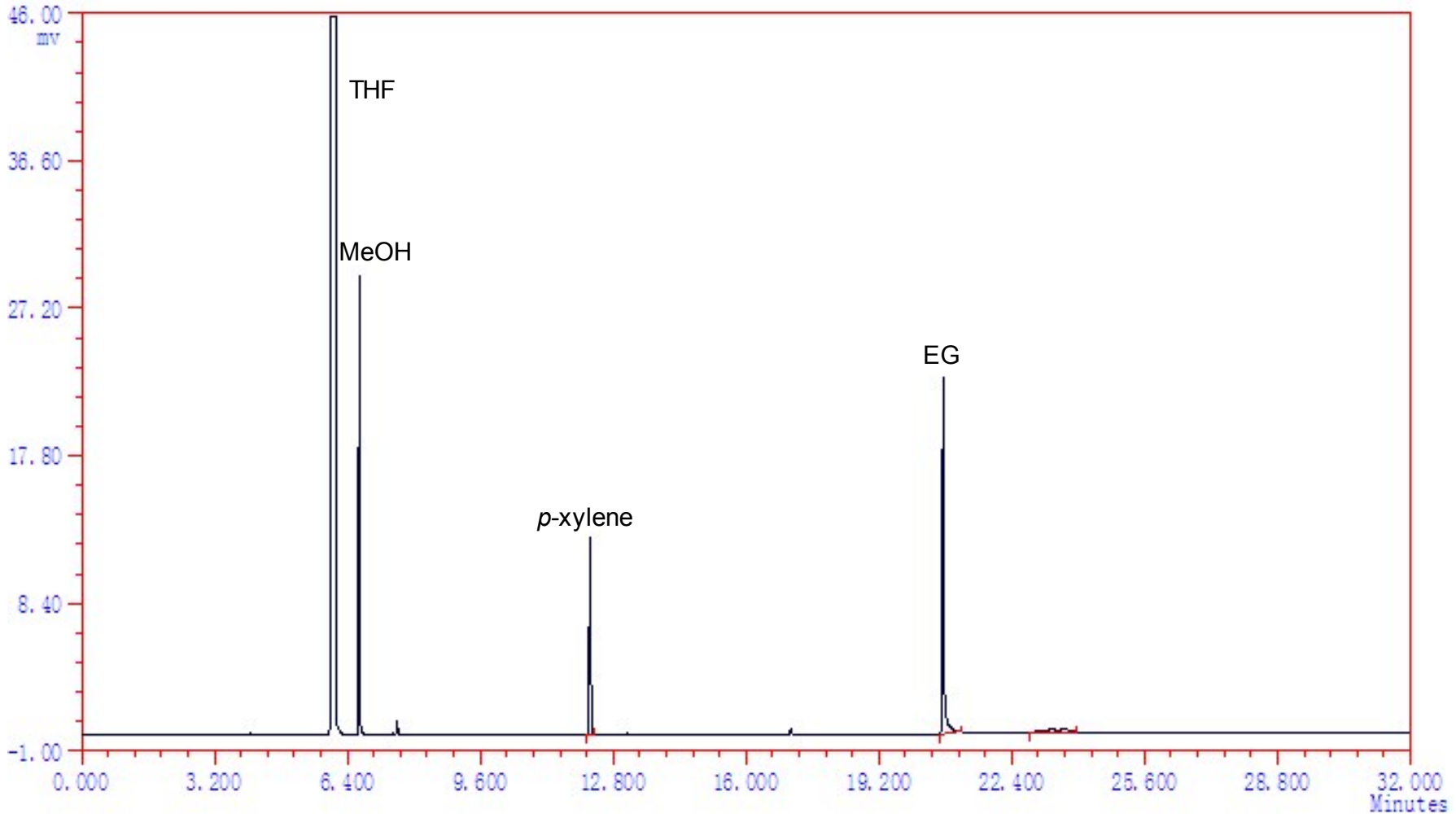

Fig. S31 GC analysis result for H_2-hydrogenation of DMO to EG by **1**/40 NaOMe (entry 25).

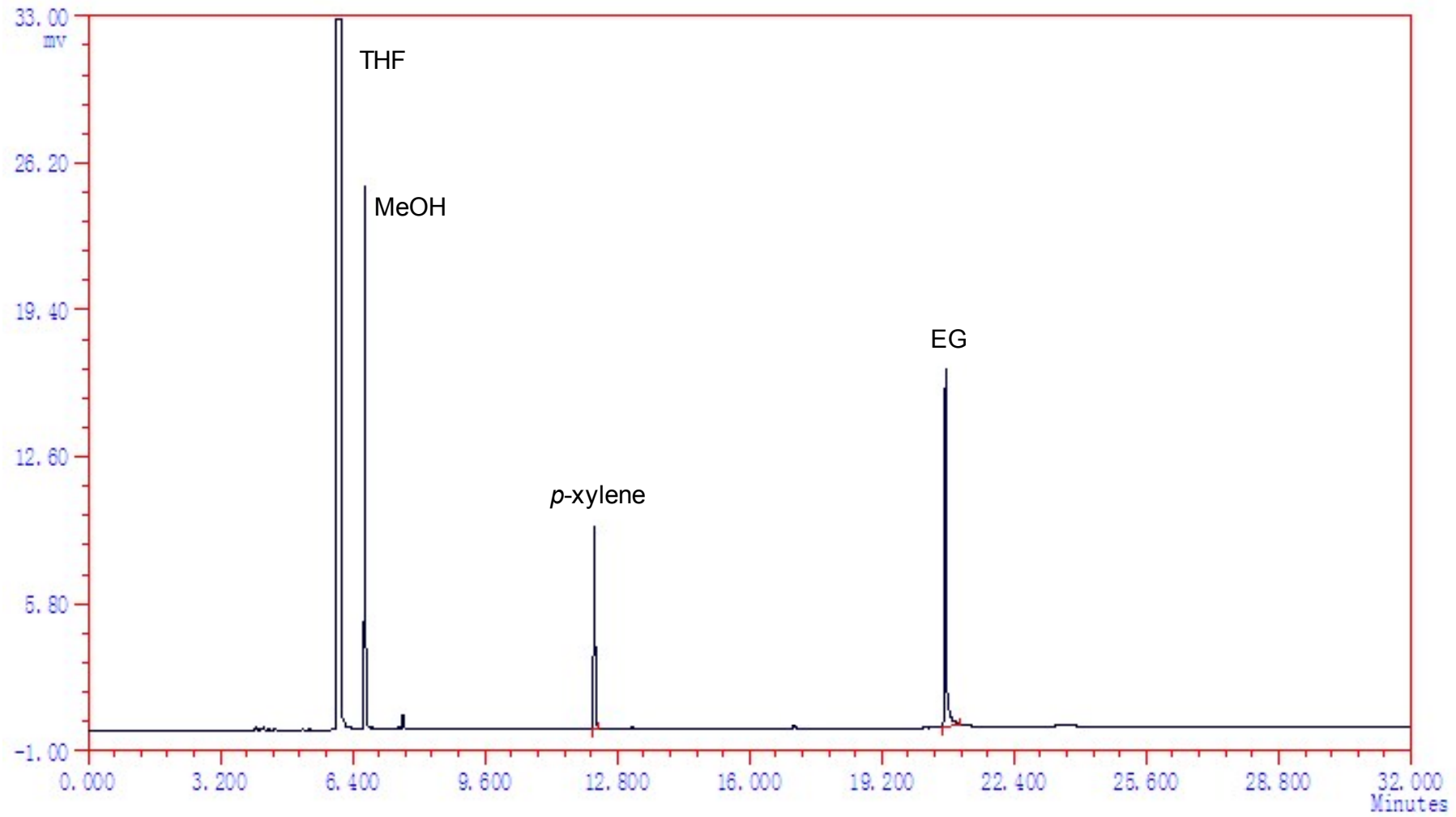

Fig. S32 GC analysis result for H_2-hydrogenation of DMO to EG by **2**/20 NaOMe (entry 29).

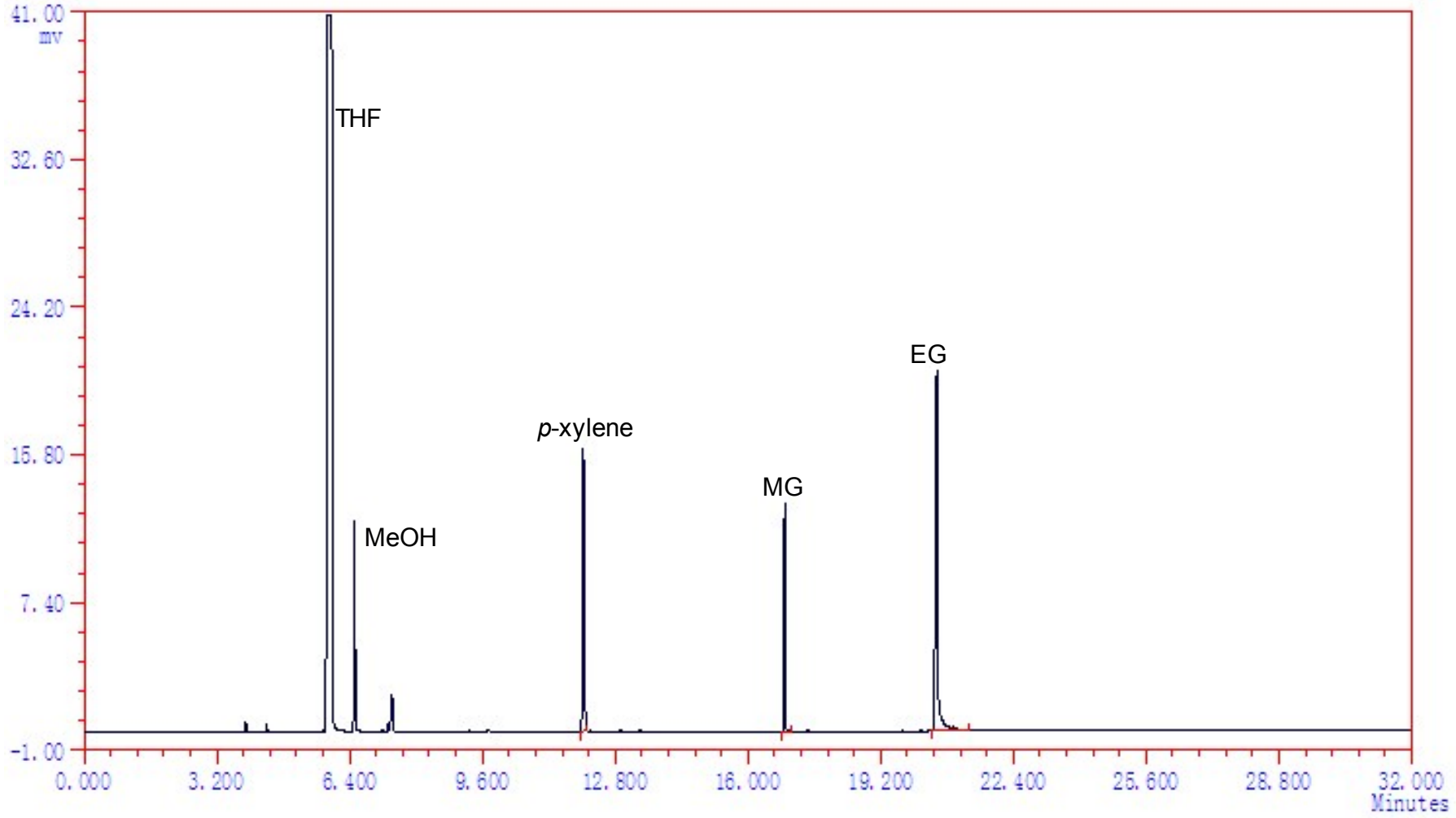

Fig. S33 GC analysis result for H_2-hydrogenation of MG to EG by **1**/40 NaOMe (entry 30).

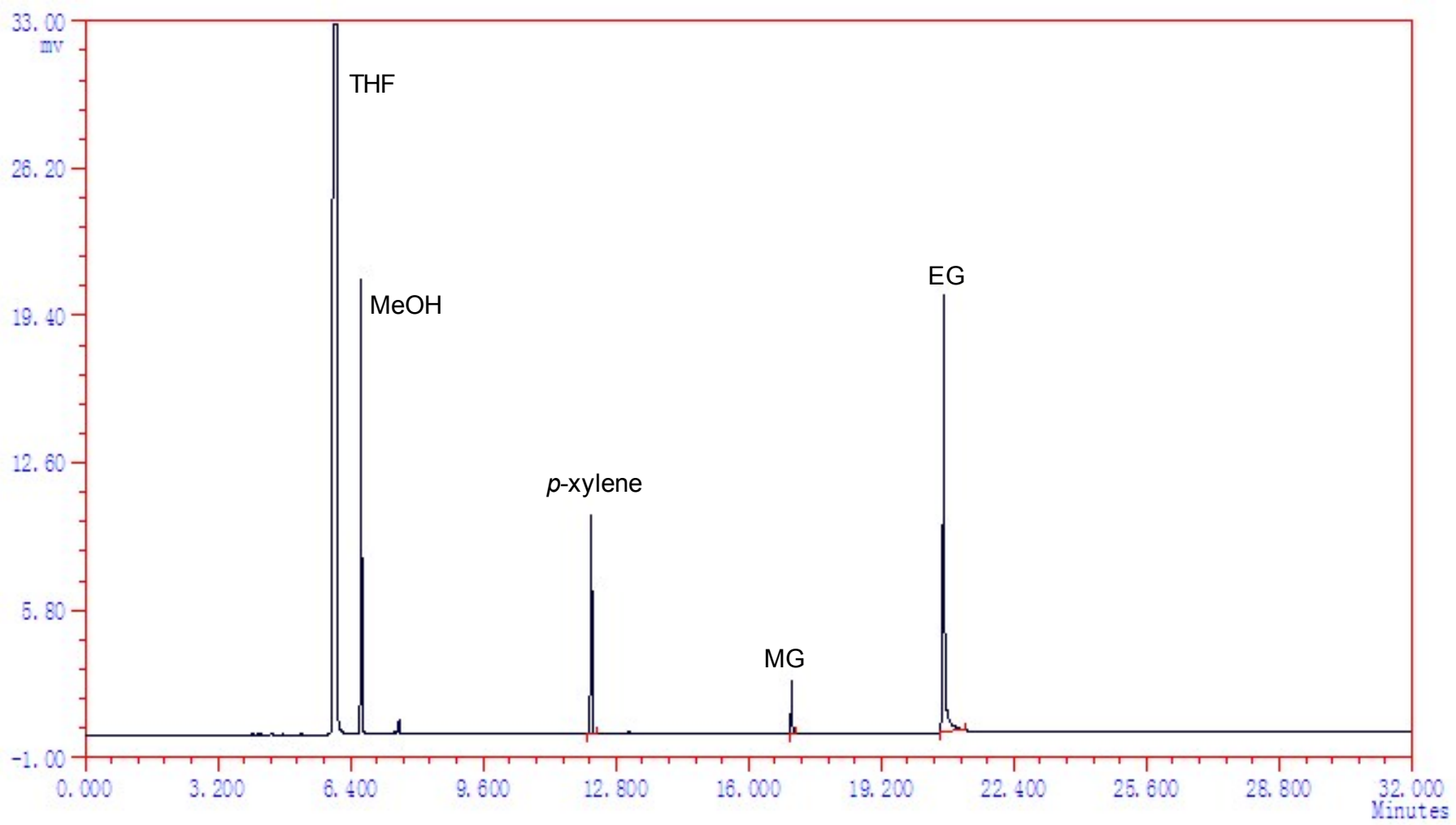

Fig. S34 GC analysis result for H_2-hydrogenation of MG to EG by **2**/20 NaOMe (entry 40).

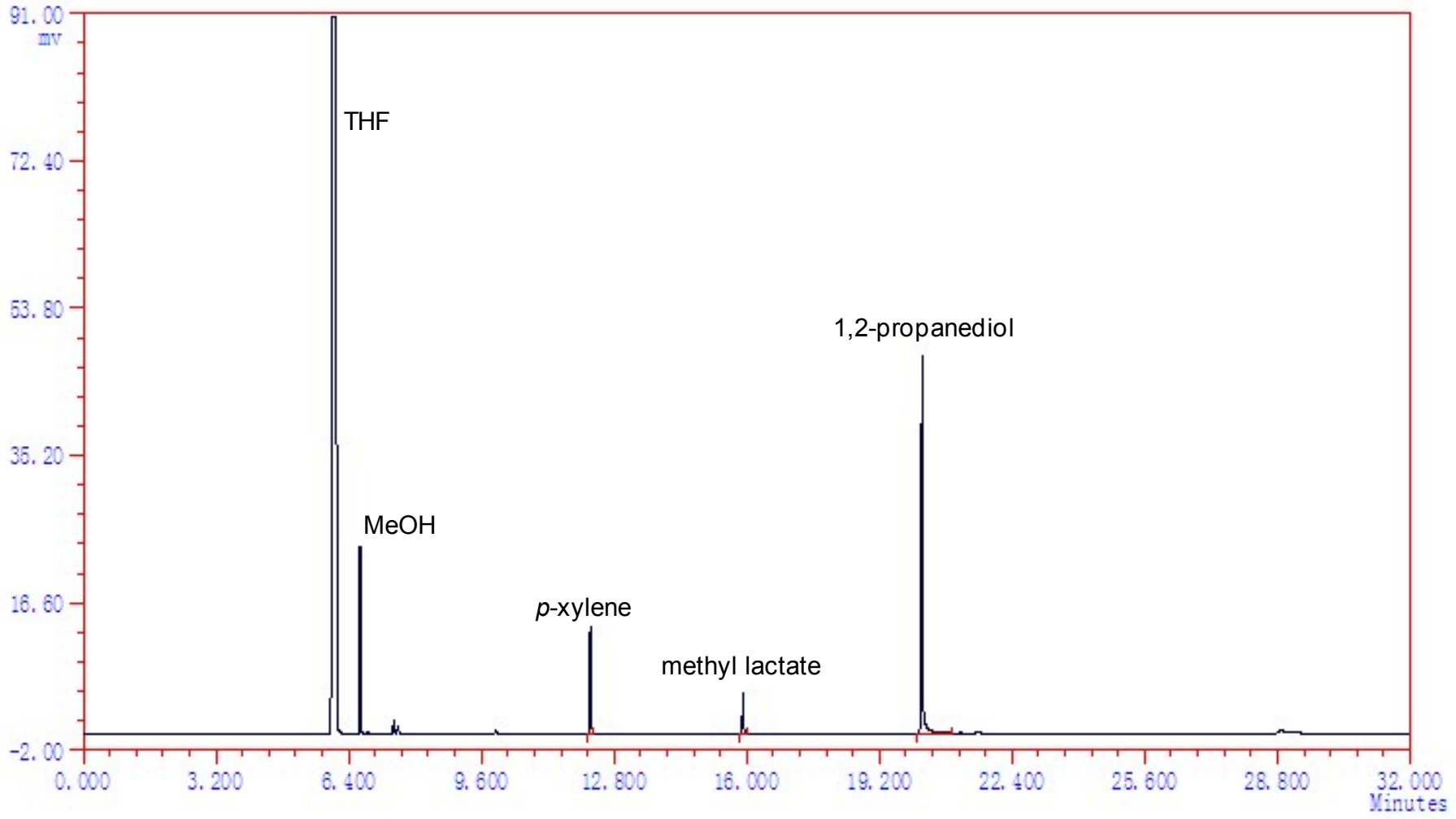

Fig. S35 GC analysis result for H_2-hydrogenation of methyl lactate to 1,2-propanediol by **1**/40 NaOMe (entry 31).

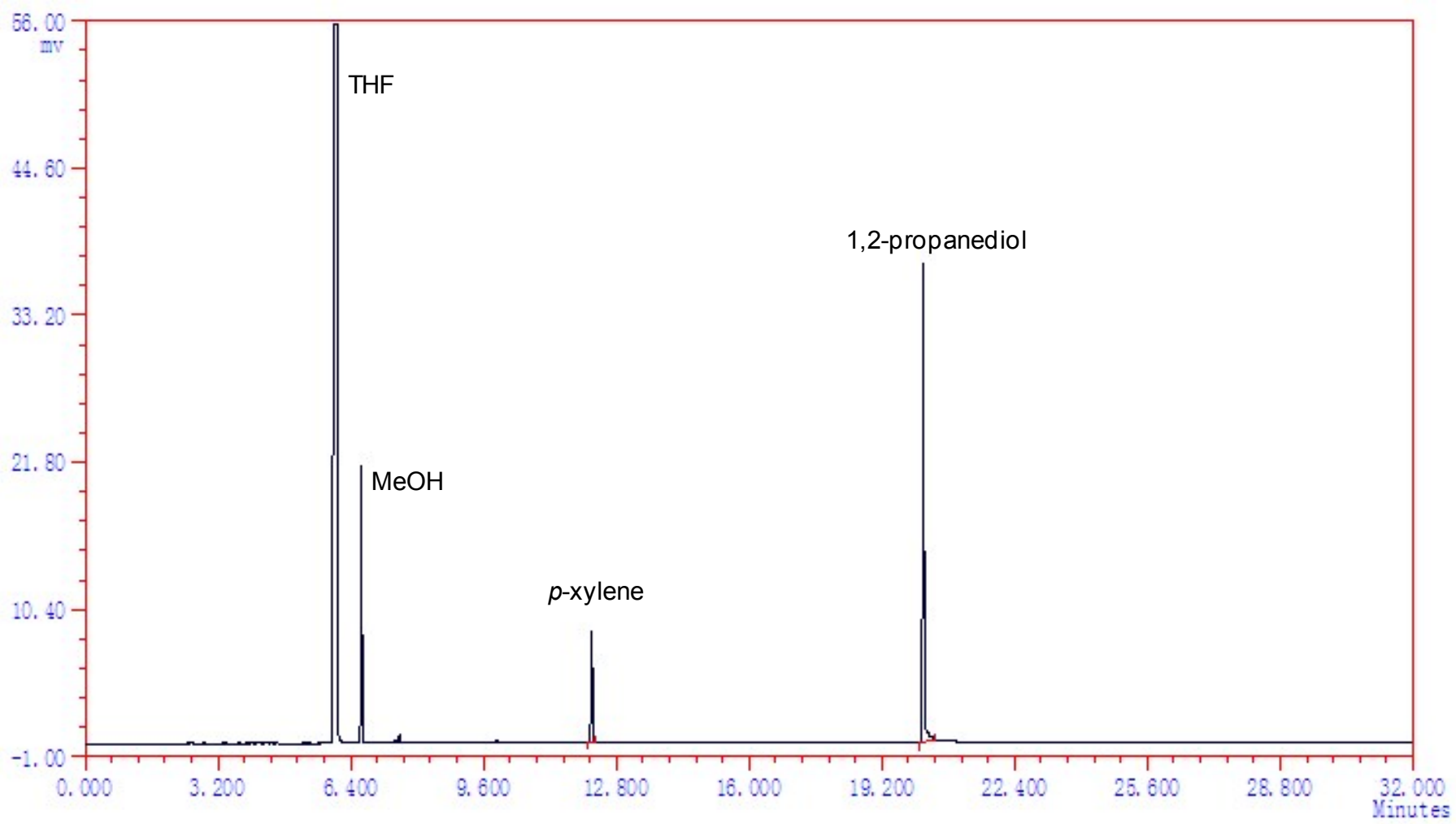

Fig. S36 GC analysis result for H_2-hydrogenation of methyl lactate to 1,2-propanediol by **2**/20 NaOMe (entry 41).

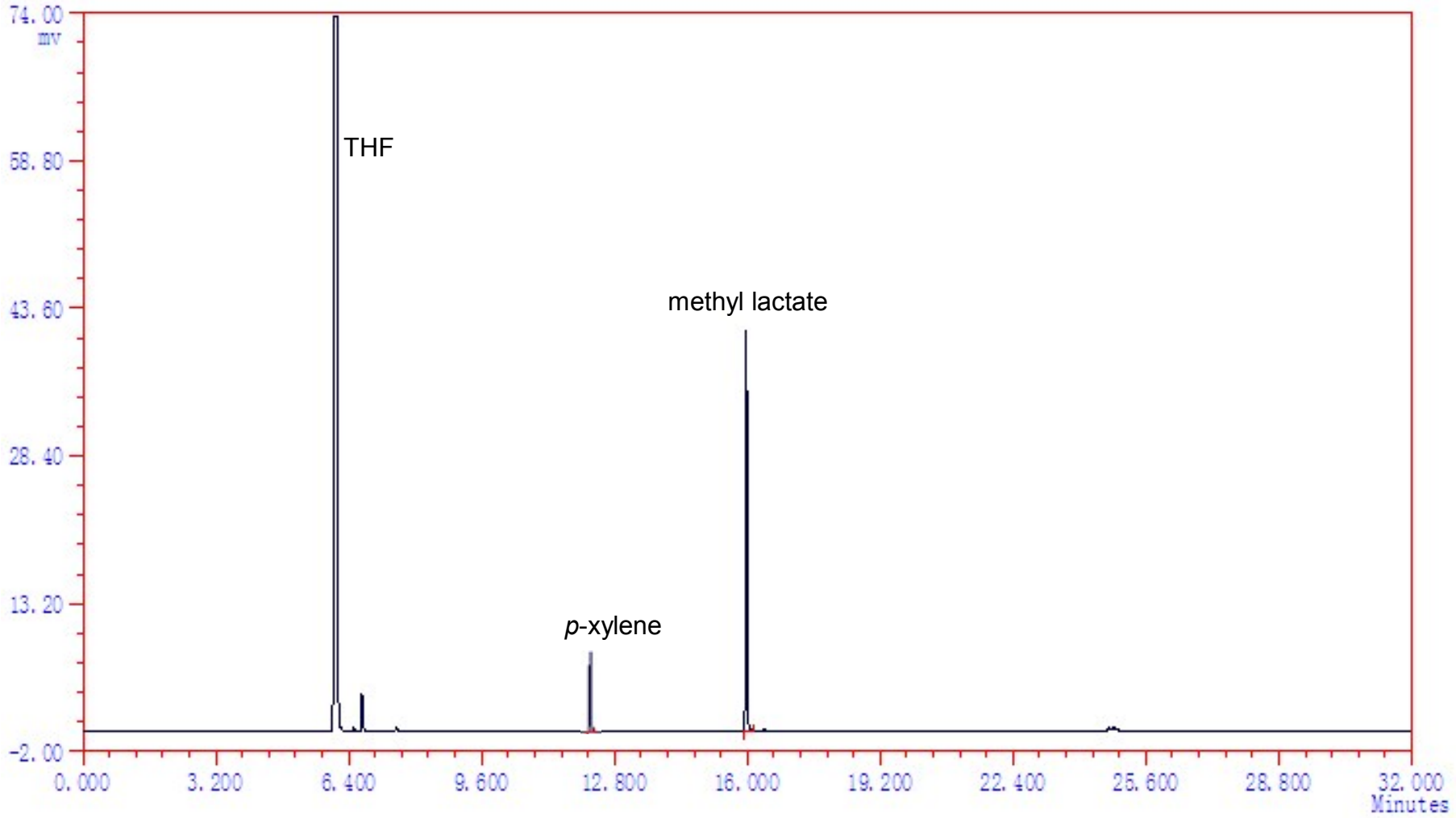

Fig. S37 GC analysis result for H_2-hydrogenation of methyl pyruvate to methyl lactate by **1**/40 NaOMe (entry 32).

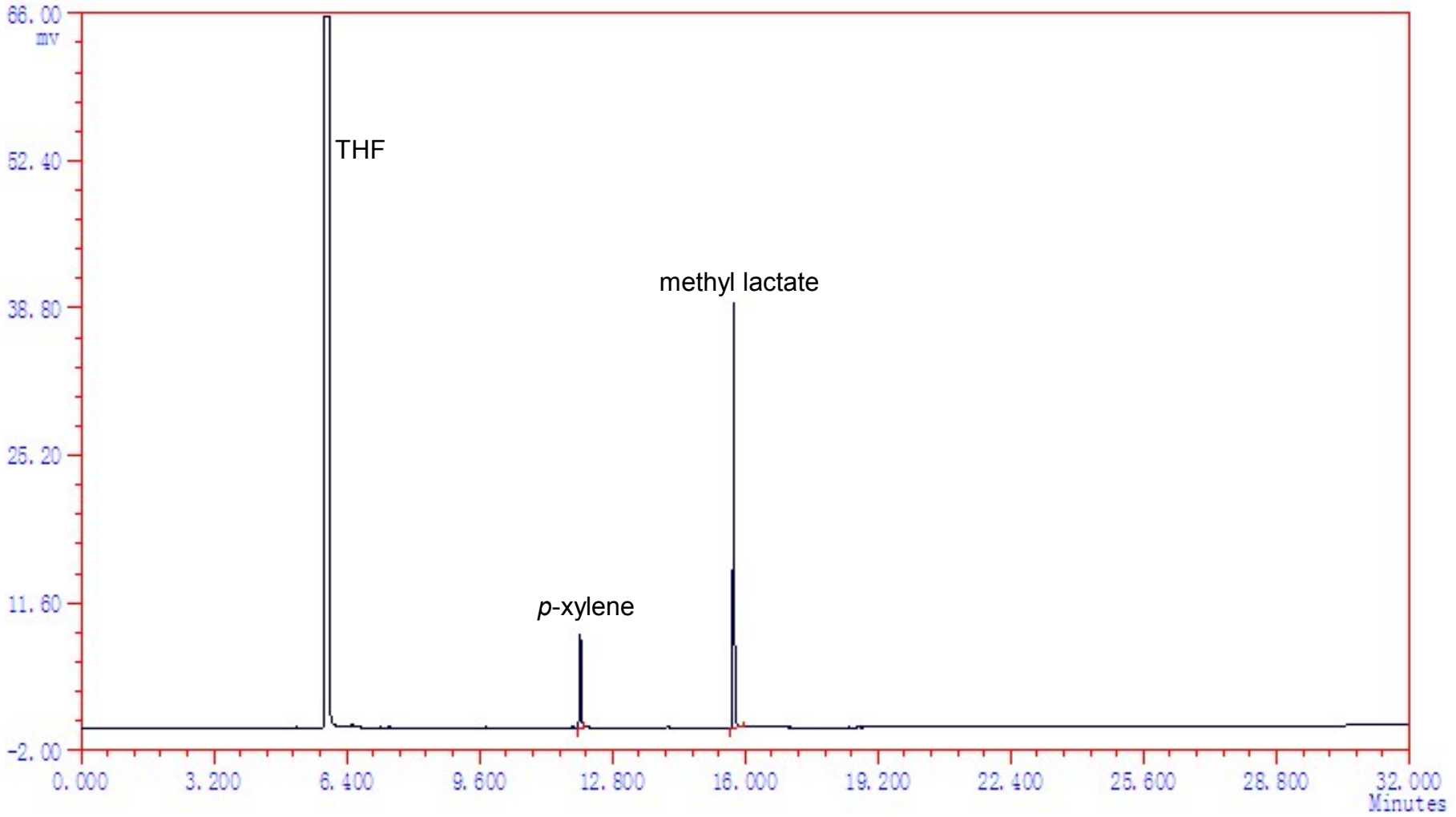

Fig. S38 GC analysis result for H_2-hydrogenation of methyl pyruvate to methyl lactate by **2**/20 NaOMe (entry 42).

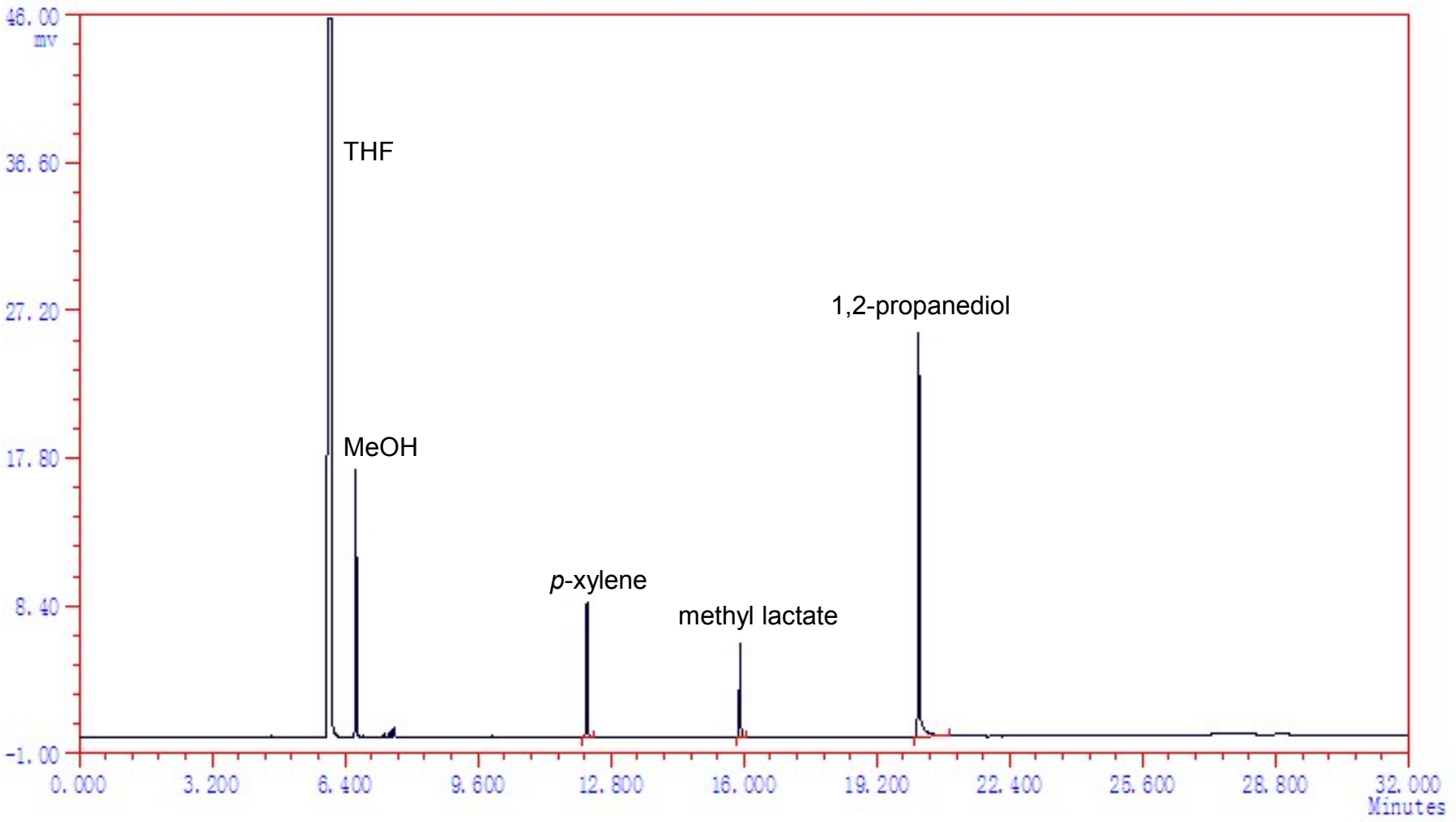

Fig. S39 GC analysis result for H_2-hydrogenation of methyl pyruvate to 1,2-propanediol by **1**/40 NaOMe (entry 33).

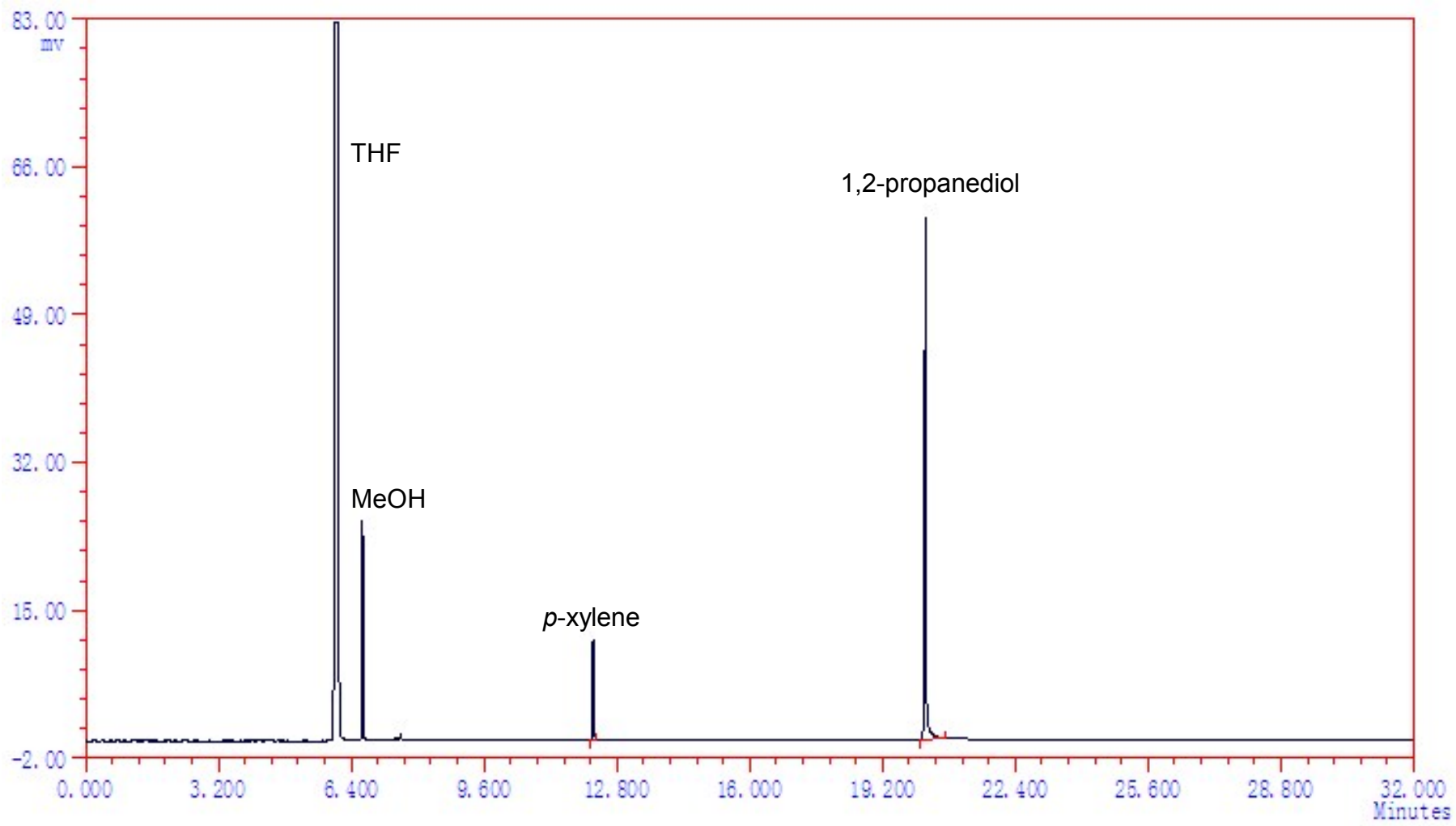

Fig. S40 GC analysis result for H_2-hydrogenation of methyl pyruvate to 1,2-propanediol by **2**/20 NaOMe (entry 43).

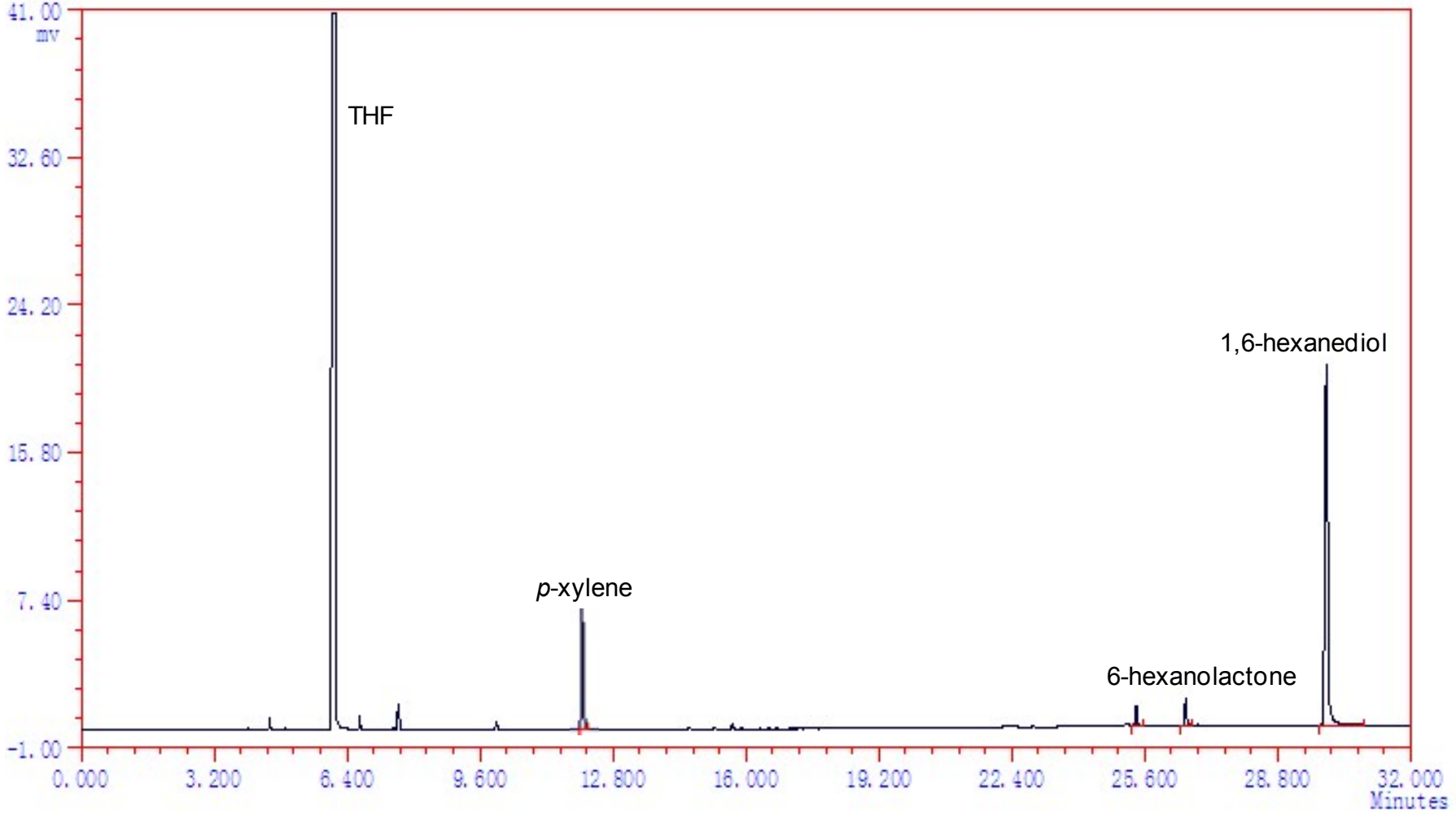

Fig. S41 GC analysis result for H_2-hydrogenation of 6-hexanolactone to 1,6-hexanediol by **1**/40 NaOMe (entry 34).

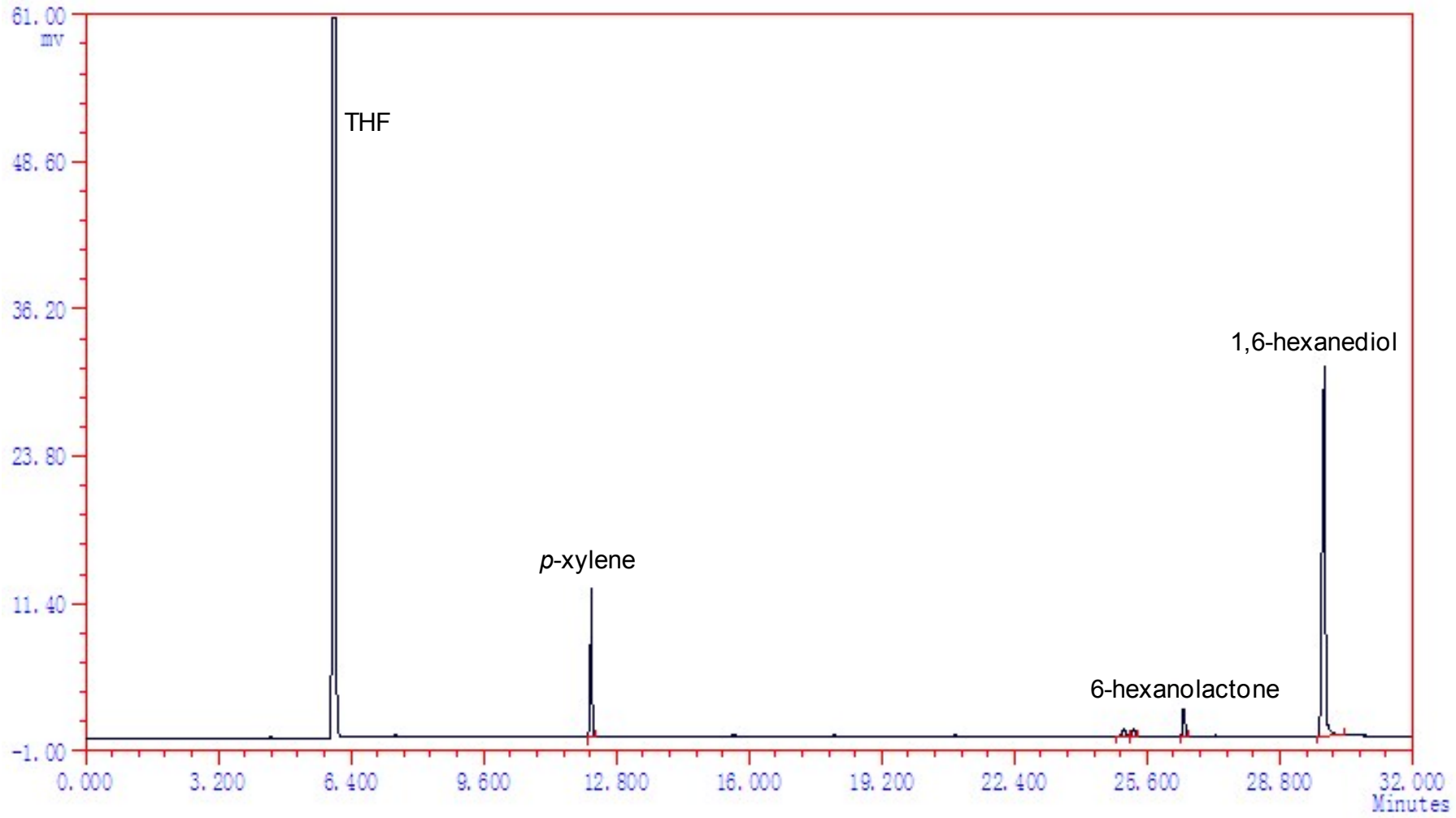

Fig. S42 GC analysis result for H_2-hydrogenation of 6-hexanolactone to 1,6-hexanediol by **2**/20 NaOMe (entry 44).

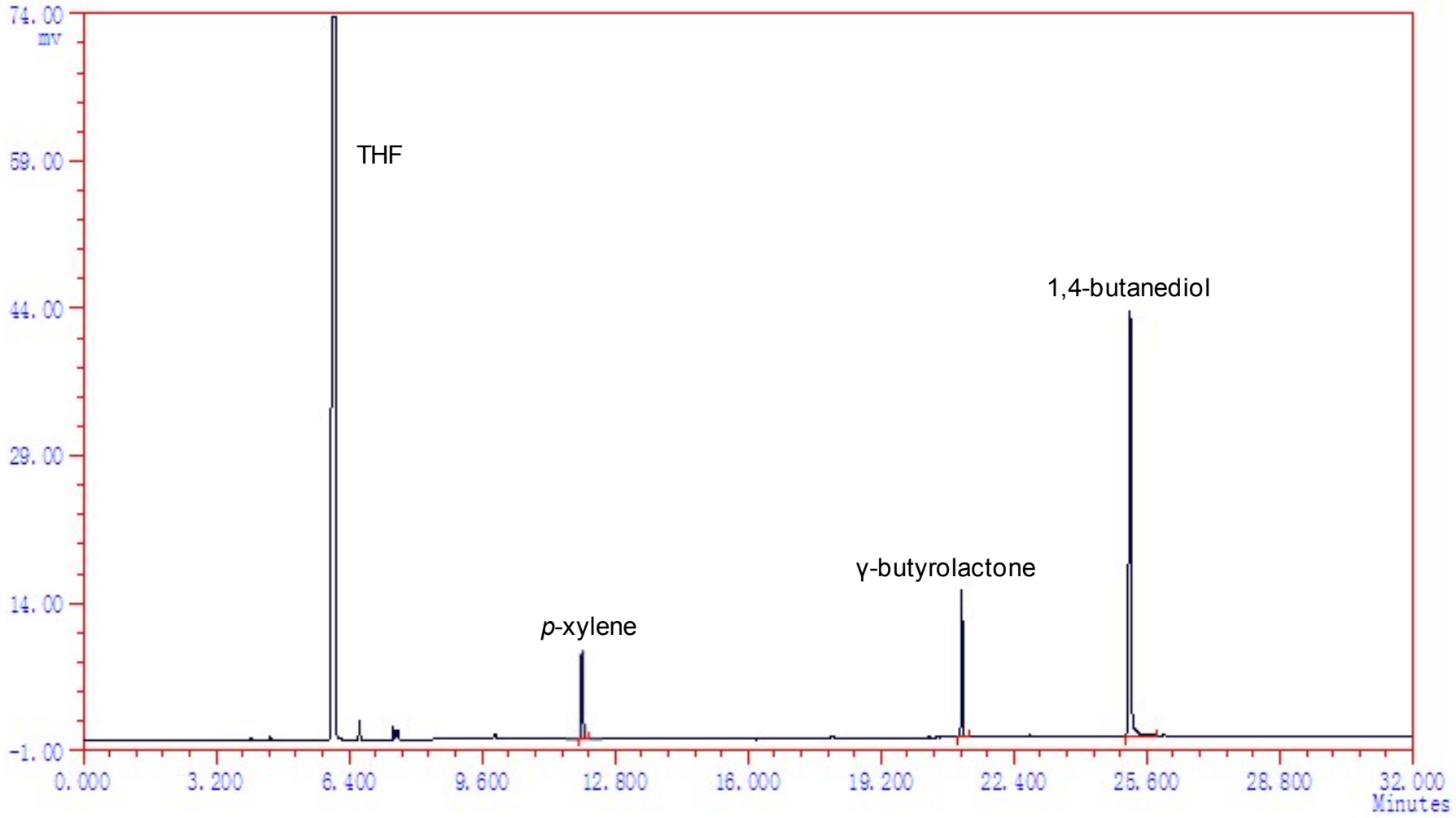

Fig. S43 GC analysis result for H_2-hydrogenation of γ-butyrolactone to 1,4-butanediol by **1**/40 NaOMe (entry 35).

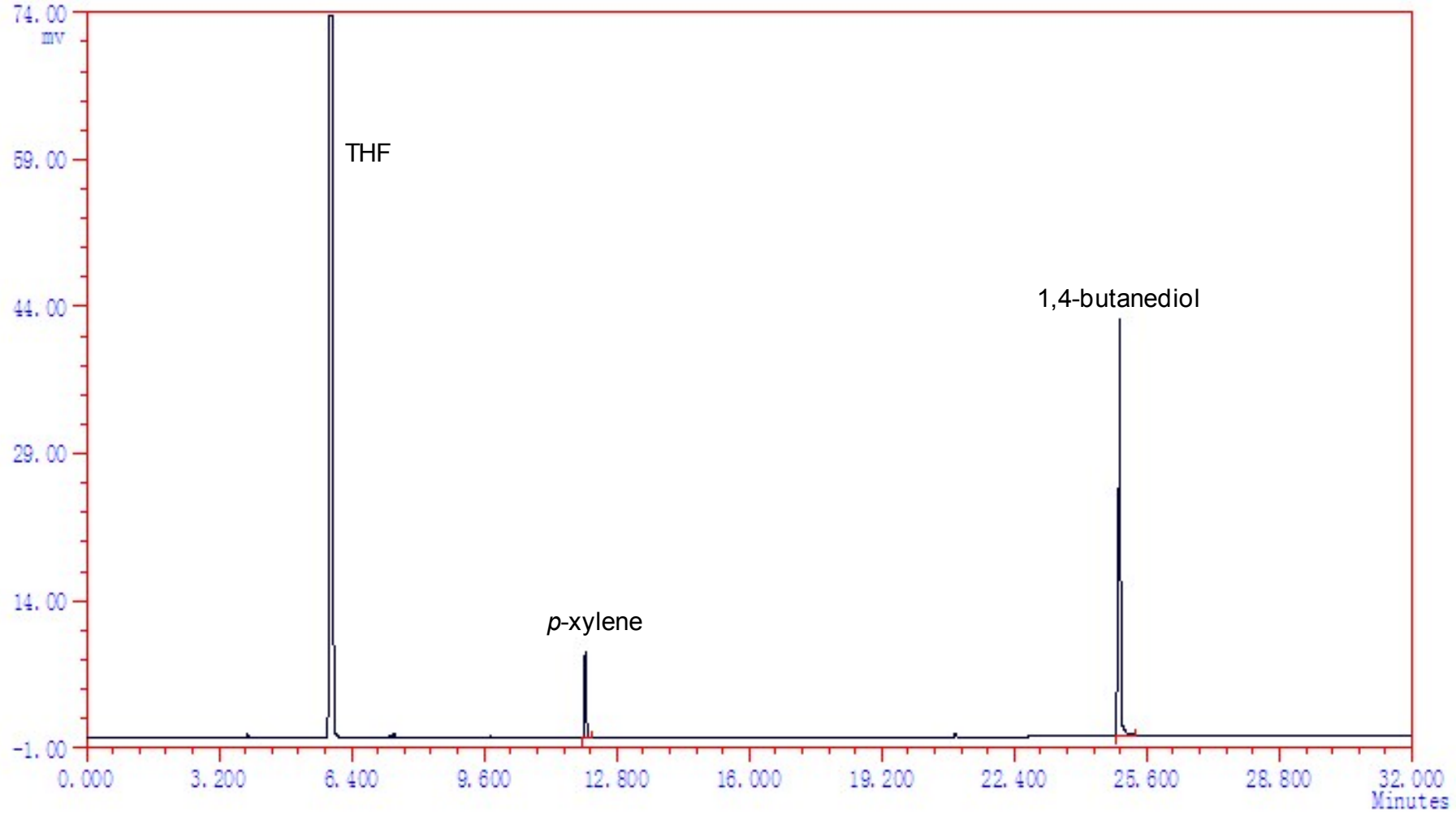

Fig. S44 GC analysis result for H_2-hydrogenation of γ-butyrolactone to 1,4-butanediol by **2**/20 NaOMe (entry 45).

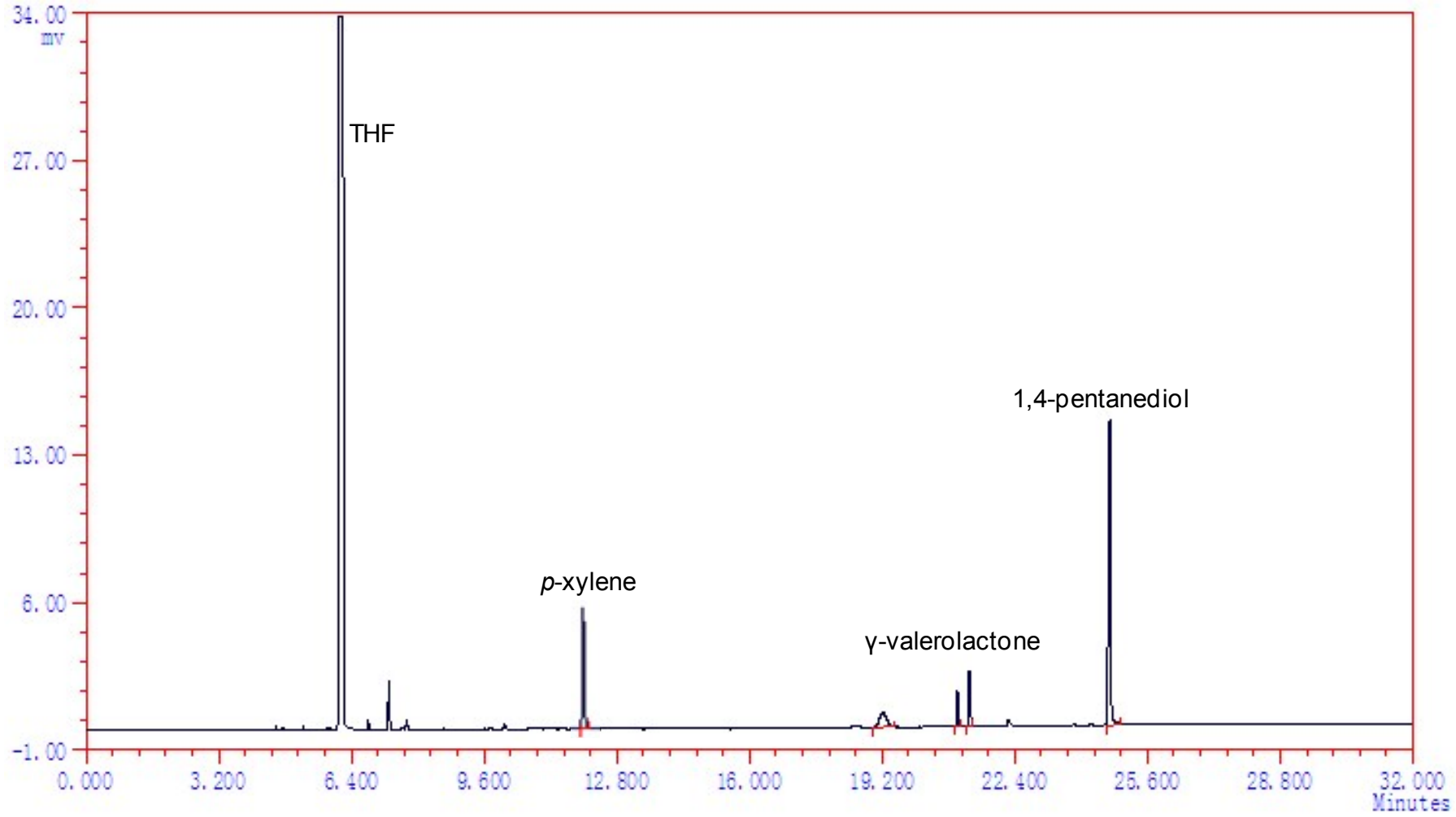

Fig. S45 GC analysis result for H_2-hydrogenation of γ-valerolactone to 1,4-pentanediol by **1**/40 NaOMe (entry 36).

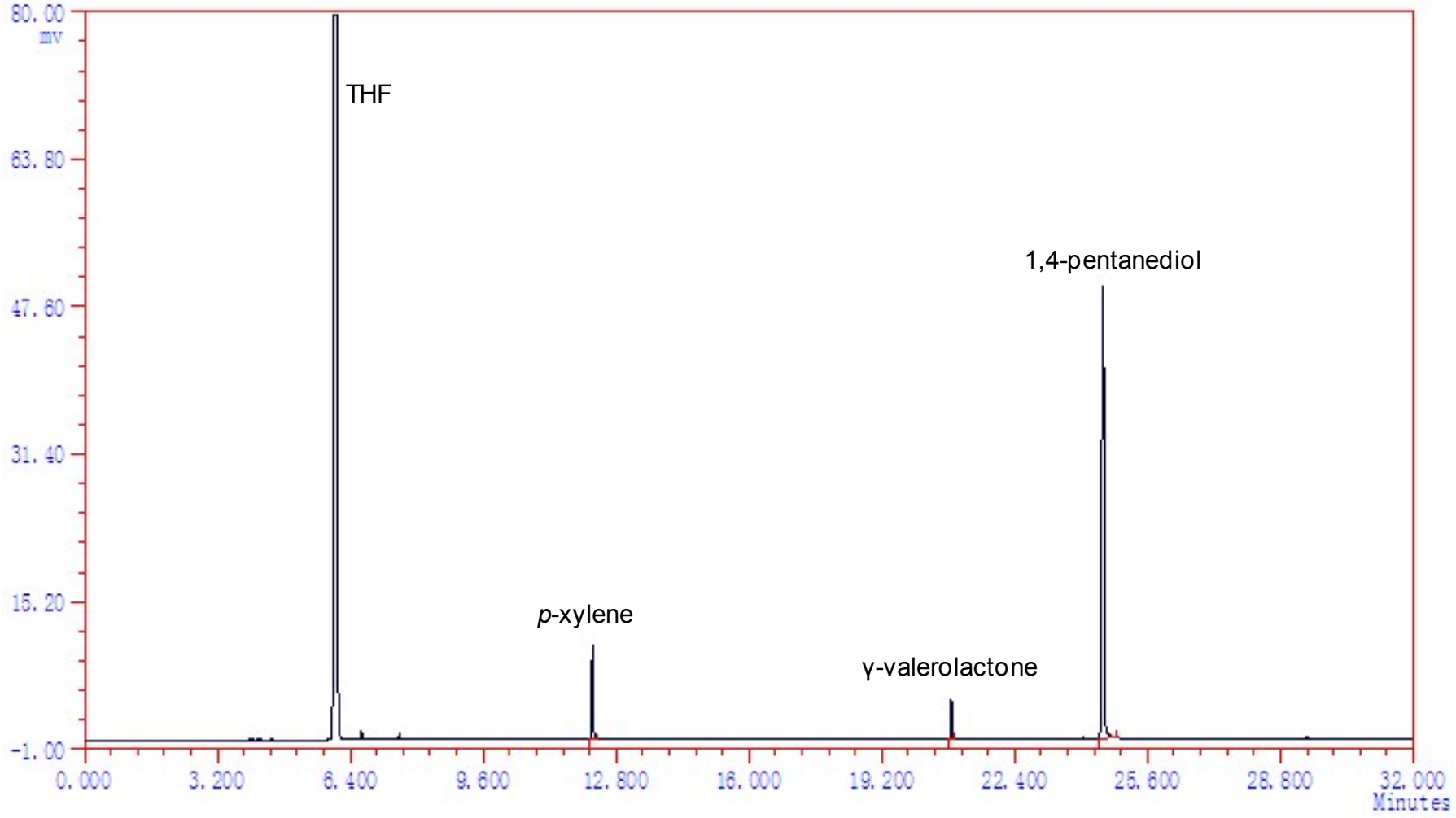

Fig. S46 GC analysis result for H_2-hydrogenation of γ-valerolactone to 1,4-pentanediol by **2**/20 NaOMe (entry 46).

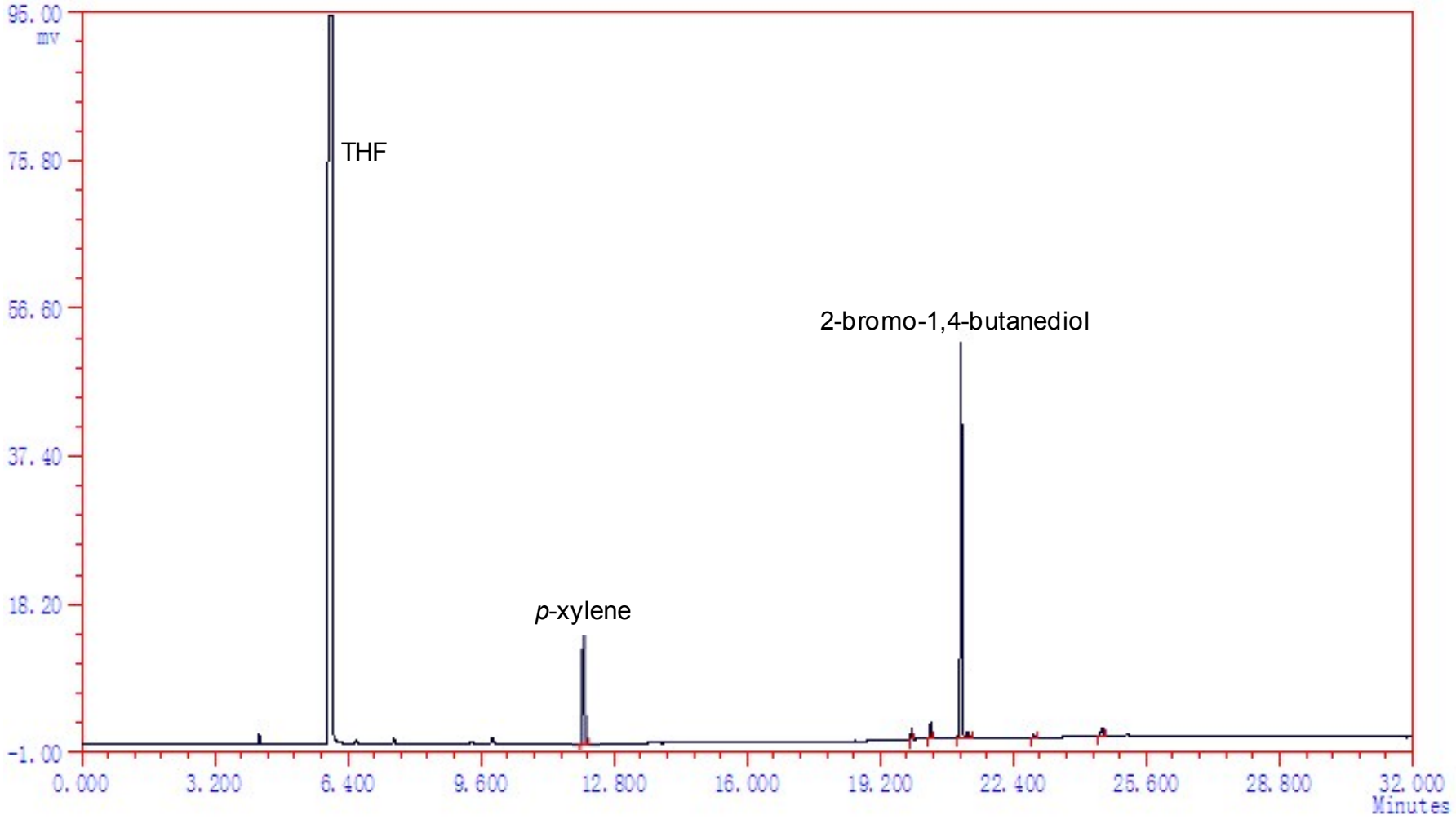

Fig. S47 GC analysis result for H_2-hydrogenation of 2-bromo-4-butanolide to 2-bromo-1,4-butanediol by **1**/40 NaOMe (entry 37).

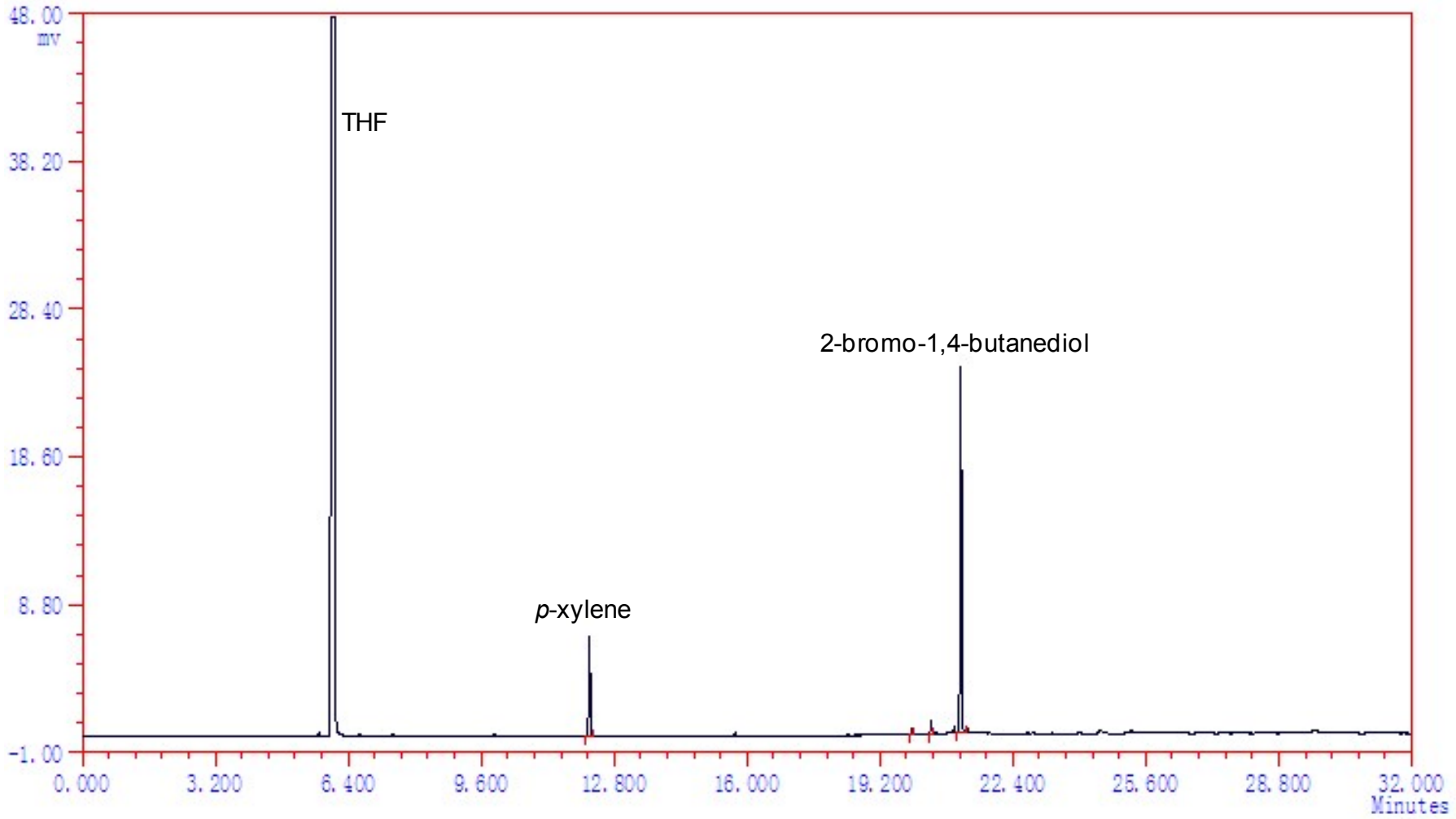

Fig. S48 GC analysis result for H_2-hydrogenation of 2-bromo-4-butanolide to 2-bromo-1,4-butanediol by **2**/20 NaOMe (entry 47).

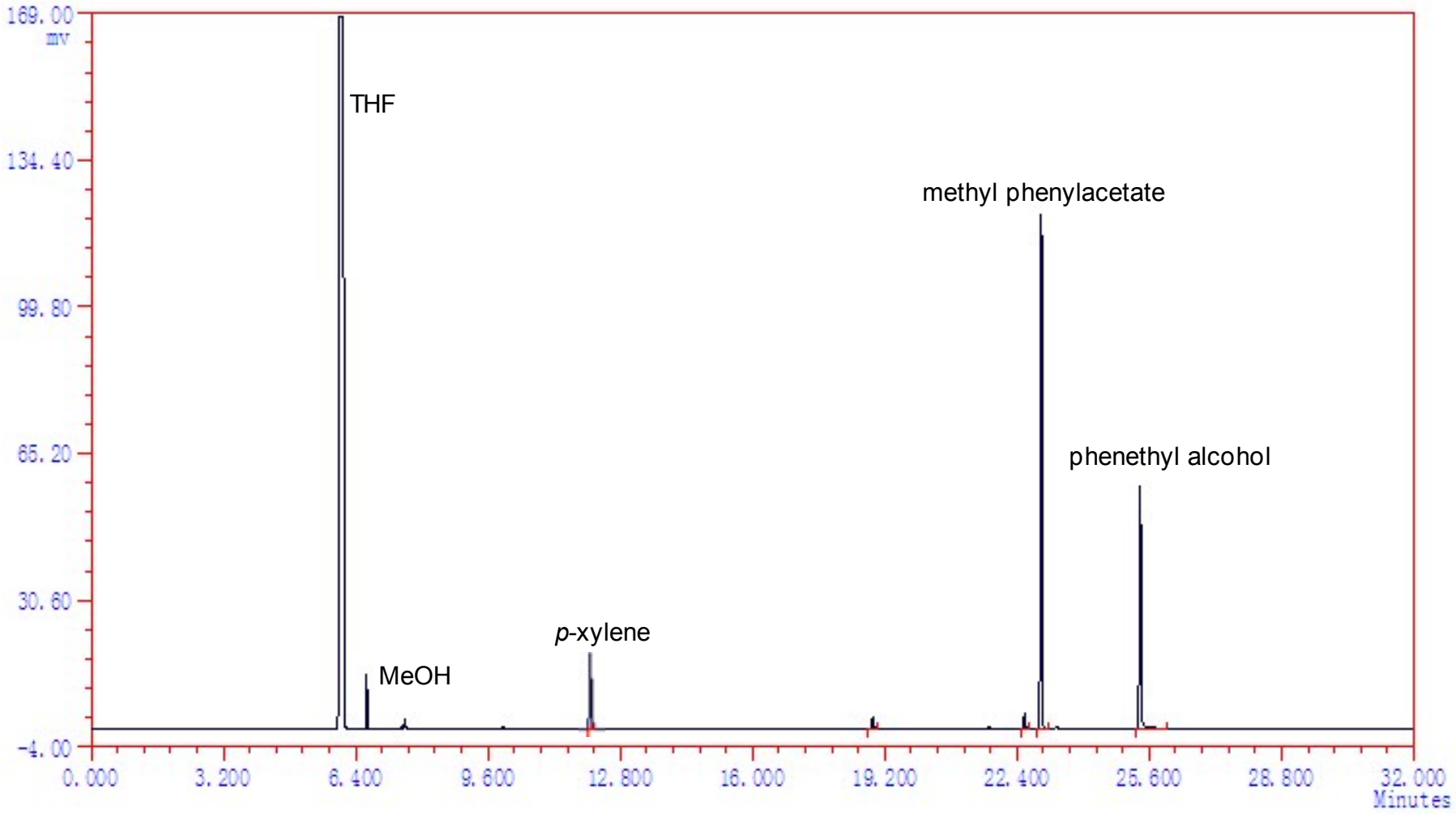

Fig. S49 GC analysis result for H_2-hydrogenation of methyl phenylacetate to phenethyl alcohol by **1**/40 NaOMe (entry 38).

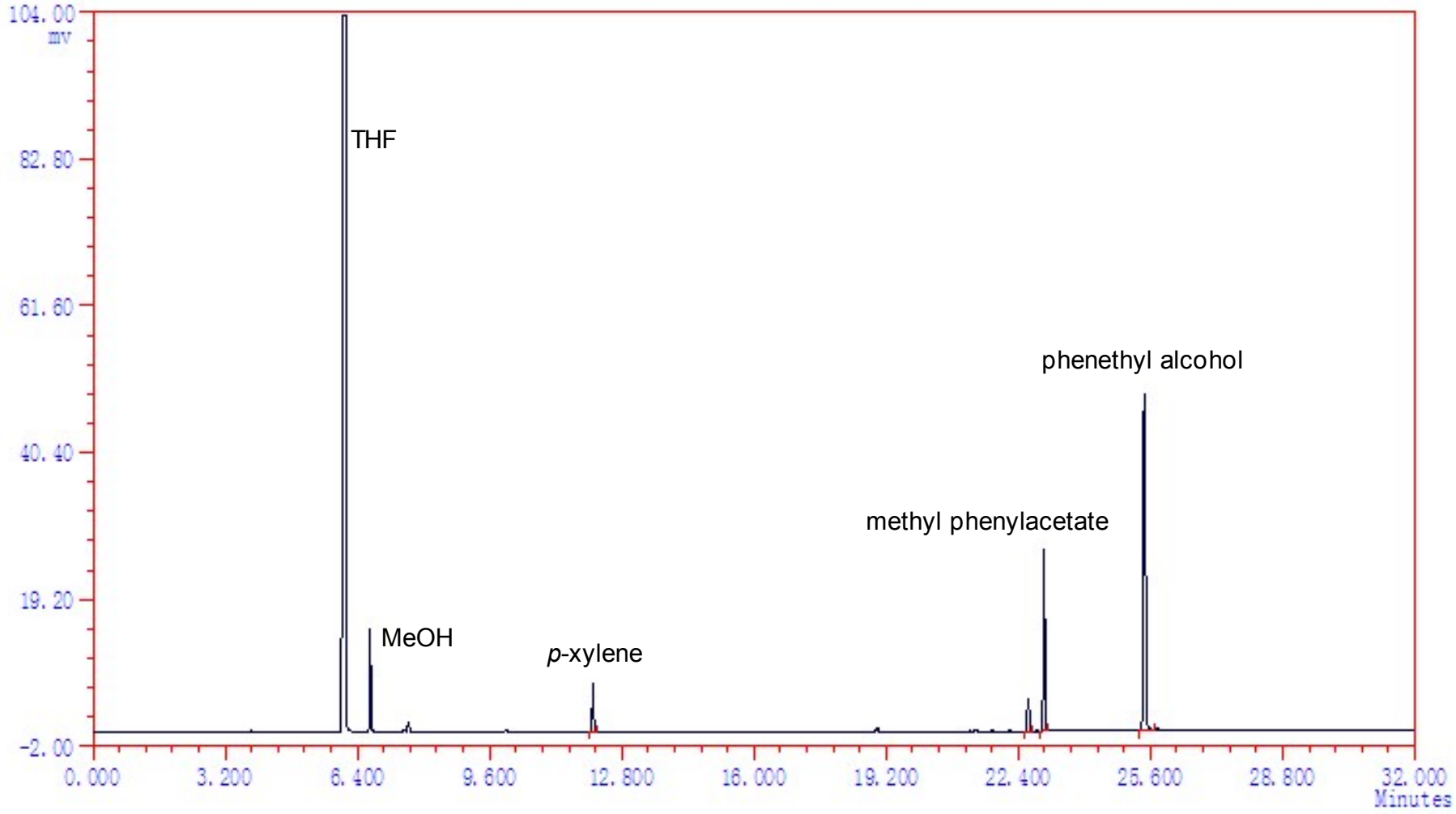

Fig. S50 GC analysis result for H_2-hydrogenation of methyl phenylacetate to phenethyl alcohol by **2**/20 NaOMe (entry 48).

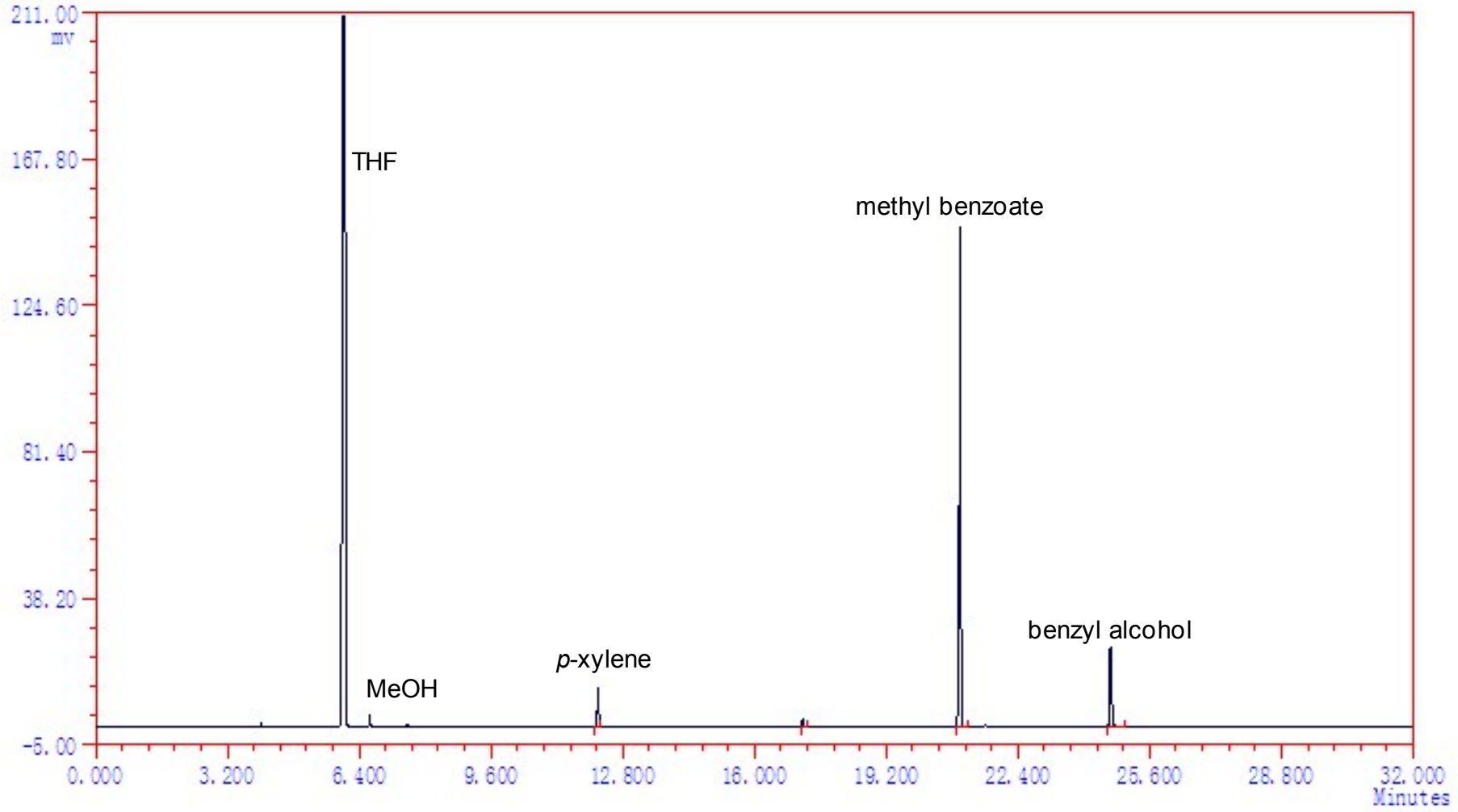

Fig. S51 GC analysis result for H_2-hydrogenation of methyl benzoate to benzyl alcohol by **1**/40 NaOMe (entry 39).

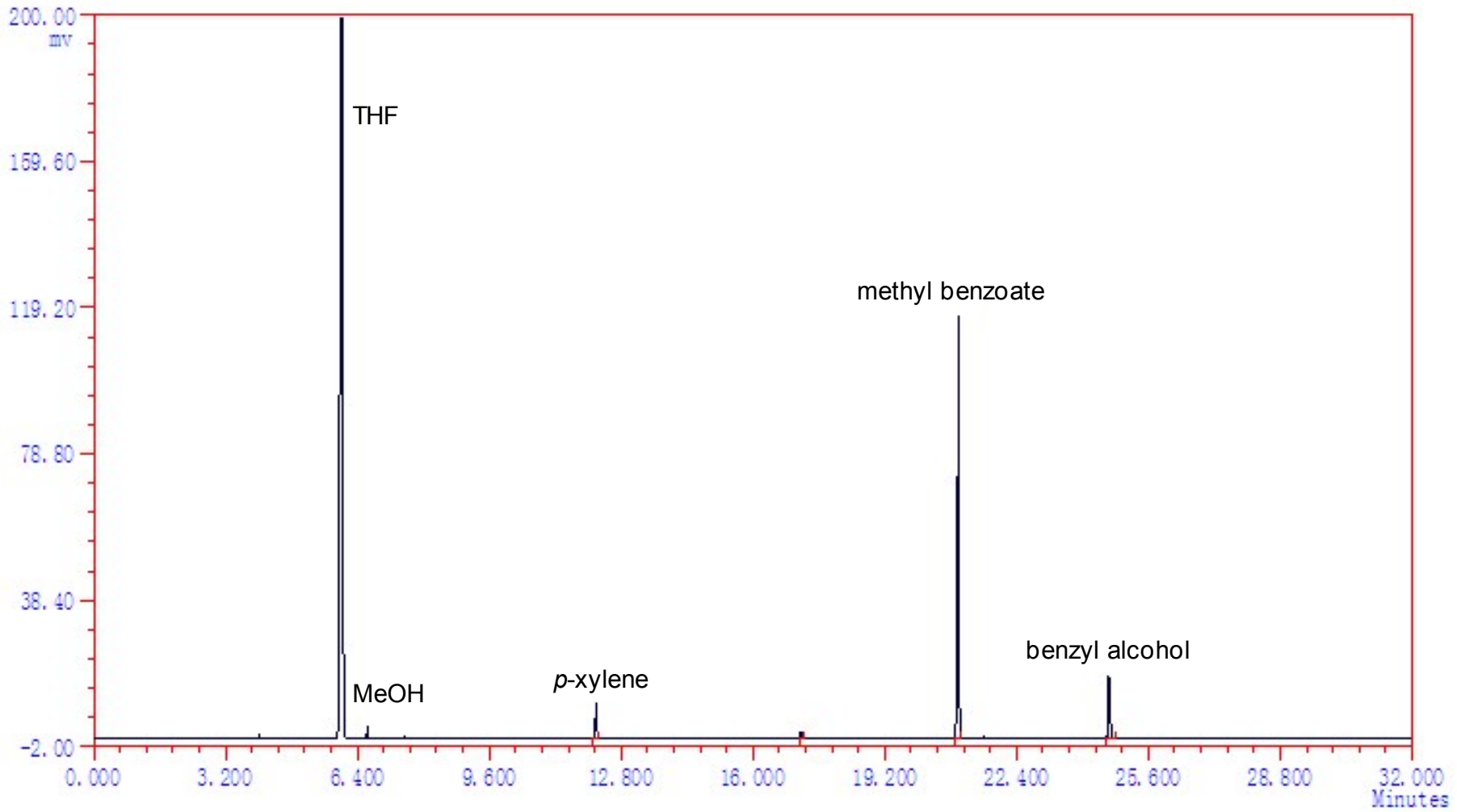

Fig. S52 GC analysis result for H_2-hydrogenation of methyl benzoate to benzyl alcohol by **2**/20 NaOMe (entry 49).

S11. References

1 O. Herd, A. Heßler, M. Hingst, M. Tepper and O. Stelzer, *J. Organomet. Chem.*, 1996, **522**, 69-76.

2 V. Richard, M. Ipouck, D. S. Merel, S. Gaillard, R. J. Whitby, B. Witulski and J.-L. Renaud, *Chem. Commun.*, 2014, **50**, 593-595.

3 S. J. La Placa and J. A. Ibers, *Inorg. Chem.*, 1965, **4**, 778-783.

4 R. A. Schunn, E. R. Wonchoba and G. Wilkinson, in *Inorg Synth*, John Wiley & Sons, Inc., 1972, pp. 131-134.

5 N. Ahmad, J. J. Levison, S. D. Robinson, M. F. Uttley, E. R. Wonchoba and G. W. Parshall, in *Inorg Synth*, John Wiley & Sons, Inc., 1974, pp. 45-64.

6 K. Abdur-Rashid, R. W. Guo, A. J. Lough, R. H. Morris and D. T. Song, *Adv. Synth. Catal.*, 2005, **347**, 571-579.

7 W. L. Jia, X. H. Chen, R. W. Guo, C. Sui-Seng, D. Amoroso, A. J. Lough and K. Abdur-Rashid, *Dalton Trans.*, 2009, 8301-8307.

8 J. X. Gao, H. L. Wan, W. K. Wong, M. C. Tse and W. T. Wong, *Polyhedron*, 1996, **15**, 1241-1251.

9 D. C. Mudalige, S. J. Rettig, B. R. James and W. R. Cullen, *J. Chem. Soc. Chem. Commun.*, 1993, 830-832.

10 C. C. Lee, Y. H. Liu, S. M. Peng, P. T. Chou, J. T. Chen and S. T. Liu, *Polyhedron*, 2012, **35**, 23-30.

11 G. M. Sheldrick, SHELXS-90, Program for Structure Solution; Acta Crystallogr., Sect. A 1990, **46**, 467–473.

12 G. M. Sheldrick, *SHELXL-97*, *Program for Crystal Structure Refinement*; University of Göttingen: Göttingen, Germany, 1997.

13 (a) K. Abdur-Rashid, S. E. Clapham, A. Hadzovic, J. N. Harvey, A. J. Lough and R. H. Morris, *J. Am. Chem. Soc.*, 2002, **124**, 15104-15118; (b) C. A. Sandoval, T. Ohkuma, K. Muñiz and R. Noyori, *J. Am. Chem. Soc.*, 2003, **125**, 13490-13503.